

Semisolid metal processing

Z. Fan

Semisolid metal (SSM) processing is a relatively new technology for metal forming. Different from the conventional metal forming technologies which use either solid metals (solid state processing) or liquid metals (casting) as starting materials, SSM processing deals with semisolid slurries, in which non-dendritic solid particles are dispersed in a liquid matrix. Semisolid metal slurries exhibit distinctive rheological characteristics: the steady state behaviour is pseudoplastic (or shear thinning), while the transient state behaviour is thixotropic. All the currently available technologies for SSM processing have been developed based on those unique rheological properties, which in turn originate from their non-dendritic microstructures. Year 2001 marks the 30th anniversary of the concept of SSM processing. Today, SSM processing has established itself as a scientifically sound and commercially viable technology for production of metallic components with high integrity, improved mechanical properties, complex shape, and tight dimensional control. Perhaps more importantly, it has demonstrated its great potential for further technological development and commercial exploitation. In this paper, progress made on the scientific understanding, technological development, and industrial applications of SSM processing are reviewed. The areas for further research and development are also discussed. IMR/335

© 2002 IoM Communications Ltd and ASM International. The author is in the Wolfson Centre for Materials Processing, Brunel University, Uxbridge, Middlesex UB8 3PH, UK (mtstzff@brunel.ac.uk).

Introduction

Year 2001 marks the 30th anniversary of the concept of semisolid metal (SSM) processing. The original experiment leading to the discovery of rheocasting was performed in early 1971 by Spenser¹ as a part of his doctorate research under the supervision of Professor Flemings at MIT. Spenser was investigating hot tearing during casting of steels. He used Sn–15Pb alloy* as a model system to evaluate the viscosity of partially solidified alloys using a Couette viscometer. In doing so, he was shearing the dendritic structure, although that was not originally intended. He discovered that when the dendritic structure is broken up, the partially solidified alloy has the fluidity of machine oil and exhibits thixotropic behaviour.^{1,2} Flemings and his team immediately recognised the importance of the discovery and, by the summer of that year, had performed industrial trials demonstrating the feasibility of the two routes, which were termed ‘rheocasting’ and ‘thixocasting’.³ In brief, rheocasting involves the

* Alloy compositions are in wt-% unless specified otherwise.

application of shearing during solidification to produce a non-dendritic semisolid slurry that can be transferred directly into a mould or die to give a final product. Thixofforming is used to describe the near net shaping of a partially melted non-dendritic alloy slug within a metal die: thixocasting if in a closed die, or thixoforging if in an open die. (These processes are described in more detail below in ‘Technologies for component shaping’.) The technology was quickly guarded by a series of patents. During the early years, many alternative approaches to mechanical stirring were suggested to achieve the required microstructures. These include isothermal coarsening of solid dendritic materials, mixing of powders, passive mixing, electrical discharge through a semisolid dendritic material, electromagnetic stirring, and intensive cold working of initially dendritic solid materials. Those explorations were partly an attempt to circumvent a strong MIT patent position, but almost certainly also a result of intense curiosity from the foundry world and perceived disadvantages of mechanical stirring. Of all those suggestions, however, only electromagnetic stirring has become a widely accepted method for the production of non-dendritic feedstock materials on a commercial scale, although small scale productions via intensive plastic deformation are being used for some components today.⁴

The feasibility of SSM processing of various alloys has been investigated in the past 30 years. Initially, the primary focus was on high temperature alloys, notably steels, and practically no attention was given to aluminium and magnesium alloys. This was mainly due to the drive for perfection of steel die casting technology for military applications. Semisolid processing was considered to be an effective means to reduce the casting temperature. However, because of the oil crises in the 1970s, and increasing environmental concerns since the 1980s, automobile market forces have been pressing hard for weight reduction using high performance light metal parts. As a consequence, since the 1990s, SSM processing has predominantly concentrated on aluminium alloys. In the past decade, SSM processing has experienced intensive research, development, and commercialisation. Today, SSM processing has established itself as a scientifically sound and commercially viable technology for the production of metallic components with high integrity, improved mechanical properties, complex shape, and tight dimensional control. Perhaps more importantly, it has demonstrated a great potential for further technological development and commercial exploitation.

Another significant aspect of SSM processing, which has not been clearly realised in the past, is that it marks the first extensive manipulation of the solidification process. Historically, for thousands of years, since the birth of metal casting, solidification of alloys of given compositions has been treated as a natural process, with the so called rapid solidification

processing being an accelerated natural process. Semisolid metal processing has, so far, clearly demonstrated that the solidification process can be manipulated positively and effectively by external means in order to achieve the desired solidification microstructures, providing inspiration for many other new processes in the years to come.

Thirty years on, much progress has been made and much is left to be done.⁵ Progress in SSM processing has been marked by six biennial international conferences.^{6–11} However, after 30 years, it is still not clear which of the two basic routes, rheocasting or thixocasting, will be of the greatest long term significance. Cast alloys are still being used for SSM processing and the basic mechanisms for the formation of the non-dendritic structures are still not clearly understood. The implications of the SSM processed microstructures as regards the mechanical properties of the final parts are still to be realised.

There have been two comprehensive reviews on the subject, one by Flemings¹² in 1991 and the other by Kirkwood in 1994.¹³ The objectives of the current review are to give a comprehensive account of the progress made in the past 30 years on various aspects of SSM processing with an emphasis on the new developments since the last review¹³ and to identify key areas for further research and development. Though perhaps once possible to cover the majority of the literature by referring to the previous two reviews, it is now no longer feasible to do so. Although every effort has been made to include most of the original contributions in the area, the present author apologises for omitting any important contribution to the field.

Rheology of semisolid metals

The rheology of SSM slurries is attracting increasing attention from research scientists owing to the complexity of the flow response, and from production engineers since it must be controlled carefully for successful forming operations. Semisolid metal slurries can be roughly divided into two broad categories; a 'liquid-like' slurry contains dispersed solid particles and behaves like a fluid under external forces, while a 'solid-like' slurry contains an interconnected solid phase and behaves like a solid, exhibiting a well defined yield strength. The deformation mechanisms for these two types of slurry are fundamentally different. In this review they will be treated separately. Semisolid metal slurries with a solid fraction less than 0.6 and a globular solid morphology usually exhibit two unique rheological properties: thixotropy and pseudoplasticity.¹⁴ Thixotropy describes the time dependence of transient state viscosity at a given shear rate, while pseudoplasticity refers to the shear rate dependence of steady state viscosity. All the SSM processing techniques rely on either or both of those properties in the same process. Therefore, successful development of SSM processing technologies requires a good understanding of the rheology of SSM slurries. In this section, the experimental techniques, experimental findings, and theoretical modelling of SSM slurries available in the literature are reviewed. It should be mentioned that in this section the author

has drawn heavily from the recent review paper on rheology by Suery *et al.*¹⁵

Experimental techniques

The concentric cylinder rheometer has been most commonly used for rheological characterisation of SSM slurries.^{14,16–23} It has two different configurations, Couette or Searle, depending respectively on whether the cup or the bob is the rotating part. In the concentric cylinder rheometer, rheological experiments for SSM slurries are often performed in three different modes:

- continuous cooling and shearing from a temperature above the liquidus
- transient or steady state experiments from a specified starting condition under fixed solid fraction and shear rate
- shearing after partial solidification or partial remelting.

The major advantages of this technique include high flexibility in terms of operating mode and well defined flow conditions. This makes it very suitable for understanding the physical mechanisms of SSM rheology. However, this technique is limited to low shear rates and relatively low solid fractions, because too high a shear rate can cause flow instability and too high a solid fraction can lead to wall slippage. Another problem associated with this technique is that it takes from several minutes up to several hours to reach steady state. Irreversible microstructural changes may occur during such experiments, which might affect the rheological properties.²⁴

Compression between parallel plates is another technique used for rheological characterisation of SSM slurries. In this method, a cylindrical sample with low aspect ratio is compressed between two parallel plates at constant deformation rate or under constant load.^{25–30} In this case, the axial velocity becomes insignificant compared to the radial velocity of the alloy during the later stage of deformation. It should be noted that the stress–strain field in this experiment is highly inhomogeneous due to the presence of friction. Therefore, comparison of results should be made with caution, especially when there are specimen size differences. This technique can be used to investigate SSM slurries with high solid fraction, and to detect the presence of yield stress. However, the flow conditions are complex, it is difficult to define the steady state and, more importantly, it is difficult to prevent solid/liquid segregation.

Capillary die and backward extrusion have also been used to characterise SSM slurries. In such techniques, the flow is pressure driven and is characterised by a variation of shear rate along the cross-section depending on material behaviour.^{22,31,32} Viscosity is usually calculated assuming linear viscous behaviour, which may not necessarily be true for all the cases.³³ As in the parallel plate technique, it is not clear whether the steady state is reached; the data obtained are not steady state values, but probably closer to isostructure data. Moreover, in the presence of strong deviation from linearity or if yield stress is present, plug flow conditions will develop. In this case, the flow conditions near the wall dominate the response

of the materials. Therefore, a true viscosity cannot be calculated. Another problem associated with this technique is that it is almost impossible to study thixotropy. Segregation may also occur due to the pressure gradient that develops as a result of the long length required by this test and the increased permeability at the walls. However, since similar flow conditions are present in an actual thixoforming process, the information extracted from such tests can be relevant when comparable values of cross-sections are used.

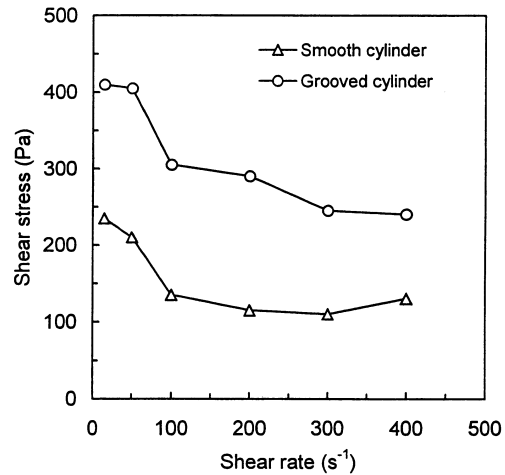
Recently, Koke and Modigell^{23,34} made a comparison of the steady state flow curves of semisolid Sn–15Pb alloy obtained by different investigators,^{21,33,35} as shown in Fig. 1. There are substantial discrepancies in Fig. 1 for the same alloy composition using similar experimental techniques (concentric cylinder rheometer). Such variations in experimental results may be attributed to the following factors:

- difference in geometry for cylinders (cylinders have either a grooved (e.g. Ref. 23) or a smooth (e.g. Ref. 35) surface; the former can promote a more uniform particle distribution, whereas the latter may lead to wall depletion or slippage (see experimental observations of Koke *et al.*³⁶ in Fig. 2) resulting in a much reduced shear stress)
- difference in the methods used for calculating the shear rate
- difference in the starting materials, which may be partially solidified or partially remelted, and consequently have different particle size and morphology.²⁴

It appears from the above analysis that it is necessary to standardise the testing methods and procedures.

Phenomenology

The first investigation of the rheology of SSM slurries was conducted on the Sn–Pb system by Spencer *et al.*² at MIT. They showed that the stirred SSM slurry at a solid fraction higher than 0.2 behaves like a non-Newtonian fluid with an apparent viscosity orders of magnitude less than that of a unstirred dendritic slurry. It is this first observation which



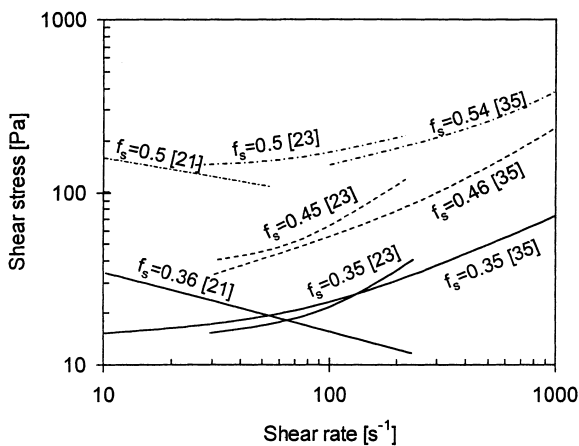
2 Steady state shear stress obtained from shear rate transient experiments (from 25 to 400 s⁻¹) in 10 min intervals using smooth and grooved cylinders (after Ref. 36)

initiated numerous rheological studies on stirred SSM slurries. Among them is the very extensive study by Joly and Mehrabian¹⁴ on the Sn–Pb system. As demonstrated by Joly and Mehrabian,¹⁴ the rheological phenomena in stirred SSM slurries can be approximately divided into three categories:

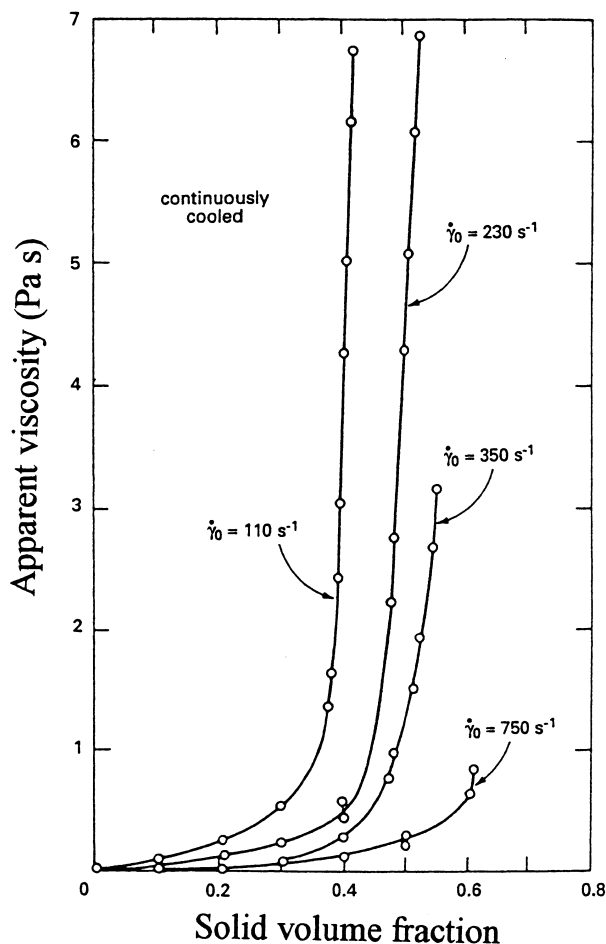
- continuous cooling behaviour, which describes the viscosity evolution during continuous cooling at constant cooling rate and shear rate
- pseudoplastic behaviour, which describes the shear rate dependence of steady state viscosity, or shear thinning behaviour
- thixotropic behaviour, which describes the time dependence of transient state viscosity.

The continuous cooling behaviour gives the first insight into the effects of solid fraction, shear rate, and cooling rate on the rheological behaviour of SSM slurries. In particular, it is more relevant to the practical conditions set in SSM processing techniques such as rheocasting and rheomoulding. Figure 3 shows an example of results obtained from the continuous cooling experiments on Sn–15Pb alloy carried out by Joly and Mehrabian.¹⁴ Generally, for a given cooling rate and shear rate, the measured apparent viscosity increases with increasing solid fraction, slowly at low solid fraction and sharply at high solid fraction. At a given solid fraction, the apparent viscosity decreases with increasing shear rate and decreasing cooling rate. This is because both increasing shear rate and decreasing cooling rate promote a more spherical particle morphology. Following the work of Joly and Mehrabian¹⁴ on the Sn–Pb system, similar studies were carried out on other alloy systems (e.g. see Refs. 37–42) and also on SSM slurries containing SiC particles (e.g. Refs. 39, 41). However, as has been pointed out by Suery *et al.*,¹⁵ such experiments are more relevant to exploiting the solidification behaviour rather than studying the rheology of SSM slurries.

The isothermal steady state experiments lead to more precise rheological characterisation and is a first step towards the determination of a constitutive



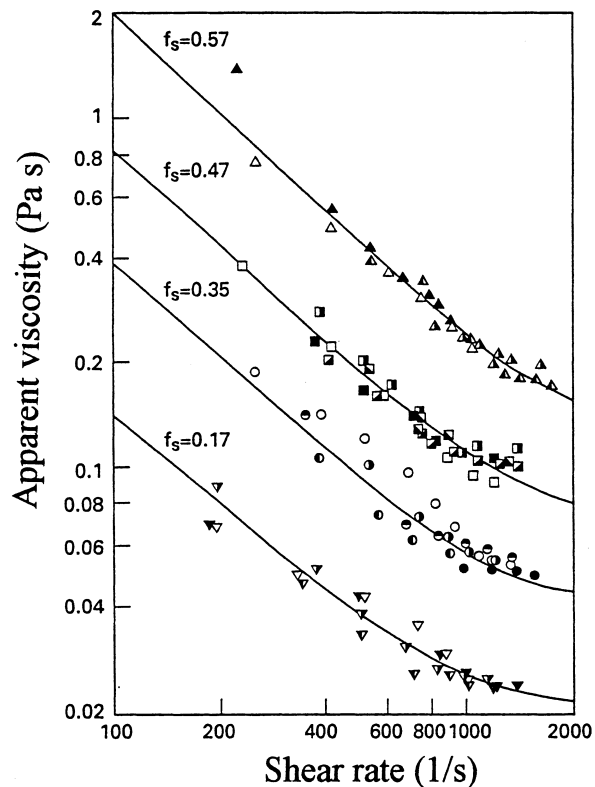
1 Comparison between flow curves of Sn–15Pb alloy determined for various solid fractions f_s by McLelland *et al.*,²¹ Modigell and Koke,²³ and Peng and Wang³⁵ (after Ref. 23)



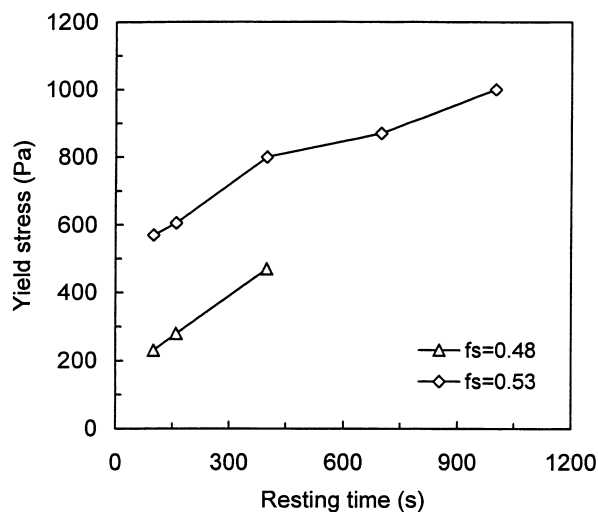
3 Apparent viscosity versus solid fraction f_s of Sn-15Pb alloy sheared continuously and cooled at 0.33 K min^{-1} at different shear rates $\dot{\gamma}_0$ (after Ref. 14)

equation. The steady state is usually defined as a state at which the viscosity of a SSM slurry with fixed volume fraction and shear rate does not vary with prolonged shearing time. Thus, for a given alloy system, steady state viscosity is a function of solid fraction and shear rate. Joly and Mehrabian¹⁴ showed on Sn-15Pb alloy that the behaviour is shear thinning (or pseudoplastic), where the apparent steady state viscosity decreases with increasing shear rate. This shear thinning was demonstrated more generally by Turng and Wang,¹⁷ as shown in Fig. 4. For a SSM slurry with a fixed solid fraction, the steady state viscosity decreases with increasing shear rate, approaching an asymptotic value when the shear rate becomes infinite. Such pseudoplastic behaviour has also been confirmed in many other systems.^{37,39-43} It is now generally accepted that the steady state viscosity at a given shear rate depends on the degree of agglomeration between solid particles, which, in turn, is the result of a dynamic equilibrium between agglomeration and deagglomeration processes.⁴⁴

Another phenomenon associated with steady state behaviour is the presence of yield stress. This phenomenon is not well understood at present.^{45,46} It is generally agreed that many suspensions have a yield point at low shear rate, resulting from the structural

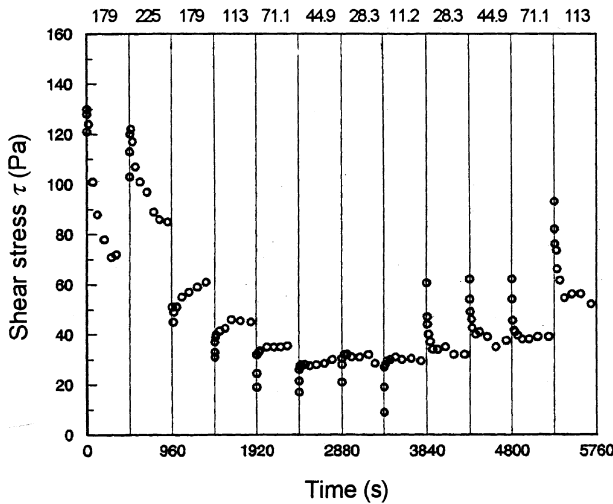


4 Steady state apparent viscosity versus shear rate in Sn-15Pb alloy for various solid fractions f_s (after Ref. 17)



5 Yield stress of semisolid Sn-15Pb alloy with solid fractions f_s of 0.48 and 0.53 as function of resting time (after Ref. 24)

formation due to the dynamic interaction between solid particles. The yield phenomenon is generally inherent to the thixotropy, however, there are very few data of yield stress for SSM slurries, as has been discussed by Sigworth⁴⁷ and Peng and Wang.³⁵ Sannes *et al.*⁴⁸ reported that the yield stress for magnesium based SSM slurries is in the range 10^2 – 10^4 Pa for solid fractions ranging from 0.3 to 0.6. More recently, Modigell *et al.*²⁴ reported the yield stress data for Sn-15Pb SSM slurries as presented in Fig. 5 as a function of resting time. They also pointed



6 Results obtained from shear rate transient experiments on Sn-15Pb alloy with solid fraction of 0.45 (after Ref. 50): along top of figure are shear rate (unit s⁻¹) values that apply to vertical sections beneath

out that the strong particle interactions are responsible for the existence of yield stresses, below which the SSM slurries behave like elastic solid. Yield stresses are ideally measured using shear stress controlled rheometers by applying shear stress ramps and measuring the stress value when the alloy starts to deform.²⁴

The thixotropic behaviour of SSM slurry was first demonstrated by Joly and Mehrabian¹⁴ on Sn-15Pb alloy by measuring the hysteresis loops during a cyclic shear deformation. Following this work, other investigators used a similar technique to study the thixotropic behaviour of other systems (e.g. Ref. 49). However, such a procedure is not sufficient to quantify the kinetics of agglomeration and deagglomeration processes. To overcome this shortcoming, special experimental procedures involving an abrupt shear rate jump or a shear rate drop were developed to characterise the kinetics of structural evolution (Refs. 17, 20, 23, 42, 49, 50). An example of such thixotropic experiments obtained by Modigell *et al.*⁵⁰ for Sn-15Pb alloy is shown in Fig. 6. It has been found that the agglomeration process dominates after a shear rate drop, whereas the deagglomeration process dominates after a shear rate jump.^{20,23,49,51}

Another group of interesting experiments associated with shear rate transient experiments are the so called isostructure tests. If the shear rate transient is fast enough, the slurry structure will not change during the shear rate ramping process. A shear thickening phenomenon was first observed experimentally in Sn-Pb alloys and aluminium based alloys by Kumar *et al.*¹⁸ using a rotational viscometer, and more recently by Modigell and Koke²³ in Sn-Pb alloys using the same technique. However, de Figueredo *et al.*³⁰ recently investigated the transient behaviour of A357 alloy using the parallel plate compression technique. They found that for a large range of solid fractions the slurry consistently showed shear thinning behaviour, and the transient shear

thickening behaviour was not detected for transition times as low as 200 μs.

Rheological modelling

To date, the experimental work has demonstrated phenomenologically a strong coupling between the slurry structure (or the state of agglomeration) and the flow behaviour under various external flow conditions, as has been reviewed by Suery *et al.*¹⁵ and Sigworth.⁴⁷ However, modelling work on those aspects of the behaviour of SSM slurries is far from satisfactory.^{52,53} The existing models either have been developed for a specific rheological phenomenon, or are difficult to link with experiments for further understanding. As already pointed out by Brown and co-workers,^{49,54} rheological models should be linked with microstructural parameters measurable metallographically, because such models coupled with experimental investigations can yield further insight into the mechanisms of agglomeration and deagglomeration processes. In this section, the progress made on rheological modelling of SSM slurries is reviewed.

Modelling of pseudoplasticity

Joly and Mehrabian¹⁴ used a simple power law to interpret the shear thinning behaviour observed during isothermal steady state experiments on Sn-15Pb alloy

$$\eta = k\dot{\gamma}^{m-1} \dots \dots \dots (1)$$

1

where η is the apparent viscosity, $\dot{\gamma}$ is the shear rate, and k and m are two solid fraction dependent factors. Following this work, there have been a number of elaborated power law models. These include the model developed by Kattamis and Piccone³⁹ to consider microstructural effects and to account for viscoplastic deformation of the solid phase, the model proposed by Nan *et al.*³⁸ to consider energy dissipation by viscoplastic deformation of the solid phase, and the model proposed by Turgung and Wang¹⁷ to account for the observed asymptotic viscosity of Sn-15Pb alloy. Those models, usually referred as power law type models, have been extensively reviewed by Kirkwood,¹³ Suery *et al.*,¹⁵ and McLelland *et al.*²¹ In general, the models based on power law are useful for engineering applications such as process simulations. They are, however, empirical by nature and do not address the origin of pseudoplasticity at microstructural level.

A totally different approach was taken by Perez *et al.*⁵⁵ to study steady state behaviour. The authors introduced a lattice model to simulate the agglomeration and deagglomeration processes within a slurry under shear. When the steady state is reached, the entrapped liquid fraction is calculated and is used to estimate the viscosity. The results obtained from simulation on the viscosity and structure of three-dimensional (3D) clusters appear to be in agreement with the experimental results.

Chen and Fan⁵⁶ developed a microstructural model that describes the rheological behaviour of liquid-like SSM slurries under simple shear flow. In this model, a liquid-like SSM slurry is considered as a suspension in which interacting spherical solid particles of low cohesion are dispersed in a liquid matrix. In a simple

shear flow field, the dynamic interactions between solid particles result in the formation of agglomerates. Under the influence of viscous forces, collisions between agglomerates lead to new agglomerates of a larger size and, at the same time, larger agglomerates also break up giving rise to agglomerates of a smaller size. At a particular time, the state of agglomeration is described by a structural parameter n , which is defined as the average particle number in agglomerates. Based on such considerations, the time evolution of the structural parameter $n(t)$ has been derived analytically as a function of both microstructural parameters and external flow conditions

$$\frac{1}{n(t)} = \frac{1}{n_e} + \left(\frac{1}{n_0} - \frac{1}{n_e} \right) \exp\{-\lambda t\} \quad \dots \quad (2)$$

where $n_0 = n(0)$, which is the average agglomerate size at $t = 0$, and n_e is the average agglomerate size at $t = \infty$ (steady state), and

$$n_e = \frac{\pi d^3 K_d + 12\alpha_1 f_s^2 K_a}{\pi d^3 K_d - 6\alpha_2 f_s K_a} \quad \dots \quad (3)$$

$$\lambda = \frac{6\alpha_1 f_s^2 K_a}{\pi d^3} + \frac{1}{2} K_d \quad \dots \quad (4)$$

where d is the particle size, f_s is the solid fraction, K_a and K_d are agglomeration and deagglomeration rates respectively, and α_1 and α_2 are model constants.

Through effective solid fraction (Φ_{eff} , defined as the sum of the actual solid fraction and the entrapped liquid fraction) both viscosity η and shear stress τ can be expressed as a function of the structural parameter n

$$\eta = \eta_0 (1 - \Phi_{\text{eff}})^{-5/2} \quad \dots \quad (5)$$

$$\Phi_{\text{eff}} = \left(1 + \frac{n-1}{n} A \right) f_s \quad \dots \quad (6)$$

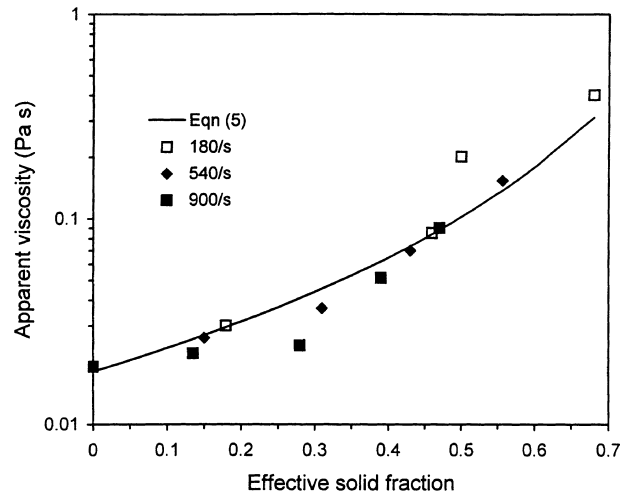
$$\tau = \eta(n, \dot{\gamma}) \dot{\gamma} \quad \dots \quad (7)$$

$$\frac{dn}{dt} = g(n, \dot{\gamma}) \quad \dots \quad (8)$$

2

where η_0 is the viscosity of the liquid matrix, A is another model parameter related to the packing mode. The value of A decreases with the increase of packing density. Equation (6) indicates that the effective solid fraction is affected by the actual solid fraction, agglomerate size, and the packing mode in the agglomerates. It is interesting to note from equation (5) that the viscosity of a semisolid slurry is a direct function of the viscosity of the liquid matrix and the effective solid fraction. The flow conditions affect viscosity only indirectly through changing the effective solid fraction. Theoretical predictions⁵⁷ from this model are in good agreement with the experimental results of Ito *et al.*,⁴⁰ as shown in Fig. 7.

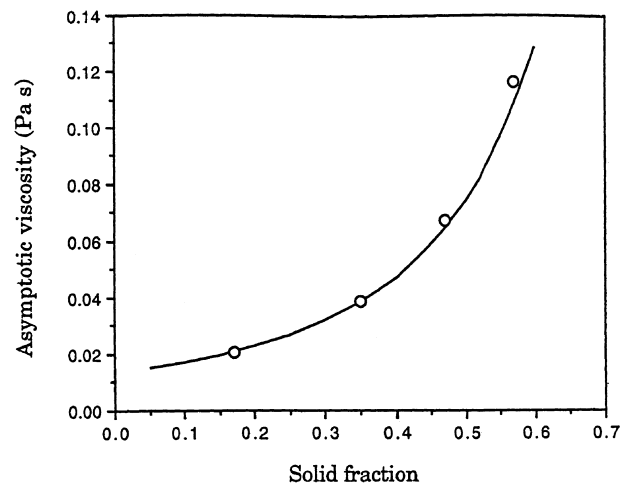
Experimental results on the steady state viscosity of Sn-15Pb slurries¹⁷ were used to determine the model parameters. Application of this model⁵⁶ to Sn-15Pb slurries has revealed a number of microstructural and rheological characteristics of SSM slurries.⁵⁷ Under simple shear flow, the steady state represents the dynamic equilibrium between two opposite processes, agglomeration and deagglomeration. At steady state, the microstructure of a SSM



7 Comparison of calculated⁵⁷ (solid line) and experimental⁴⁰ (symbols) data for apparent viscosity of Al-6.5Si alloy as function of effective solid fraction

slurry is characterised by spherical particle morphology, uniform particle size, constant average agglomerate size, and constant effective solid fraction. The theoretical analysis shows that there is a strong coupling between the microstructure and the steady state viscosity. Shear rate affects the viscosity of SSM slurries by changing the amount of entrapped liquid between solid particles in the agglomerates, and therefore altering the effective solid fraction. The predicted steady state viscosity of a SSM slurry decreases with increasing shear rate and approaches an asymptotic viscosity, which is in good agreement with the experimental observation of Turng and Wang¹⁷ (see Fig. 8). The asymptotic viscosity is only a function of solid fraction and corresponds to a microstructure in which there is no particle agglomeration ($n = 1$).

In order to consider the possible existence of finite yield stress, SSM slurries have recently been treated as Bingham fluids and the Herschel-Bukley type of model⁵⁸ has been used to describe the deformation



8 Comparison of calculated⁵⁷ (solid line) and experimental¹⁷ (open circles) data for asymptotic viscosity of Sn-15Pb alloys as function of solid fraction

characteristics of SSM slurries (e.g. Refs. 23, 35). The steady state flow curve is given by the following equation

$$\tau = \tau_a + k_1 \dot{\gamma}^n \quad \dots \quad (9)$$

where τ_a is the apparent yield stress and k_1 and n are model parameters. Equation (9) is normally used to fit the experimental flow curve to determine the yield stress data and the model parameters. However, substantial differences exist between results from different investigators. For example, the shear rate exponent n for a SSM Sn–15Pb slurry with a solid fraction of 0.45 was found to be 0.83 by Peng and Wang,³⁵ 1.29 by Modigell and Koke,²³ and –0.31 by McLelland *et al.*²¹ It appears that the importance of the existence of yield stress in SSM slurries is being realised and that modelling work should include the effect of finite yield stress, especially for SSM slurries with high solid fractions and under low shear rates. It should be noted, however, that Barnes⁵⁹ has commented that the existence of a yielding point may depend on the experimental technique employed and may not therefore be a fundamental property of the system.

Modelling of thixotropy

Modelling of thixotropic behaviour has been performed using predominantly the internal variable framework^{20,23,50,51,54} or based on the Cross model.^{60–62} A structural parameter s is normally used as a scalar measure of the degree of agglomeration in a SSM slurry. The parameter s varies between 1 and 0, corresponding to a fully agglomerated state and a fully deagglomerated state, respectively. The objective of such thixotropic modelling is to derive the time evolution of the structural parameter s . This is done by using constitutional equations similar to equations (7) and (8).

Mada and Ajersch^{20,51} used this general framework to model the thixotropic behaviour of A356 alloys and the effect of SiC particles on it. The authors derived the following equation to describe the relationship between the shear stress $\tau(t)$ at time t and the shear rate after the jump where deagglomeration processes are dominant²⁰

$$\tau(t) = \tau_a + (\tau_0 - \tau_a) \exp \left\{ - \frac{\dot{\gamma}_f}{a_1 + b_1 \dot{\gamma}_f} t \right\} \quad (10)$$

where τ_0 and τ_a are the isostructural shear stress and the steady state shear stress respectively, and a_1 and b_1 are constants. In the case of reagglomeration during resting, the evolution of the shear stress with time at rest t_r after resuming shear is given by²⁰

$$\tau(t_r) = \tau_\infty - (\tau_\infty - \tau_e) \exp \left\{ - \frac{\dot{\gamma}_0}{a_2 + b_2 \dot{\gamma}_0} t \right\} \quad (11)$$

where α is a model constant, τ_∞ and τ_e are the shear stresses for a fully agglomerated state and the shear stress when the shear rate is dropped respectively, and a_2 and b_2 are constants.

Quaak *et al.*⁴⁴ further elaborated equation (10) by proposing, in the case of evolution of the shear stress after a shear rate jump in A356 and A356/SiC alloys,

a double exponential expression

$$\tau(t) = \tau_e - (\tau_0 - \tau_e) \times \left[\alpha \exp \left\{ - \frac{t}{\lambda_1} \right\} + (1 - \alpha) \exp \left\{ - \frac{t}{\lambda_2} \right\} \right] \quad \dots \quad (12)$$

where λ_1 and λ_2 are fitted characteristic times that depend on the initial and final shear rate and solid fractions.

Brown and co-workers have also used the general framework of internal variable models to propose, based on micromechanical considerations, a flow equation^{18,54}

$$\tau = A(s) \frac{(c/c^*)^{1/3}}{1 - (c/c^*)^{1/3}} \eta_L \dot{\gamma} + (n + 1) C(T) s f_s \eta_L^{n+1} \dot{\gamma}^n \quad \dots \quad (13)$$

and an evolution equation⁴⁹ for the structural parameters

$$\frac{ds}{dt} = H(T, f_s)(1 - s) - R(T, f_s) s \dot{\gamma}^n \quad \dots \quad (14)$$

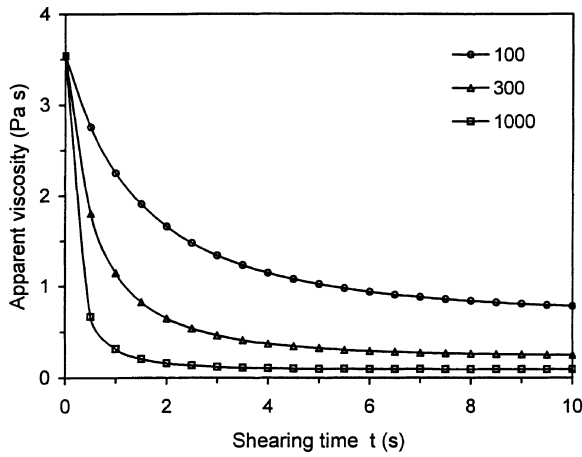
where $c = f_s(1 + 0.1s)$ takes into account the entrapped liquid due to agglomeration, $c^* = 0.625 - 0.1s$ is a critical solid fraction, $A(s)$ is a hydrodynamic factor, η_L is the viscosity of the liquid phase in the SSM slurry, $C(T)$ is a temperature dependent factor with an Arrhenius form, $H(T, f_s)$ is the agglomeration function that represents agglomeration of solid particles, $R(T, f_s)$ is the deagglomeration function representing shear induced rupture of particle–particle bonds, and $n = 4$. The steady state flow equation is given by setting $ds/dt = 0$ such that

$$s = s_{st} = \frac{1}{1 + (R/H) \dot{\gamma}^n} \quad \dots \quad (15)$$

The model was identified and validated on Sn–15Pb and Al–7Si–0.6Mg alloys, and used by Zavaliangos and Lawley⁶³ for simulation of the thixoforging process. It was further used qualitatively for high solid fraction ($f_s > 0.60$) semisolid Sn–Pb alloys stirred in a Couette rheometer.⁶⁴

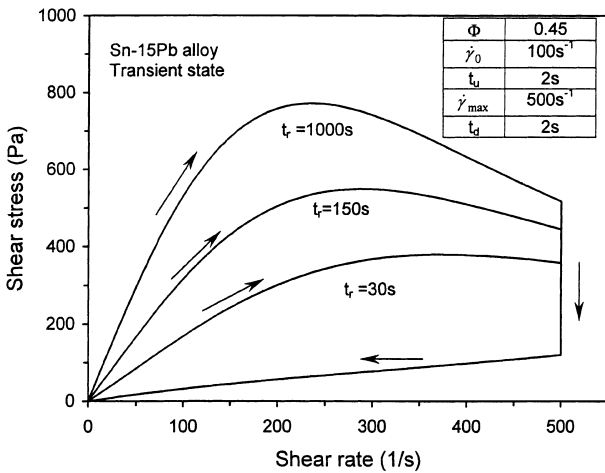
Further modelling work on thixotropy using the structural parameter s , but considering the presence of finite yield stress, includes the work by Koke and co-workers^{34,65} and Burgos and Alexandrou.⁶⁶ However, the structure parameter s is not a well defined parameter, and it is difficult to link with other microstructural parameters measurable using metallographic techniques, and therefore difficult as regards direct insight into the kinetics of structural evolution during shearing.

The microstructural model developed by Chen and Fan⁵⁶ has also been applied to study the transient state behaviour of SSM slurries under various deformation conditions, such as isothermal shearing (Fig. 9), isothermal resting, isostructural shearing, shear rate transient, and cyclic shearing (Fig. 10).⁶⁷ Theoretical predictions of the hysteresis loops under various cyclic deformation conditions have revealed that the physical origin of thixotropy lies in the fact that the deagglomeration kinetics is much faster than the agglomeration kinetics, with the former being a



9 Comparison of calculated transient state viscosity of Sn-15Pb alloy with solid fraction of 0.4 under different shear rates (unit s⁻¹) as function of shearing

3



10 Calculated hysteresis loops for Sn-15Pb alloy showing effect of resting time t_r on degree of thixotropy. t_u and t_d are respectively time used for ramping-up and ramping-down of shear rate

4

few seconds and the latter a few hundred seconds. In addition, the theoretical analysis also shows that, for a given SSM slurry, deformation under isostructure conditions always results in a constant viscosity, showing no shear thickening behaviour.⁶⁷

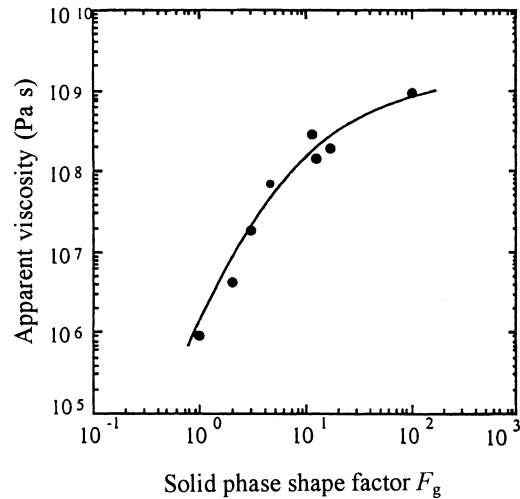
Modelling of continuous cooling

To explain the experimental result on continuous cooling of Sn-15Pb alloy, Joly and Mehrabian¹⁴ applied a standard model for suspensions to correlate the apparent viscosity η to the solid fraction f_s

$$\eta = A \exp \{Bf_s\} \dots \dots \dots (16)$$

where A and B are shear rate dependent coefficients. This equation has also been applied to other alloys.^{37,42}

A more elaborate equation, introducing explicitly the effect of the shear rate γ̇, has been proposed by Turng and Wang¹⁷ to account for the viscosity of continuously cooled Sn-15Pb alloy. Hirai *et al.*⁶⁸



11 Apparent viscosity of Al-7Si-0.6Mg alloy with solid fraction of 0.5 as function of particle shape factor (after Ref. 69): F_g is dimensionless grain-specific shape factor, see equation (20)

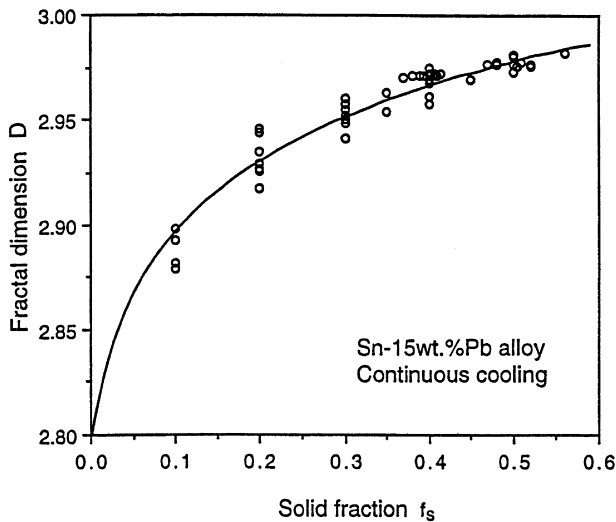
have also proposed, based on an earlier general model of suspensions, a model for the apparent viscosity.

Although the fact that particle morphology has a strong influence on the flow behaviour of SSM slurries is well established (Fig. 11),⁶⁹ the scientific understanding is very limited. The normalised specific surface area³⁹ or the simple shape factor^{69,70} has been used to describe the morphological evolution of solid particles during either a rheological experiment or SSM processing. Qin and Fan⁷¹ have recently used fractal dimension D to quantify the solid particle morphology. The value of D is 3 for perfectly spherical particles, and D decreases with increasing complexity of particle morphology. The authors have derived⁷¹ a mathematical expression for the equivalent solid fraction Φ as a function of D and actual solid fraction f_s

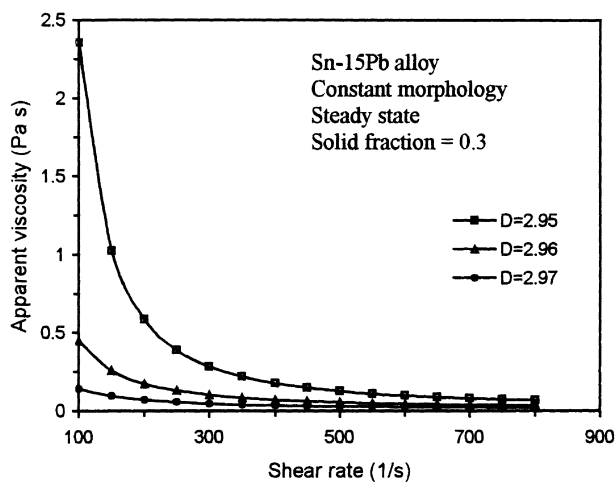
$$\Phi = k(3)k(D)^{-3/D} \left(\frac{N}{Q}\right)^{(3-D)/D} f_s^{3/D} \dots \dots (17)$$

where N/Q is a dimensionless factor.

The microstructural model⁵⁶ was used by Fan and Chen⁷² to estimate the D data from the experimental results on continuous cooling of Sn-15Pb alloys.¹⁴ Within the range of experimental conditions concerned, D is predominately affected by solid fraction or, equivalently, local solidification time, while shear rate and cooling rate have only limited effect on D (see Fig. 12). The microstructural model⁵⁶ was applied to predict the apparent viscosity of SSM slurries with non-spherical particle morphology during continuous cooling and subsequent isothermal holding. Under constant morphology assumption, the shear thinning effect is much more pronounced for SSM slurries with solid particles of lower fractal dimension, i.e. a more dendritic morphology (see Fig. 13), and the degree of thixotropy increases with decreasing fractal dimension of solid particles. In addition, it has also been demonstrated that as a diffusion controlled process, particle spheroidisation takes many thou-



12 Fractal dimension D deduced⁷² from experimental viscosity data from continuous cooling experiments¹⁴ as function of solid fraction



13 Calculated steady state viscosity for Sn-15Pb slurries under constant morphology as function of shear rate⁷²

sands of seconds, and is much slower than the deagglomeration process (a few seconds) and the agglomeration process (a few thousand seconds).

Deformation behaviour of SSM slurries with high solid fractions

Semisolid metal slurries with high solid fractions are characterised by the existence of a solid skeleton, which can be formed by either partial solidification at low temperature or partial remelting at high solid fraction. Owing to its high relevance to the thixoforming process, the deformation behaviour of such high solid fraction slurries has been subjected to both experimental and theoretical studies, but to a much lesser extent than the amount of work done on liquid-like SSM slurries. Several methods have been used to evaluate the flow characteristics of high solid fraction slurries. The most commonly used method is compression between parallel plates.^{25–27} This method is

relatively easy to implement, but the applied shear rate is generally limited to less than 1 s^{-1} . To improve upon this, rapid compression rheometers have been recently developed,^{28,30,73} with which shear rates comparable to thixoforming and shear rate change of 1500 s^{-2} are obtainable. Martin *et al.*⁶⁴ used a Couette rheometer to examine the flow behaviour of Sn–Pb slurries with solid fraction up to 0.6 and shear rates up to 10 s^{-1} . Loue *et al.*³¹ characterised two aluminium alloys at shear rates up to 1000 s^{-1} using a back extrusion technique. A similar technique has also been recently used to characterise partially remelted Sn–Pb alloys.⁷⁴ The experimental results so far have identified the following deformation characteristics:

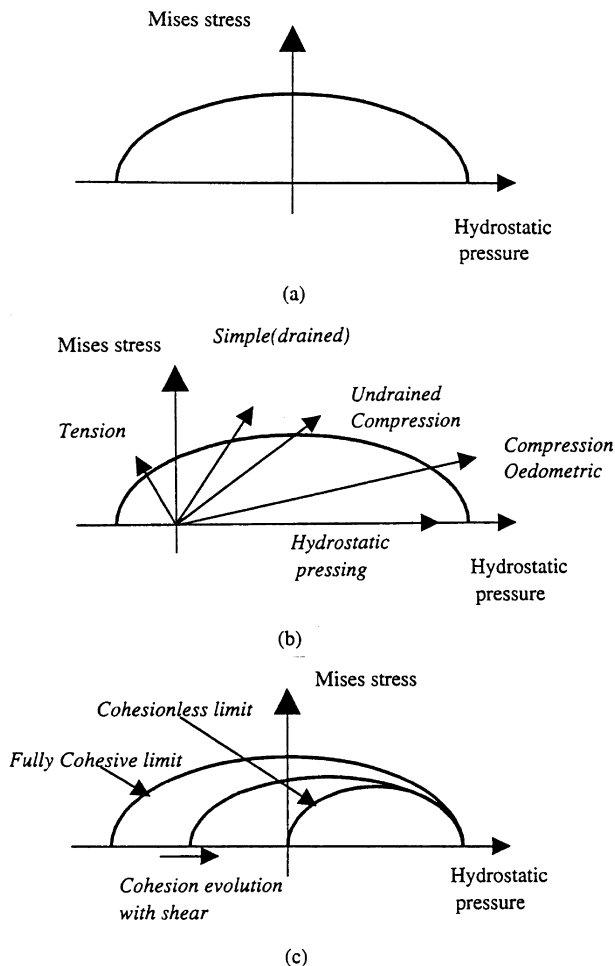
- the existence of large yield stress
- the occurrence of solid phase cracking and liquid phase separation.

Owing to the formation of a solid phase skeleton, the solid phase responds to the macroscopically applied hydrostatic pressure by densification through either particle rearrangement or by slight deformation at the contacts between the solid particles.²⁷ The reduction of the interstitial volume leads to the development of hydrostatic pressure in the liquid phase. The presence of the spatial gradient of hydrostatic pressure in the liquid phase will cause phase separation.⁵² Conditions that promote segregation include:

- low deformation rates (or low die filling rates)
- high pressure gradients, e.g. in the case of filling narrow and long channels
- high fraction of solid
- large and non-spherical particles.

In spite of the importance of understanding the deformation behaviour of SSM slurries to the thixoforming process, due to the complexity involved with both theoretical and experimental studies, modelling work on this aspect started only in recent years.^{50,75,76}

Semisolid slurries with high solid fractions are usually treated as a two phase system in which a solid skeleton is saturated with a near-Newtonian liquid phase.^{50,77–82} These models are aimed at predicting the deformation behaviour of the solid skeleton and the fluid flow through the solid skeleton, and therefore understanding the liquid phase segregation during the thixoforming process. Early work described the flow of the solid skeleton by a yield surface or plastic potential that combines the equivalent stress and hydrodynamic pressure in a symmetric ellipsoidal form (Fig. 14a).^{63,83–86} The flow of the liquid is usually described by Darcy's law and volumetric strain compatibility couples the solid and liquid motions.^{63,84} It was quickly realised that due to the partial level of cohesion, the behaviour of semisolid slurries under tensile and compressive hydrostatic stress is not symmetric and, consequently, asymmetric ellipse models have been proposed and elaborated on the basis of triaxial tests (Fig. 14b).²⁷ To account for the transient behaviour, an asymmetric model with thixotropy has also been proposed (Fig. 14c).⁸⁷ In addition, there have also been models that attempt to address the two phase problem by introducing a relative motion of the liquid with respect to the solid, but ignoring any resistance to pressure offered by the solid phase.⁷⁹ In this case, the pressure dependence of viscosity is



a symmetric ellipse; b asymmetric ellipse; c thixotropic asymmetric ellipse

14 Two phase models (after Ref. 52)

ignored and the validity of the model is limited to low solid fraction.

Microstructural evolution during slurry preparation

The ideal microstructure for a semisolid slurry before the component shaping process would be an accurately specified volume fraction of fine and spherical solid particles uniformly dispersed in a liquid matrix. A primary goal of slurry preparation is to create such a structure to ensure the favourable rheological characteristics to facilitate the subsequent component shaping process. Technically, this structure can be achieved by a number of different techniques. They can be categorised into two different approaches. The first approach involves partial solidification of a melt under forced convection induced by either electromagnetic or mechanical stirring, or partial solidification under the influence of an external field, such as ultrasonic vibration or pulsed electrical current. The second approach involves partial remelting of solid feedstock material, which has been solidified earlier under specific conditions or worked thermo-mechanically. In this section, the scientific understanding of microstructural evolution during slurry preparation by those two approaches is reviewed. The

section starts with the techniques available for describing and quantifying the slurry microstructures.

Microstructural characterisation

For a fixed alloy composition, complete description of the microstructure of semisolid slurry involves quantifying the volume fraction, size, shape, and distribution of the solid particles. This is normally done with a solid material quenched from the semisolid temperature. So far, nearly all the quantifications have been done on a two-dimensional (2D) polished surface using conventional metallographical techniques.⁸⁸ This might be satisfactory for measuring particle size and volume fraction, but it is inadequate for measuring particle shape and distribution. Solid particles in a semisolid slurry are usually not spherical, but have a complex shape; more importantly, solid particles tend to agglomerate forming complex 3D clusters. In the following subsections, the techniques available for quantification of the above microstructural parameters are summarised.

Measurement of solid volume fraction

Accurate knowledge of solid fraction in semisolid slurry is critical for both scientific understanding and effective process control. For a given alloy, solid fraction can only be defined uniquely at a given temperature under equilibrium conditions. In any other case, it depends on the prior thermal history. Solid fraction can be evaluated either directly or through its effect on the physical properties. The following methods have potential for the determination of solid fraction.⁸⁹

- utilisation of thermodynamic data (equilibrium phase diagram)
- thermal analysis techniques
- quantitative metallography on microstructures quenched from the semisolid state
- ultrasonic monitoring (measurement of propagation speed of ultrasonic waves)
- measurement of electrical resistivity/ magnetic permeability
- measurement of mechanical properties (by indentation and extrusion etc.).

The last three methods not only require calibration, but also there is no unique correlation between the characteristic parameter measured and the solid fraction because wave propagation and electrical, magnetic, and mechanical properties of semisolid alloys depend strongly on microstructure, especially on the connectivity and the distribution of the solid phase. For these reasons, the first three methods seem to be more practical for the determination of solid fractions. Although these three methods are all approximate, each one has its own significance and unique advantages: the use of thermodynamic data is a fast tool for alloy design, thermal analysis provides one with comparable information and reveals the prior thermal history of an alloy, and quantitative microscopy after quenching reveals more microstructural information, such as morphology and distribution of the solid phase in the semisolid state.

Particle morphology

Three-dimensional structures are usually characterised by measurement on 2D sections. Using image

analysing systems, one can measure number, interface length, and areas of objects.⁸⁸ To quantify particle morphology, an object-specific shape factor F is usually used. Two different expressions for the shape factor F have been used in the literature

$$F_1 = \frac{4\pi A}{P^2} \quad \dots \quad (18)$$

$$F_2 = \frac{P^2}{4\pi A} \quad \dots \quad (19)$$

where A and P represent the area and perimeter of the object, respectively. In both cases, $F = 1$ refers to a perfectly spherical morphology, while for very complex shapes, $F_1 \rightarrow 0$ and $F_2 \rightarrow \infty$. Equations (18) and (19) are generally adequate for morphological quantification of compact and well dispersed particles. However, for more open particles such as dendrites, a 2D cut of such a particle gives rise to several apparently isolated images, which are usually treated by an image analysing system as several individual particles. Thus, an average of object-specific shape factor may not reflect the true complexity of particles with an open structure.

Loue and Suery⁷⁰ introduced a modified dimensionless grain-specific shape factor F_g , as defined by the following equation

$$F_g = \frac{1}{6\pi f_s} \frac{S_V^2}{N_A} \quad \dots \quad (20)$$

where S_V is the solid/liquid interfacial area per unit volume and N_A is the number of grains per unit area. The authors have demonstrated that F_g describes more accurately the particle morphology than does F (equations (18) and (19)). However, the parameter N_A in equation (20) measured by image analysis may not accurately reflect the true particle density.

In most cases of SSM processing, the geometry of the solid phase is irregular rather than spherical. By noting that the dendrite is a typical fractal structure⁹⁰ and that the irregular geometry of solidifying crystals can be quantitatively characterised by the fractal theory,⁹¹ Qin and Fan⁷¹ proposed describing the morphology of equiaxed dendrites using the fractal dimension D . The fractal dimension of a solid particle can be measured by many different methods, such as slit island analysis,⁹¹ profile analysis,⁹² direct surface area analysis,⁹³ and variation-correlation analysis.⁹⁴ It has been shown recently that for a well developed dendrite under diffusion controlled condition $D = 2.5$ (Ref. 95), while for a perfectly spherical particle $D = 3$. The concepts of fractal dimension D and the equivalent solid fraction Φ have been successfully applied to model the rheological behaviour of SSM slurries with non-spherical particles.⁷²

Particle distribution

For a given slurry system with a fixed solid fraction, particle distribution in the liquid matrix has a pronounced influence on the slurry rheology and has a strong implication regarding the quality of the SSM processed components. Despite such importance, currently there is no mature method for the quantification of particle distribution in the liquid matrix.

To model the deformation behaviour of SSM slurries, a structural parameter s has often been used to describe the particle distribution.^{18,49,54} In a completely agglomerated state $s = 1$, while for a completely dispersed state $s = 0$. Thus, $0 \leq s \leq 1$. However, this parameter is not well defined and is extremely difficult to measure experimentally.⁹⁶

Another way to describe the particle distribution in semisolid slurry is to use the stereological parameter 'contiguity volume', which was originally developed^{97,98} by Gurland and Lee and defined by the following equation

$$f_{sc} = C_s f_s \quad \dots \quad (21)$$

where f_{sc} is the contiguity volume and C_s is the contiguity of the solid phase. Uggowitzer and co-workers^{99,100} recently applied the contiguity volume to characterise the particle distribution in SSM slurries. Their experimental results showed that the contiguity volume should not exceed a value of 0.3 for maximum thixotropic material flow; however, on the other hand, a value below 0.1 is not suitable for thixofforming because of the poor stability of the slug for handling. They also demonstrated that the contiguity volume could be improved by addition of minor alloying elements.¹⁰⁰

More recently, Chen and Fan⁵⁶ proposed using the average number of particles in agglomerates as a parameter to describe the degree of particle agglomeration in SSM slurry. Obviously, this parameter can be determined experimentally using a standard metallographical method. The concerned parameter has been successfully used for the development of a microstructural model for SSM slurries.⁵⁶ The authors have demonstrated that the viscosity of a specified SSM slurry has a one-to-one correspondence to the average number of particles in agglomerates.

Most of the experimental investigations of semisolid microstructure are based on 2D observations that do not allow straightforward conclusions about the exact state of agglomeration. Attempts have been made to obtain 3D images by serial sectioning.^{40,101-104} However, serial sectioning is very time consuming and, more importantly, this technique may not be adequate to characterise the degree of agglomeration in slurries with fine particle size due to its low resolution (about 20 μm). More recently, advanced techniques, such as electron back scattered diffraction^{96,105} and X-ray microtomography,⁹⁶ have been used.

Solidification behaviour under forced convection

Nearly all the alloys of commercial importance solidify dendritically, with either a columnar or an equiaxed dendritic structure.¹² During dendritic solidification of castings and ingots, a number of processes take place simultaneously within the semi-solid region. These include crystallisation, solute redistribution, ripening, interdendritic fluid flow, and solid movement. The dendritic structure is greatly affected by the interdendritic flow and solid movement, which, in conventional solidification, is caused by internal factors such as density difference and heterogeneous distribution of temperature. The effects

of those processes on the solidified microstructures have been reviewed previously by Flemings,¹⁰⁶ and more recently by Boettinger *et al.*¹⁰⁷ In this review, discussion is confined to forced convection with a much larger intensity.

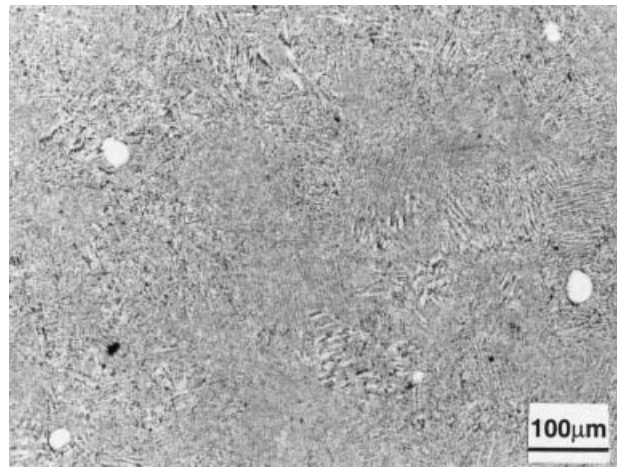
Phenomenology

In studying conventional solidification, transparent organic alloys have been intensively used to investigate the solidification behaviour at microstructural level by direct observation. However, this may not be possible for solidification under forced convection, even using organic analogue, due to the blurred image caused by intensive stirring.¹⁰⁸ For this reason, current understanding of the solidification behaviour under forced convection is obtained indirectly by examination of the final solidified microstructures.

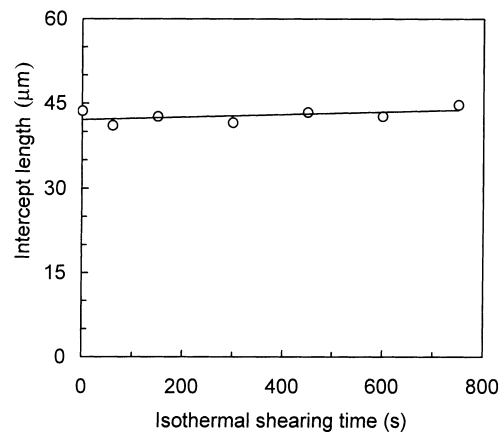
It has been conclusively established from experimental observations that solidification under melt stirring produces non-dendritic structures, as has been summarised in previous reviews.^{12,13} The early work by Spencer *et al.*² and Joly and Mehrabian¹⁴ on the Sn–Pb system using rotational rheometers confirmed that the solid phase in the semisolid state has either a degenerated dendritic structure or rosette morphology. With prolonged stirring time, such particles change to a more or less spherical morphology containing entrapped liquid by a ripening process. Increasing the shear rate accelerates this morphological transition and reduces the amount of entrapped liquid inside the solid particles.¹⁴ The rosette morphology of solid particles has also been observed in many stirred alloys by other investigators^{109–112} using rod and impeller types of stirrer. Later work on solidification under magnetohydrodynamic (MHD) stirring confirmed the formation of a fine and degenerated dendritic structure (*see* summary in Refs. 12, 13).

For Al–Cu alloys, Vogel *et al.*¹⁰⁹ observed that with applied shear the primary particles grow as rosettes until a certain limit beyond which further growth does not occur but subsequent solidification takes place by formation of more (new) particles. However, quenching the liquid 1 min after the initiation of solidification and counting through the ingots showed equivalent numbers of growth centres in stirred and unstirred melt. Molenaar *et al.*¹¹³ observed rosette type and radially grown cellular particles in intermediate and fast cooled and sheared Al–Cu alloys. At slow cooling rate, rosettes were observed. Similar to the observation by Vogel *et al.*,¹⁰⁹ stirring speed was not found to influence the particle density or size significantly. The cell spacing was considerably greater than the secondary dendrite arm spacing from unstirred melt, indicating that stirring promotes crystal growth. Smith *et al.*¹¹⁴ studied the microstructural evolution during solidification of a stirred Al–19Si alloy. They found that with increasing shear rate the average particle diameter decreases, while the particle density increases. It should be mentioned that in all those investigations on melt stirring the flow conditions are generally characterised by largely laminar flow with relatively low shear rate achieved by using rod or simple impeller as stirrer.

Ji and Fan^{115,116} studied the effect of turbulent flow on the solidification morphology of Sn–15Pb alloy

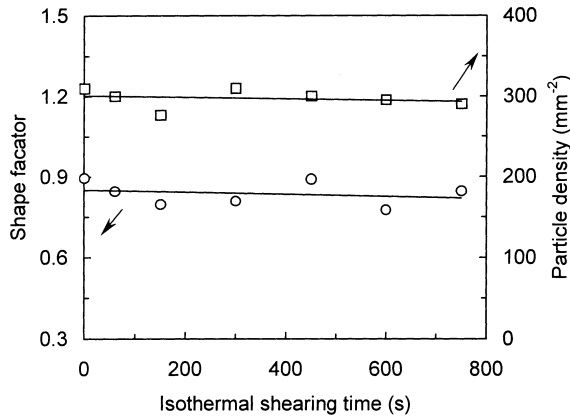


15 Quenched microstructure of Sn–15Pb alloy at early stage of solidification in twin screw rheomoulding (TSRM) machine¹¹⁵



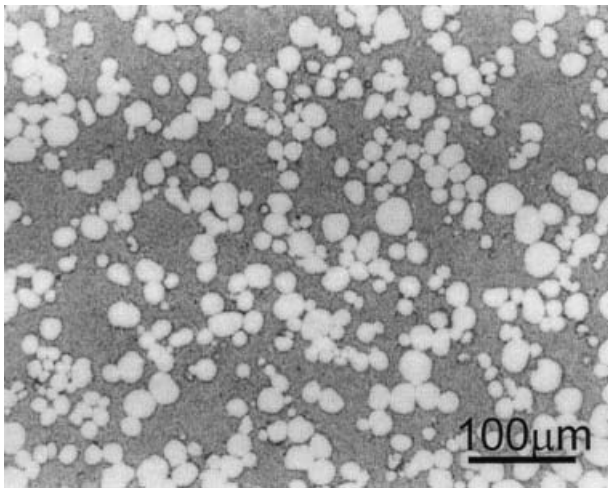
16 Effect of isothermal shearing time on intercept length of primary particles in Sn–15Pb alloy processed in TSRM machine¹¹⁶

using a laboratory scale twin screw rheomoulding (TSRM) machine developed recently. They found that under intensive turbulent flow, the solidification morphology is spherical even at the very early stage of solidification (Fig. 15).¹¹⁵ Their isothermal shearing experiments showed that the size, shape factor, and density of the solid particles are almost constant with increasing isothermal shearing time (Figs. 16, 17).¹¹⁶ This is in good agreement with the early work by Ryoo and Kim¹¹⁷ on Mg–Al–Zn–Si alloys. The particle size distribution was found to be very close to that of randomly dispersed monospheres.¹¹⁸ They also found that in the low shear rate region, increasing shear rate increases particle density and decreases particle size, while in the high shear rate region both particle size and density reach a plateau. This work has, for the first time, demonstrated the importance of turbulent flow as regards the formation of spherical morphology, i.e. intensive turbulent flow stabilises the solid/liquid interface. Following this work, Das *et al.*¹¹⁹ have recently conducted a systematic study on the growth morphology under various fluid flow conditions using different stirring devices. Cylindrical rod with low rotation speed creates essentially simple



17 Effect of isothermal shearing time on shape factor F_1 (see equation (18)) and particle density of primary particles of Sn-15Pb alloy processed in TSRM

5

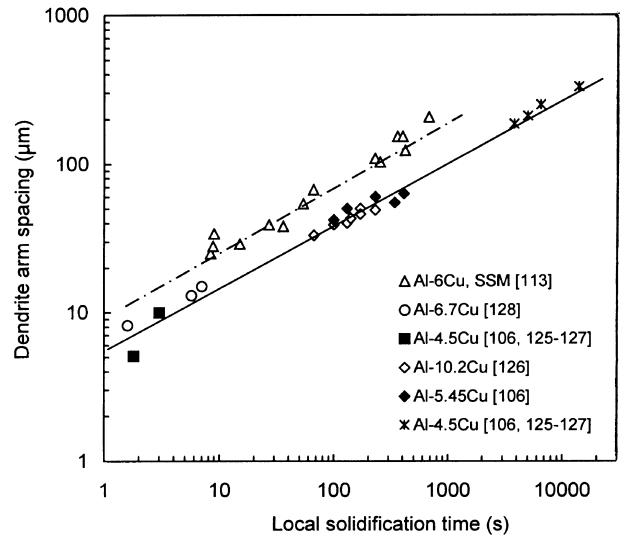


18 Microstructure of Sn-15Pb alloy solidified under high intensity of turbulent flow in TSRM machine¹¹⁹

laminar flow, propellers induce predominantly laminar flow with limited degree of turbulence, while a TSRM machine produces basically turbulent flow. The important findings from these investigations¹¹⁵⁻¹¹⁹ are:

- Turbulent flow is crucial for the formation of spherical particles during solidification under forced convection (see Fig. 18).
- The observed rosette and spherical particle morphologies are more likely to be a growth phenomenon during solidification under forced convection.

Furthermore, it is generally observed that melt stirring accelerates crystal growth during solidification. Under full diffusion control, spheroidisation of the initially dendritic structure in the semisolid state usually takes a few tens of minutes or even up to a few hours,¹²⁰⁻¹²³ while formation of spherical particles takes only a few minutes under predominantly laminar flow conditions.¹¹⁷ The recent work by Ji and Fan¹¹⁶ has demonstrated that this process requires only a few seconds under intensive turbulent flow conditions, even with a fully dendritic structure before stirring.¹²⁴



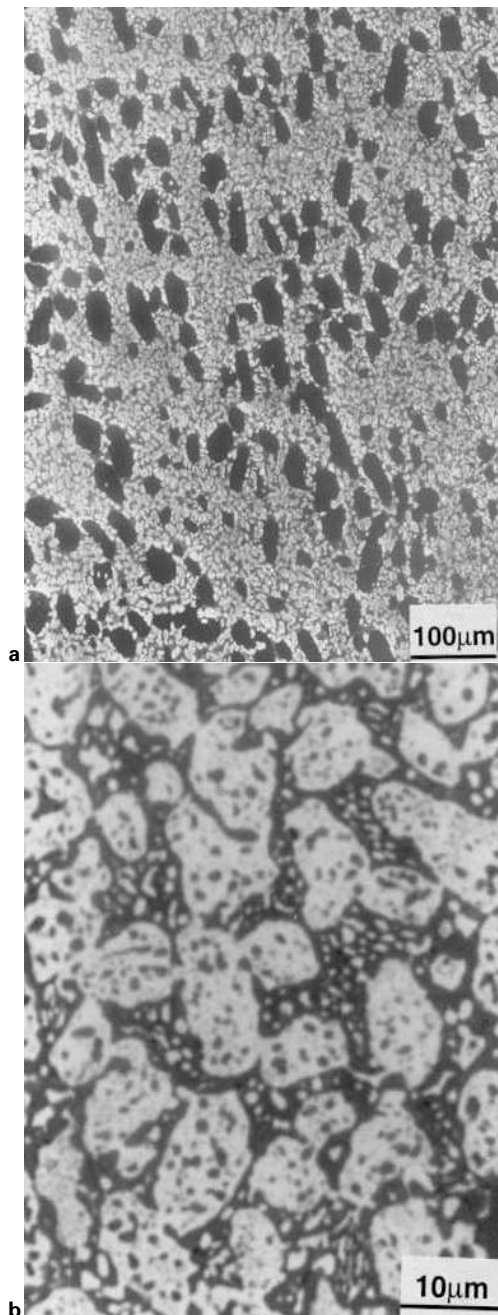
19 Experimental correlation of secondary dendrite arm spacing with local solidification time for Al-Cu alloys solidified with¹¹³ (----) and without^{106,125-128} (—) melt stirring

Figure 19 compares the growth rate of Al-Cu alloys under stirred¹¹³ and unstirred^{106,125-128} conditions. Figure 19 shows that for the same local solidification time, dendritic arm spacing with melt stirring is consistently larger than without melt stirring.

Another interesting and potentially important phenomenon created by melt stirring was found in eutectic alloys. A laboratory scale TSRM machine was used to shear a Sn-38.1Pb eutectic alloy during continuous cooling from the fully liquid state.¹²⁹ It was found that substantial undercooling could be obtained under high shear rate and high intensity of turbulence. The typical microstructure obtained by quenching from the undercooled state is presented in Fig. 20. In contrast to the microstructure formed by coupled growth during conventional solidification, Fig. 20a shows a hypereutectic type structure (dark particles are primary tin phase), indicating the suppression of the formation of the lead phase under intensive shear. From Fig. 20a, it appears that the alloy was quenched from the semisolid state, where the primary tin particles (dark particles) are dispersed in a metastable lead rich liquid phase. Upon quenching, the remaining liquid phase solidifies into a two phase structure, where both the tin rich (dark) and lead rich (bright) phases contain substantial amounts of fine precipitates of the other phase (Fig. 20b). This work¹²⁹ has clearly demonstrated that intensive shearing can create metastable phenomena during solidification.

The experimental findings so far on solidification under forced convection can be summarised as follows:

- Forced convection promotes finer particles with a non-dendritic morphology.
- Forced convection accelerates crystal growth.
- Turbulent flow influences much more significantly the particle size and morphology than does laminar flow.



a at low magnification; b microstructure of matrix

20 Microstructure of undercooled Sn-38.1Pb eutectic alloy after shearing in TSRM machine¹²⁹

- With increasing shear rate and intensity of turbulence the particle morphology changes from dendritic to spherical via rosette.

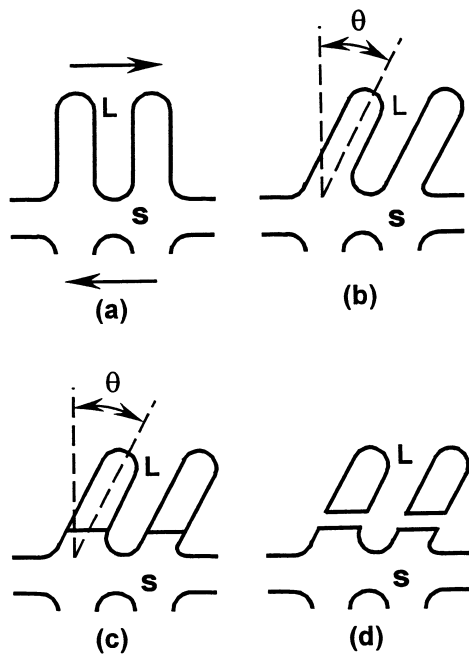
Mechanisms for formation of non-dendritic structure

To explain the observed fine particle size and non-dendritic morphology under forced convection several mechanisms have been proposed. These include: dendrite arm fragmentation, dendrite arm root remelting, and growth controlled mechanisms. Any proposed mechanism has to address two basic aspects of solidification under forced convection, namely, grain refinement and morphological transition. It should

be mentioned that solid particles with any morphology in the semisolid state would, with prolonged isothermal holding, spheroidise by a ripening process under the driving force for reduction of interfacial free energy, even under full diffusion control. The discussions in this paper will be confined to the process from nucleation to the stage when solid fraction reaches a defined value. Structural evolution during isothermal holding without melt stirring will be addressed in a later section.

Vogel and Cantor¹³⁰ developed a boundary layer model to investigate the effects of stirring on the growth of spherical particles from the melt. The effect of stirring was introduced by the use of stagnant thermal and diffusional boundary layers. The particle growth rate and the interface stability are determined by solving Laplace equations for the thermal and solute profiles. They found that stirring destabilises the solid/liquid interface for both low and high mobility interfaces. Further analysis by the same authors for dendritic solidification under fluid flow revealed that stirring increases the dendrite tip velocity and decreases the tip radius.¹³¹ The apparent contradiction to the observed experimental results prompted Vogel¹³² to suggest that the non-dendritic microstructure observed during rheocasting might be a result of overlapping diffusion fields of a large number of growing particles. A high density of nuclei growing even under full diffusion control can give rise to stable non-dendritic growth with shape stability due to reduced concentration gradients arising out of overlapping diffusion fields.¹³³

To explain the observed grain refinement by melt stirring, Vogel *et al.*¹⁰⁹ have proposed a dendrite arm fragmentation mechanism to account for grain multiplication, as schematically illustrated in Fig. 21.¹³⁴ They suggested that dendrite arms bend plastically under the shear force created by melt stirring. Plastic bending introduces large misorientations into the dendrite arms in the form of 'geometrically necessary dislocations'. At high temperature, such dislocations rearrange themselves to form high angle grain boundaries through recrystallisation. Any grain boundary with an energy greater than twice the solid/liquid interfacial energy is then wetted by liquid metal, resulting in the detachment of dendrite arms. Observation of bent (but unrecrystallised) regions and low angle/coincidence site boundaries in stir cast structures were presented^{109,111,134,135} in support of the theory. However, the presence of a high proportion of low angle grain boundaries in the rheocast samples has been challenged by the recent work by Niroumand and Xia,^{103,104} in that the particles with low angle grain boundaries observed on a 2D section could be parts of a single dendrite or rosette in 3D. This would imply that the higher than average proportion of low angle grain boundaries would not occur in slurry containing spherical particles, as indeed observed by Sannes *et al.*¹⁰¹ using the electron back scattered diffraction technique in a magnesium alloy. Another point to be clarified is whether alloys have such dynamic recrystallisation behaviour. Doherty *et al.*¹³⁴ performed hot bending tests on single crystals of aluminium and observed the formation of high and low angle grain boundaries for



a undeformed dendrite; b after bending; c formation of high angle grain boundary by recrystallisation; d fragmentation through wetting of grain boundary by liquid metal

21 Schematic illustration of dendrite arm fragmentation mechanism (after Ref. 134)

bending angles in excess of 55° . However, a question that needs to be answered is whether melt shearing can impose such high bending moment on the dendrite arms.

Following the early suggestion by Flemings,¹² Hellawell¹³⁶ suggested that secondary dendrite arms can detach at their roots because of remelting due to solute enrichment and thermosolutal convection. To explain the crystal multiplication in semisolid processing, the author suggested that temperature fluctuations in the MHD rheocasting process play a significant role in the structural evolution. A continuous nucleation might take place in the absence of a distinct recalescence where each volume element of the liquid passes periodically through different temperature zones. To explain the non-dendritic structure, the author suggested that vigorous stirring prevents the establishment of stable diffusion fields for continued dendrite evolution. Eventually, smooth rounded shapes are expected out of solidification.

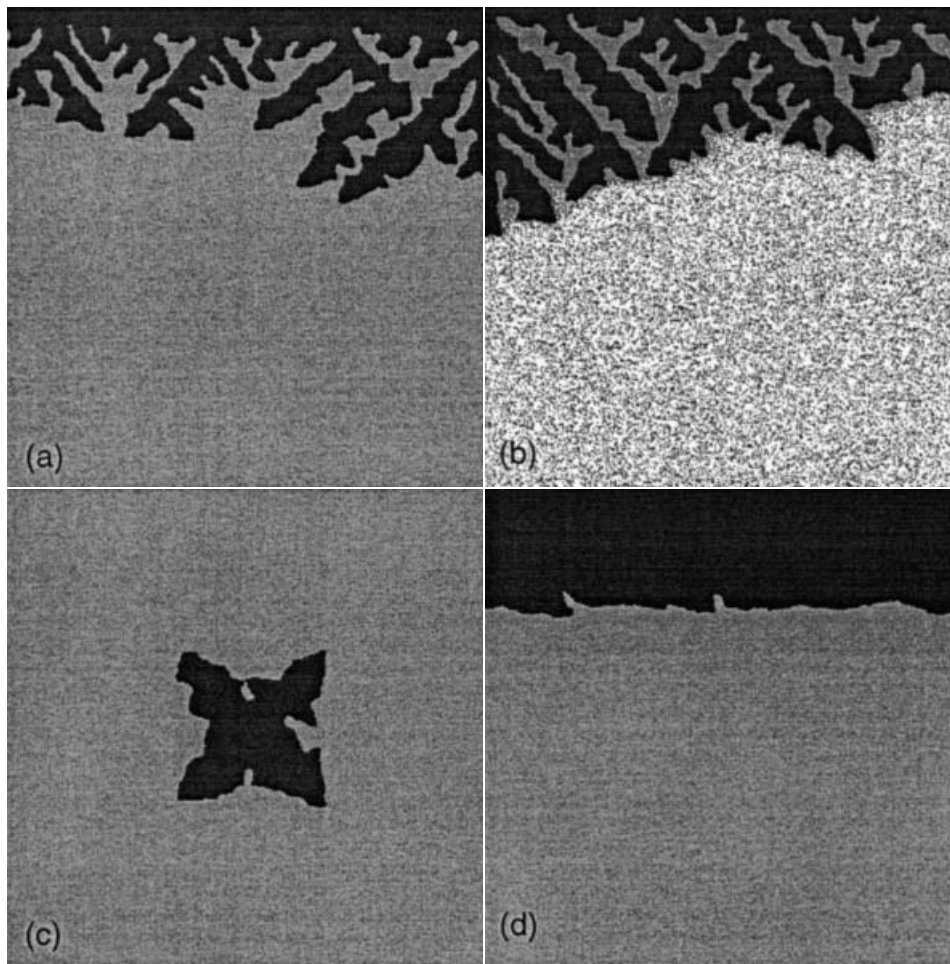
It should be remembered that the actual conditions obtaining in the melt under stirring are difficult to visualise. The inability to observe the microstructural formation during the early stages of solidification (during nucleation and early growth) adds to the difficulty of direct correlation of morphological development with a possible explanation. Most of the proposed theories, therefore, are based on indirect observations. Nucleation is almost certain to be heterogeneous, and there is no indication that stirring induces homogeneous nucleation. However, multiple nucleation due to periodic passage through different temperature zones as described by Hellawell¹³⁶ is unlikely in the TSRM process developed by Fan *et al.*¹³⁷ The very intense turbulent flow between the

closely meshed twin screws is able to homogenise instantaneously the melt with respect to both temperature and composition (see 'Rheomoulding' below). The dendrite fragmentation mechanism attempts to rationalise the final microstructural features observed in the solid, but the biggest question remaining to be answered is how likely is it that shearing can exert such a high bending moment to small dendrite arms to fracture them. According to the theoretical work by Vogel,¹³² the microscale of turbulence has to be of the order of particle size for the viscous forces to be active on bending the dendrite arms, and that is possible only at a very high shear rate. Moreover, fragmented dendrite arms are expected to grow dendritically in the melt, at least during the initial period of growth, until impingement of diffusion fields occur. Figure 15 shows the microstructure of Sn-15Pb alloy during the very early stages of solidification in the TSRM machine.¹¹⁵ Primary particles are very few in the microstructure and widely apart, but still the growth morphology is spherical. Furthermore, both fragmentation and remelting mechanisms do not offer an explanation for the rosette type morphology formed under low shear.

In recent years, there has been an increasing belief that the evolution of particle morphology under forced convection is a growth phenomenon. By coupling a free boundary model of dendrite formation with a cellular automaton model of rosette formation, Mullis¹³⁸ proposed that dendrite bending could give rise to rosette formation without any need to invoke mechanical effects. However, the predicted extensive dendritic arm bending by this model has never yet been observed.

The intensity of shear is expected to determine the fluid flow characteristics in the melt. But none of the proposed theories has, so far, tried to rationalise the observation on the basis of fluid flow characteristics. At low and intermediate shear rate the flow is essentially laminar, and it is unlikely that a laminar flow can interact with the secondary dendrite arms to exert a bending moment. In fact, under a laminar flow, the secondary dendrite arms are not expected to experience any relative fluid motion at the solid/liquid interface. But the intensity of laminar flow will certainly determine the thickness of diffusion boundary layer around a growing particle, and therefore determine the growth morphology of the solid. At a high shear rate, the flow characteristics change to turbulence, and liquid penetration into the interdendritic region is likely to take place. This would bring about a significant change in the solidification structure, as solute transport away from the secondary dendrite arms would take place.

Based on the above considerations, Qin and Fan¹³⁹ have recently elaborated the boundary layer model to account for liquid penetration into the interdendritic region under turbulent flow. Their numerical analysis using a boundary element method has shown that the penetration of the liquid phase into the interdendritic region results in a relative change in growth rate along the solidification interface. With increasing intensity of turbulent flow, the local growth rate increases laterally and at the root of dendrite arms, resulting in the formation of rosettes and even



a pure diffusive flow; *b* laminar flow (from left to right); *c* rotating particle in laminar flow; *d* penetration of interdendritic region by turbulent flow

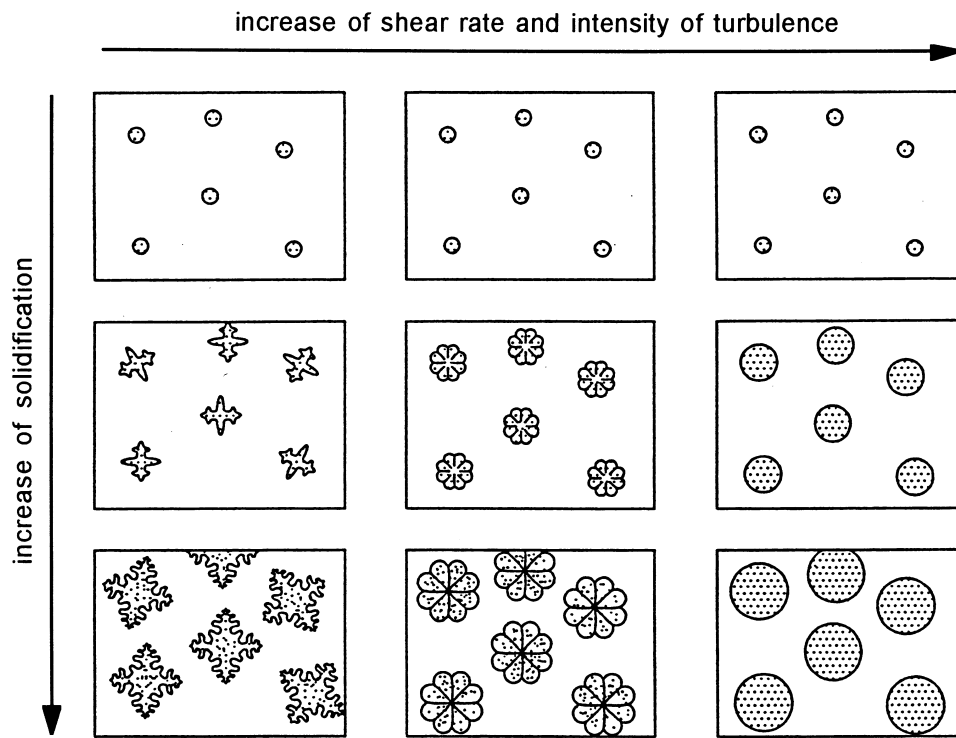
22 Monte Carlo simulation showing effect of fluid flow on growth of primary phase¹⁴⁰

spheres at sufficient intensity of turbulence. They concluded that turbulent flow stabilises the solidification interface. Their analysis also indicates that turbulent flow can enhance crystal growth more effectively than laminar flow.

More recently, Das *et al.*¹⁴⁰ have developed a Monte Carlo technique to simulate the microstructural evolution under forced convection. The model takes into account diffusive and forced fluid flow, the kinetics of atomic attachment at the solid/liquid interface, and structural modification under the influence of capillarity. It has been shown that at low shear rate, where the flow characteristics are laminar, growth of dendrite from a substrate is enhanced (compare Fig. 22*a* and 22*b*), which is in agreement with the earlier prediction by Vogel and Cantor.¹³⁰ However, the Monte Carlo simulation shows further that isolated particles rotating in a laminar flow grow with rosette type morphology (Fig. 22*c*). This explains why, at a low shear rate, rosette type morphology is observed instead of dendritic morphology during solidification under forced convection. At a higher shear rate, where the nature of fluid flow is expected to be turbulent, it has been shown that the growth morphology is compact with a stable planar front from the initiation of solidification (Fig. 22*d*). The interaction of turbulent flow with the interdendritic

region, transporting away the rejected solute atoms, stabilises the solid/liquid interface and explains why spherical particles are normally observed when the melt is sheared at a very high intensity.

The experimentally observed grain refinement under high shear rate and high intensity of turbulence was explained by a copious nucleation mechanism.^{116,119} Under the intensive mixing action offered by the TSRM machine, both temperature and composition fields inside the liquid alloy are extremely uniform. During the continuous cooling under forced convection, heterogeneous nucleation takes place at the same time throughout the whole liquid phase. Compared with conventional solidification, the actual nucleation rate in the rheomoulding process may not be increased, but all the nuclei formed will survive due to the uniform temperature field, resulting in an increased effective nucleation rate. In addition, the intensive mixing action will disperse the clusters of potential nucleation agents, giving rise to an increased number of potential nucleation sites. In fact, this situation not only occurs under intensive turbulent flow in the rheomoulding machine, but also applies to nucleation under forced convection in general. However, it seems that laminar flow is much less effective for homogenising the temperature and composition and for dispersing the potential nucleation



23 Schematic illustration of morphological transition from dendritic to spherical via rosette with increase in shear rate and intensity of turbulence¹¹⁶

agents. Consequently, laminar flow is less powerful for structural refinement and spheroidisation of the solid particles, which is in good agreement with the experimental observations described in the previous sections.

The understanding of the microstructural evolution obtained from the above investigations^{116,119,139,140} can be schematically illustrated as in Fig. 23 and summarised as follows:

- Forced convection promotes crystal growth due to enhanced mass transport during solidification.
- Laminar flow changes the normal dendritic growth morphology to rosette, while turbulent flow changes the growth morphology from rosette to sphere.
- It appears that the observed rosette and spherical morphologies under forced convection are more likely to be a growth phenomenon rather than resulting from a mechanical fragmentation mechanism.
- The structural refinement under intensive stirring is most probably caused by a copious nucleation mechanism, which is facilitated by homogeneous temperature and composition fields and well dispersed heterogeneous nucleation agents. However, at lower shear rates, the dendrite arm remelting^{12,136} and fragmentation¹⁰⁹ mechanisms noted above may also be of significance.

Structural evolution during partial remelting and isothermal holding

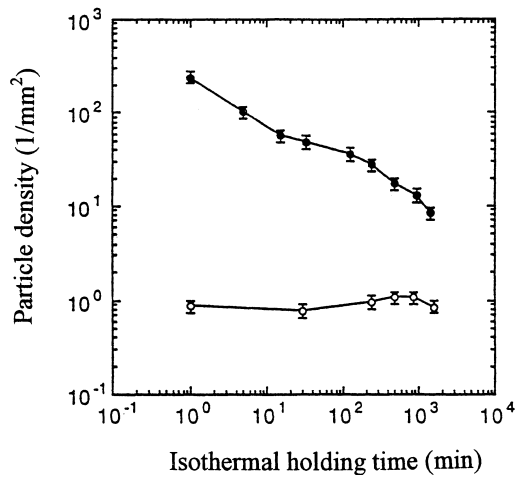
Remelting of alloys is of importance to various industrial processes, such as thixoforming and recycling procedures. However, from a fundamental point of view, remelting has been much less frequently studied

than solidification. In contrast to solidification from the liquid state, the variety of solid state structures that can be encountered during remelting give rise to a rich range of melting behaviour. As a result, the microstructural evolution during remelting and subsequent holding before thixoforming has received only limited attention. In this section, the information available in the literature is summarised.

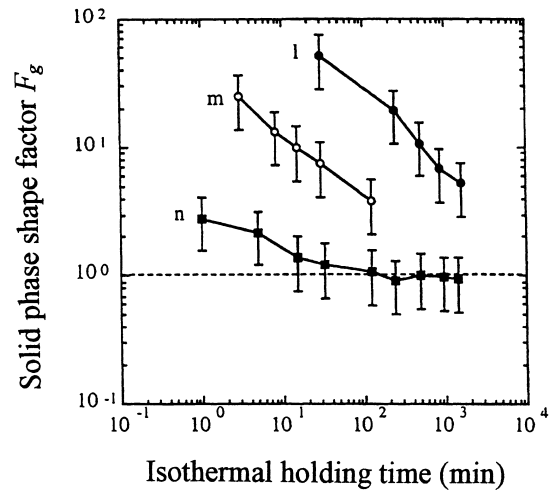
Phenomenology

Slug reheating is a critical stage in the thixoforming process. Its purpose is not only to obtain the desirable nominal liquid fraction, but also to ensure transformation of the solid phase to a spheroidal morphology with fine particle size. The driving force for such morphological evolution in the semisolid state is the reduction of the interfacial energy between the solid and liquid phases. Microstructural evolution during reheating is therefore a diffusion controlled process. On the one hand, the holding time should be long enough to complete the morphological transition from dendritic (or rosette) to spherical, but, on the other hand, the holding time should be short enough to prevent excessive grain growth, which is detrimental to the mechanical properties of thixoformed parts. Consequently, the reheating process needs to be optimised to achieve the most desirable slurry characteristics for thixoforming. Understanding the structural evolution would be a critical step towards such optimisation.

The kinetics of structural evolution during isothermal holding in the semisolid state has been subjected to a number of studies, e.g. Refs. 70, 75, 141–143. Sannes *et al.*¹⁰¹ investigated the structural evolution of semisolid ZE33 magnesium alloy at different solid fractions. They found that the coarsen-



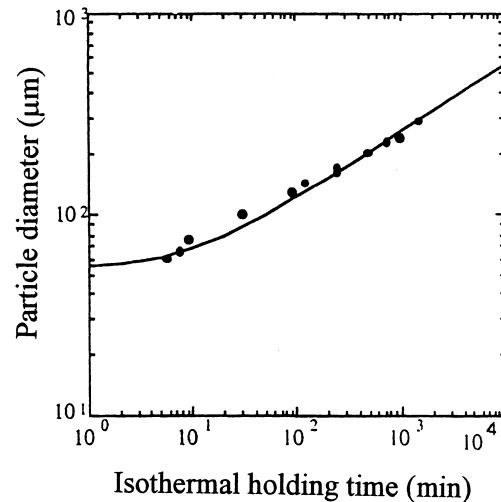
24 Particle density N_A as function of isothermal holding time during partial remelting at 580 °C ($f_s = 0.45$) of conventional, initially globular (\circ) and MHD stirred, initially dendritic (\bullet) Al-7Si-0.6Mg alloy (after Ref. 70)



25 Particle shape factor F_g (see equation (25)) as function of holding time at 580 °C ($f_s = 0.5$) for Al-7Si-0.6Mg alloy obtained by classical continuous casting, without (l) and with (m) grain refining, and by MHD stirring (n) (after Ref. 146)

8

ing kinetics follows the Lifshitz–Slyozov–Wagner (LSW) theory^{144,145} and that the coarsening rate increases with decreasing solid fraction. Based on the experimental results, the authors proposed that at high solid fraction, growth by coalescence ripening makes a major contribution to the total microstructural coarsening in the semisolid state, while at low solid fraction, Ostwald ripening is the dominant mechanism for structural coarsening. Loue and Suery⁷⁰ studied the influence of thermomechanical history on the microstructural evolution of A357 alloy during partial remelting and isothermal holding. They found that during the coarsening process, particle density for the initially globular structures decreases with increasing isothermal holding time, while that for initially dendritic structures remains fairly constant, as shown in Fig. 24.⁷⁰ They also found that longer solidification time and smaller initial grain size accelerate the coarsening kinetics. The effects of initial particle morphology on the coarsening process were investigated by Blais *et al.*¹⁴⁶ During isothermal holding in the semisolid state, regardless of the initial particle morphology, the solid phase always evolves towards a spherical morphology. However, the kinetics of such evolution is governed by the initial microstructure; as shown in Fig. 25, the larger the initial shape factor F_g , the faster the kinetics for spheroidisation, and the longer the holding time required to obtain spherical particles. The kinetics of coarsening of a MHD stirred A357 alloy follows the prediction of Ostwald ripening (Fig. 26). The work by Hong *et al.*¹⁴⁷ on SiC particulate reinforced magnesium alloy metal matrix composites (MMCs) indicated that, during coarsening, the presence of ceramic particulates leads to fine globules of the solid phase, and finer globules are achieved with increasing ceramic volume fraction. They also found that the coalescence is also reduced, since the globules are more isolated with respect to each other by the presence of ceramic particulates in the intergranular region.



26 Average particle size as function of holding time at 580 °C ($f_s = 0.5$) for Al-7Si-0.6Mg alloy obtained by MHD stirring: solid line represents predictions by LSW theory (after Ref. 146)

Another phenomenon observed during microstructural coarsening is the entrapped liquid inside the solid particles. Several authors indicated that coalescence of dendrite arms is responsible for the presence of the entrapped liquid (e.g. Refs. 120, 128), but only a few investigations have been performed on the evolution of the entrapped liquid during isothermal holding in the semisolid state.^{75,120,142} Based on the available experimental results, it appears that both Ostwald ripening and particle coalescence contribute to the process of entrapping liquid, but with opposite effects. On the one hand, Ostwald ripening leads to a loss of entrapped liquid, since the small particles with entrapped liquid will dissolve and the entrapped liquid will join the bulk liquid. On the other hand, coalescence of complex shaped particles results in liquid entrapment.^{75,120,128,142} In the latter

case, the liquid entrapped in the solid particle will remain entrapped. This makes the evolution of entrapped liquid rather complex, especially during short holding time.⁷⁵

Plastic deformation before reheating has been found to be an important factor as regards the coarsening kinetics. Loue and Suery⁷⁰ found that cold working before partial remelting of A356 alloy allows the most rapid globularisation of the solid phase once the threshold for crystallisation is surpassed. Similar work by Yunhua *et al.*¹⁴⁸ on Zn–12Al alloy showed that increasing the amount of plastic deformation and the recrystallisation temperature promote the morphological transition from dendritic to globular structure, but too much plastic deformation and too high a temperature will lead to grain coarsening.

Tzimas and Zavaliangos¹⁴⁹ compared the reheating behaviour of three different initial microstructures obtained by MHD stirring, the SIMA (stress induced and melt activated process), and spray casting. (These technologies for the production of non-dendritic feedstock are discussed below.) They concluded that at medium liquid fraction, the microstructure of spray cast and SIMA alloys consists of discrete equiaxed grains uniformly dispersed in the liquid matrix, while the corresponding microstructure of MHD alloys exhibits extensive agglomerates consisting of incompletely spheroidised grains. Their results also demonstrated that the reheated MHD microstructures are less equiaxed compared with SIMA and spray cast alloys even after 5 min soaking in the semisolid state.

The kinetics of semisolid thermal transformation of initially dendritic structure has been investigated by a number of workers, e.g. *see* Refs. 120–122, 147, 149. The general findings are summarised here. On increasing the temperature, partial remelting was found to start at grain boundaries, followed by an apparent decrease in the proportion of eutectic phase. During partial remelting and the subsequent isothermal holding in the semisolid state, coarsening first proceeds predominately through coalescence of dendritic arms. As the dendritic arms of the same cell have a perfectly matching crystallographic orientation, coalescence of the dendrite arms is supposed to be extremely rapid. Such a mechanism of rapid coalescence causes substantial entrapment of the liquid phase in the interdendritic region, while in the case of electromagnetically stirred alloys the coalescence of short dendritic arms leads to a more spherical morphology. After this rapid coalescence stage, the much slower coarsening by diffusion of solid atoms from areas of high curvature to areas of low curvature can take place. As long as the particles are not spherical, coarsening will lead to an increase in the mean free path in the solid phase, but the number of particles remains constant until eventually the solid phase becomes spherical. Further coarsening will then take place through dissolution of the small globules and the particle density will then decrease.

From this review, it appears that the microstructural evolution during reheating and subsequent isothermal holding is characterised by the following processes:

- partial remelting of the low melting point phase starting at grain boundaries

- rapid coalescence of dendritic arms resulting in liquid entrapment
- spheroidisation of individual particles due to atomic flux from the areas of high curvature to the areas of low curvature
- coarsening by both dissolution of smaller particles and coalescence between particles, resulting in a decrease in particle density.

Modelling of microstructural coarsening

The LSW theory^{144,145} describes Ostwald ripening in the limit of infinite particle separation in a surrounding matrix with no convection. Strictly speaking, for the case of coarsening in the semisolid state, the theory is valid only for solid fraction approaching zero. The LSW theory is expressed by

$$\bar{R}^3(t) - \bar{R}^3(0) = Kt \dots \dots \dots (22)$$

where $\bar{R}(t)$ is the average particle radius at time t , $\bar{R}(0)$ is the average particle radius at $t = 0$ when the system has reached a steady state distribution, and K is the coarsening rate constant for growth solely by Ostwald ripening in the limit of zero volume fraction of the growing phase.

Takajo *et al.*¹⁵⁰ and Wan and Sahn¹⁵¹ believe that coarsening by coalescence plays a major role in the ripening process of semisolid alloys. When two or more particles coalesce, they become interconnected by solid necks and spheroidise by mass transport essentially restricted to the necking regions. Takajo *et al.*¹⁵⁰ developed a theory for growth by pure coalescence ripening. The increase in the average particle size is treated under the assumption that the rate determining step is diffusion of solute atoms in the liquid. Also, in this case growth follows cubic kinetics according to equation (22). An expression for the rate constant solely by coalescence has been given by Wan and Sahn.¹⁵¹ Assuming an equal coalescence frequency for all existing particles, the theory of Takajo *et al.*¹⁵⁰ predicts a normalised steady state particle size distribution given by

$$f(\rho) = 2.136\rho^2 \exp\{-0.712\bar{1}\rho^3\} \dots \dots \dots (23)$$

where $\rho = R/\bar{R}$. Takajo *et al.*¹⁵⁰ showed that even a small contribution of coalescence broadens the particle distribution significantly compared to coarsening according to the LSW theory. Under the assumption that both mechanisms operate independently and additively, Wan and Sahn¹⁵¹ have developed a coarsening law for concurrent growth by both Ostwald ripening and coalescence ripening. The rate constant is then replaced by the sum of the rate constants for both mechanisms.

The driving force for the change in semisolid structure is the reduction in the total area of the solid/liquid interface in the system. Using a statistical approach, Marsh *et al.*¹⁵² have extended the LSW theory to dendritic microstructures. The variation of the solid/liquid interfacial area per unit volume S_v as a function of the holding time in the semisolid state is given by

$$S_v = K_1 t^{-1/3} \dots \dots \dots (24)$$

where K_1 is a complex function of liquid fraction, the solid/liquid interfacial tension, the diffusion coefficient in the liquid phase, and the initial morphology of the

solid phase. By applying the shape factor proposed by Loue and Suery⁷⁰ (equation (20)), Blais *et al.*¹⁴⁶ have derived the following equation to describe the morphological evolution

$$F_g = \frac{K_1^2}{6\pi f_s N_A} t^{-2/3} \dots \dots \dots (25)$$

Equation (25) indicates that the shape factor F_g decreases with increasing holding time, solid fraction, and particle density. This means that the spheroidisation kinetics is enhanced by the high solid fraction and smaller particle size. In addition, equation (25) also suggests that, regardless of the initial microstructure, during holding in the semisolid state the solid phase always evolves towards a spherical morphology, for which the area of interface per unit volume is a minimum. However, the kinetics of this transformation is governed by the initial microstructure through the values of K_1 and N_A in equation (25).

Alloy development for SSM processing

Demand for specifically designed alloys

The alloys commonly used for SSM processing are limited to a few casting alloys, only a limited number of trials have been carried out on wrought alloys.⁷⁵ If the materials are properly cast and the mould is well designed, the resulting mechanical properties are generally better than those of conventionally cast alloys. However, the mechanical properties offered by SSM processed cast alloys may not be sufficient for specific applications when higher strength, especially higher fatigue strength, is required. Wrought alloys could be an alternative for such applications. However, wrought alloys are very difficult to cast or shape in the semisolid state owing to the very strong temperature dependence of the liquid volume fraction, lower fluidity compared with silicon containing cast alloys, and problems related to hot tearing.^{153–155} Table 1 summarises the calculated thermal properties of some conventional wrought and cast aluminium alloys, which have been used in the past for SSM processing.¹⁵⁶ All the data in Table 1 were calculated using Thermo-Calc (KTH, Stockholm) in combi-

nation with Al-Data (ThermoTech Ltd, Guildford, UK). For the wrought alloys, a small variation in temperature induces a large change in solid fraction. Therefore, a small decrease in temperature can lead to a considerable increase in solid fraction resulting in a microstructure absolutely not favourable to semisolid forming. In this case, deformation is inhomogeneous and liquid segregation occurs often during mould filling. On the other hand, when temperature increases, the liquid fraction becomes too high, which makes slug handling very difficult due to the reduced shape stability.¹⁵⁷ In addition, SSM processing, as a new forming technology, is currently utilised without taking advantage of its unique features and is judged by suboptimal trials using existing alloys, which are optimised either for casting or for forging.¹⁵⁸ For those reasons, in the past few years, there has been a strong appeal for the development of new alloys specifically optimised for SSM processing (e.g. see Refs. 5, 154, 155, 158–160). In this section, the work in the literature on alloy design for SSM processing and some of the design principles are summarised. Briefly, the objectives of new alloy design for SSM processing are:

- to improve upon the mechanical properties offered by the existing cast and wrought alloys
- to take full advantage of the benefits offered by SSM processing techniques
- to facilitate SSM processing, such as enlarged processing windows and improved mould filling as a result of improved rheological properties
- to cut the production cost, and thus reduce component cost.

Current status of alloy design

The first commercial attempt at alloy development especially suited for thixoforming was carried out by Pechiney.¹⁶¹ To optimise the strength and ductility in the T5 condition, an Al–6Si–1Cu–Mg alloy was developed based on the A357 compositions. The properties of Al–6Si–1Cu–Mg alloy after thixoforming match or exceed those of permanent mould cast A356 alloy under T6 conditions. There have also been trials on modified hypereutectic alloys based on A390 alloy.^{159,161–163} The other approach for alloy design

Table 1 Thermal properties of aluminium alloy¹⁵⁶

Alloy/nominal composition	$T, ^\circ\text{C}$ (Ref. 184)			$T, ^\circ\text{C}$ (Scheil model)			$T, ^\circ\text{C}$ (Equilibrium)			Slope of f_s - T curve	
	T_L	T_S	ΔT_{S-L}	T_L	T_S	ΔT_{S-L}	T_L	T_S	ΔT_{S-L}	$f_s = 0.3$	$f_s = 0.6$
Wrought aluminium alloys											
2024/Al-4.4Cu-1.5Mg-0.6Mn	638	502	136	640.6	507.0	133.6	640.6	515.8	124.8	0.0339	0.014
3004/Al-1.2Mn-1.0Mg	654	629	25	653.8	522.0	131.8	653.8	640.8	13.0	0.149	0.084
4032/Al-12.2Si-1.0Mg-0.9Cu-0.9Ni	571	532	39	571.5	519.0	52.5	571.5	535.4	36.1	0.0676	0.0244
5056/Al-5.0Mg-0.1Mn-0.1Cr	638	568	70	635.7	298.0	337.7	635.7	578.8	56.9	0.0335	0.0188
6061/Al-1.0Mg-0.61Si-0.30Cu-0.20Cr	652	582	70	652.1	532	120.1	652.1	590.5	61.6	0.0707	0.0331
7075/Al-5.6Zn-2.5Mg-1.6Cu-0.23Cr	635	477	158	634.9	471.4	163.5	665.4	517.7	147.7	0.031	0.0147
Cast aluminium alloys											
296.0/Al-4.5Cu-2.5Si	635	530	105	632.5	525.1	107.4	632.5	527.8	104.7	0.0192	0.0078
356.0/Al-7Si-0.3Mg	615	555	60	615.6	557.2	58.4	615.6	567.5	48.1	0.0118	0.201
357.0/Al-7Si-0.5Mg	615	555	60	614.9	557.2	57.7	614.9	560.7	54.2	0.0117	0.121
390.0/Al-17.0Si-4.5Cu-0.6Mg	650	505	145	661.4	510.2	151.2	661.4	510.2	151.2	0.06	0.0241
520.0/Al-10Mg	605	450	155	608.7	450.1	158.6	608.7	508.0	100.7	0.016	0.0094
771.0/Al-7Zn-0.9Mg-0.13Cr	645	605	40	644.8	468.2	176.6	644.8	612.8	32.0	0.0586	0.0349

for SSM processing is based on existing wrought alloys for improving processability and maintaining the good combination of mechanical properties. Efforts in this direction have been mainly concentrated on the Al–Mg–Si system with increased magnesium and silicon contents and minor additions of other alloying elements.¹⁵⁴ It was found that such alloys have sufficient thixoformability and good combinations of mechanical properties. In addition, hot cracking was eliminated. Other preliminary work on alloy development focused primarily on self-hardening alloys aimed at reducing the heat treatment cost.¹⁵⁴

To facilitate SSM processing, microalloying elements were added to AA 6082 alloy.¹⁰⁰ It was found that minor additions of iron and chromium can effectively slow down the grain coarsening kinetics, while minor additions of surfactant elements such as barium can reduce the solid/liquid interfacial tension resulting in a dramatic reduction of the tendency for particle agglomeration, and hence improving the rheological characteristics for SSM processing.

In contrast to semisolid aluminium, the use of semisolid magnesium is relatively unknown.¹⁶⁴ So far, there has been no serious attempt at the development of magnesium alloys for SSM processing. However, due to the fast growth of the magnesium industry in the past few years, and the great demand from the automobile industry,¹⁶⁵ SSM processing of magnesium alloys and associated alloy development could be an exciting area for future research.

Basic considerations for alloy development

To achieve the above mentioned objectives for alloy design specifically for SSM processing, a number of scientific and technological factors need to be considered. Based on the prior experimental work, and the recent analysis by Witulski *et al.*,¹⁵³ Atkinson *et al.*,¹⁵⁵ and Liu and Fan,¹⁶⁶ such basic considerations are summarised in this section.

Solidification range

The solidification range is usually defined as the temperature range between the solidus and liquidus. It is mainly determined by alloy composition and affected by processing conditions, such as cooling rate. Solidification range is an important factor and needs to be optimised during alloy development for SSM processing. On the one hand, pure metals and eutectic alloys have very poor castability due to the lack of solidification range. On the other hand, too wide a solidification range could lead to poor resistance to hot tearing and poor fluidity of the liquid alloy.

Temperature sensitivity of solid fraction

For a given alloy composition, solid volume fraction v_s of a SSM slurry is usually determined by the SSM processing temperature. The temperature sensitivity of v_s can be defined by the slope of the f_s – T curve, i.e. df_s/dT . Since df_s/dT is usually negative, for simplicity, the absolute value of df_s/dT is used to represent temperature sensitivity of solid fraction. Alloys designed for SSM processing should have a small temperature sensitivity of solid fraction.

Potential for age hardening

To take full advantage of the fact that SSM processed components are heat treatable, alloys designed for SSM processing need to have large ΔC , which is defined as the solid solubility difference between SSM temperature and aging temperature. The advantage of such alloys is that it may be possible to utilise the more cost effective T5 heat treatment, rather than the more expensive T6 heat treatment. The potential for age hardening may be achieved by careful selection of alloy composition.

Castability

During SSM processing, the forming process is carried out in the semisolid state, the semisolid slurry is injected into the die cavity, and then the liquid phase solidifies in the die. The liquid is thus subject to the laws of conventional casting, so that the castability of an alloy, or rather the castability of the liquid phase, plays a major role in the success of SSM processing. The composition of the liquid phase in the SSM slurry may be quite different from that of the actual alloy. Therefore, good fluidity of the liquid phase needs to be ensured through composition selection during alloy design.

Morphology of solid phase

An ideal slurry for SSM processing has a controlled volume fraction of fine and spherical solid particles distributed uniformly in a liquid matrix with good fluidity. Such a SSM slurry can ensure smooth mould filling and fine and uniform microstructure after solidification. However, the ease with which the fine and spherical particles can form during SSM processing depends on the actual composition. Accordingly, composition selection during alloy design should facilitate the creation of such an ideal SSM slurry.

Rheological properties in semisolid state

It is the characteristic rheological properties of SSM slurries that make SSM processing unique and advantageous compared with other conventional casting techniques. The processing condition, and the morphology, size, and distribution of the solid phase in the liquid matrix, all have great influence on the viscosity of SSM slurries. The variation in viscosity, on the other hand, will influence the castability. In addition, particle agglomeration strongly affects the rheology of SSM slurries. A reduced tendency for particle agglomeration will facilitate SSM processing and can be achieved through addition of alloying elements.

Basic approaches to alloy design

Conventional alloy development has been primarily based on experimental approach and is frequently performed by the trial and error method. However, alloy development for SSM processing need not be from scratch; the vast information on the development of both cast and wrought alloys can be utilised. More importantly, the Calphad approach, combined with an appropriate thermodynamic database, can be a very powerful tool to guide the development of new alloys. Generally, thermodynamic calculations can be used to select the major alloying elements and to narrow down the alloy composition ranges. Experimental work is then carried out to select the

9

minor alloying elements and to determine the final alloy composition.

Based on current understanding, it appears that there are three basic directions for alloy development for SSM processing:

- modification of existing cast alloys for improved strength and ductility, while maintaining their superb castability
- modification of existing wrought alloys for enhanced processability, such as improved fluidity and temperature sensitivity of solid fraction and reduced tendency for hot tearing
- alloys tailored for specific applications; this might be particularly necessary for automobile components.

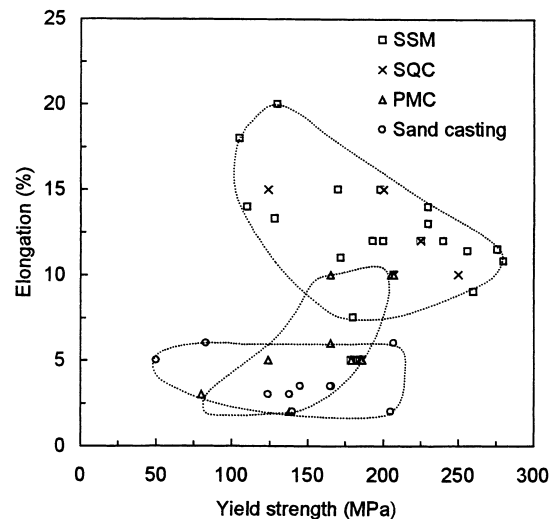
The Calphad technique has been recently applied to design new aluminium alloys for SSM processing based on the Al–Si–Mg system.¹⁶⁶ In Table 2, the thermodynamic characteristics of the newly designed alloys can be compared with those of conventional cast and wrought alloys based on the same system. Generally, the new alloys have a more suitable solidification range, reduced temperature sensitivity of solid fraction, and enhanced potential for age hardening, and therefore improved processability and increased potential for property enhancement compared with the conventional alloys.

Mechanical properties

Tensile properties

Although substantial efforts have been made to evaluate the mechanical properties of SSM processed alloys since Kirkwood's review,¹³ especially in the past few years, data in the literature are still insignificant for the purpose of accurate evaluation of the currently available processing technologies or for accumulation of a design database. It seems that most of the effort has been confined to cast aluminium alloys, with less attention being given to wrought alloys. Data for magnesium based alloys are particularly scarce.

Mechanical property data for SSM processed aluminium cast alloys can be found in Refs. 161, 163,



SQC squeeze casting; PMC permanent mould casting

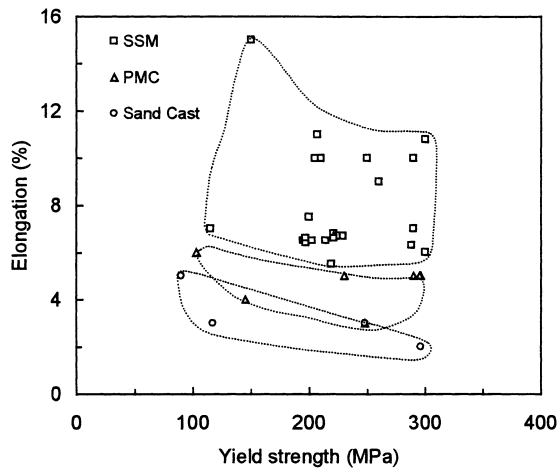
27 Literature values of elongation of A356 alloy plotted against yield strength showing advantage of SSM processing (thixoforming) over conventional processing routes

167–187. Figure 27 is a plot of elongation against yield strength for A356 alloys processed by thixoforming, squeeze casting (SQC), permanent mould casting (PMC), and sand casting. It is apparent from Fig. 27 that the mechanical properties of thixoformed A356 alloy in the fully heat treated condition (T6) are superior to those obtained by sand casting and PMC, but comparable to those achieved by SQC; the improved ductility of thixoformed specimens is particularly noteworthy. Such improvements of both strength and ductility can be attributed to two basic factors: one is reduced or even eliminated porosity and the other one is refined microstructure coupled with increased chemical homogeneity. The effect of porosity on strength and ductility has long been established. Porosity decreases both strength and ductility, the latter in particular. The effect of structural refinement on properties can be understood

Table 2 Thermodynamic characteristics of Al–Si–Mg alloys designed for SSM processing in comparison with those of commercial alloys based on same system¹⁶⁶

Alloy	Potential for heat treatment of (Al) phase, wt-%*							
	$T_L, ^\circ\text{C}$	$\Delta T_{S-L}, ^\circ\text{C}$	$ df_s/dT $		$f_s = 0.3$		$f_s = 0.6$	
			$f_s = 0.3$	$f_s = 0.6$	$\Delta C(\text{Si})$	$\Delta C(\text{Mg})$	$\Delta C(\text{Si})$	$\Delta C(\text{Mg})$
SSM alloys designed for rheo-route								
Al–7Si–3Mg	605.8	48.6	0.0104	...	0.923	0.697
Al–8Si–3Mg	599.6	42.4	0.0091	...	1.083	0.637
Al–9Si–2Mg	596.4	39.2	0.0083	...	1.340	0.391
SSM alloys designed for thixo-route								
Al–2Si–3Mg	634.6	57.3	...	0.0112	0.357	1.353
Al–3Si–2Mg	633.5	76.3	...	0.0093	0.613	0.816
Al–4Si–2Mg	627.7	70.5	...	0.0071	0.844	0.729
Al–5Si–2Mg	621.8	64.6	...	0.0058	1.090	0.645
Commercial alloys based on Al–Si–Mg system								
356.0	615.6	48.1	0.0116	0.2027	1.113	0.068
357.0	614.9	54.2	0.0115	0.1271	1.098	0.116
6061	652.1	61.6	0.0712	0.0332	0.131	0.494

* ΔC is solid solubility difference (wt-%) between SSM temperature and aging temperature.



28 Literature values of elongation of A357 alloy plotted against yield strength showing advantage of SSM processing over conventional processing routes

from the Hall–Petch type equation for yield strength σ_y and strain to fracture ϵ_f (Refs. 188–190)

$$\sigma_y = \sigma_y^0 + k_y d^{-1/2} \dots \dots \dots (26)$$

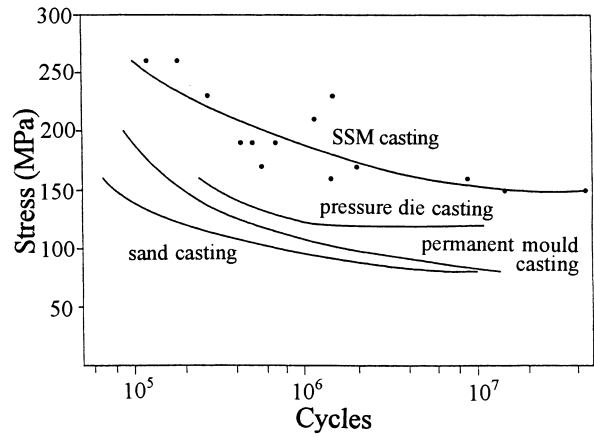
$$\epsilon_f = \epsilon_f^0 + k_\epsilon d^{-1/4} \dots \dots \dots (27)$$

where, and k_ϵ are Hall–Petch constants. It is apparent from the above equations that both strength and ductility increase with decreasing grain size, and that the ductility increase is more dramatic than the strength increase due to a less negative exponent for the former. Similar arguments apply to cast A357 alloys, as shown in Fig. 28.

However, a completely different picture for wrought aluminium alloys is presented in the literature (Refs. 171, 174, 180, 185–187). It seems that most thixoformed wrought alloys do not quite achieve the highest strength and ductility that they are potentially capable of in the wrought form.¹⁸⁴ This may reflect the presence of defects in the thixoformed wrought alloys, such as hot cracks,¹⁵⁴ residual porosity, and oxide inclusions.¹⁹¹ Such defects may originate from processing difficulties during thixoforming, for example, lack of fluidity and a narrow processing window. This emphasises again the need for new alloys developed specifically for SSM processing.

Fatigue strength and fracture toughness

Gabathuler *et al.*¹⁹² studied the fatigue strength of SSM formed A356 alloy. Their results indicate that at high cycles ($N > 10^6$), the fatigue strength of SSM formed samples has been improved substantially compared with that of samples produced by high pressure die casting (HPDC), PMC, and sand casting (Fig. 29). Valer *et al.*^{193,194} investigated the fatigue behaviour and fracture toughness of hypereutectic Al–Si alloys produced by a combination of spray forming, extrusion, and thixoforming. In the case of Al–25Si–5Cu alloy, thixoformed samples have better toughness than extruded samples, while in the case of Al–30Si–5Cu alloy, both processes produced similar toughness. The authors also showed that thixoformed samples have better fatigue resistance than



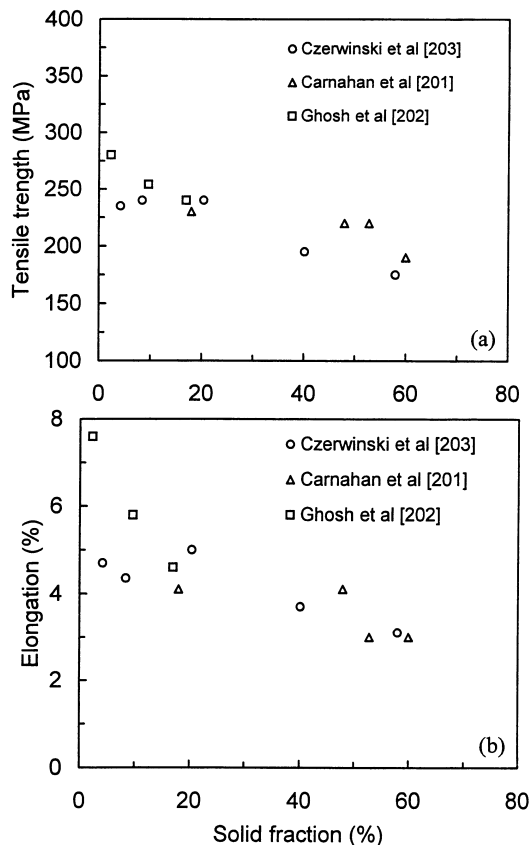
29 Comparison of S–N curve for SSM (thixoformed) A356 alloy with curves obtained for alloys processed by conventional routes (after Ref. 192)

extruded samples due to the unique distribution of primary silicon particles in the thixoformed samples. More recently, Bergsma *et al.*¹⁷⁸ measured the fatigue strengths of SSM formed A357 and modified A319 alloys. Their results also showed substantial increase in fatigue strength in SSM formed samples compared with the strengths of the same alloys produced by other processing routes. However, the recent work by Ferreira and Teixeira¹⁹⁵ on rheoforged Al–7Si and Al–4.5Cu alloys has shown an interesting trend regarding the effect of shear rate on fracture toughness and fatigue strength. For Al–7Si alloys, fracture toughness is higher for SSM samples than for die cast samples. For Al–4.5Cu alloys, fracture toughness decreases with increasing shear rate. They also found that SSM Al–Si alloys exhibit lower fatigue life and higher crack propagation rate when the shear rate is increased. Badiali *et al.*¹⁹¹ examined the initiation sites of fatigue cracks in SSM formed A356 alloy in the T6 condition. They found that the fatigue strength of SSM formed A356 alloy in the T6 condition is determined by either oxides or pores, but oxide defects have less detrimental effects on the fatigue life than shrinkage pores of the same size.

It is clear from this review that further investigations are necessary to understand the fatigue and fracture behaviour of SSM processed alloys and to correlate the fracture behaviour with the corresponding microstructural features, particularly those unique to SSM processing.

Mechanical properties of magnesium alloys

Compared with aluminium alloys, mechanical property data for SSM processed magnesium alloys are scarce.^{196–203} The available tensile property data in the literature show that the strengths of SSM processed magnesium alloys compare well, but are not superior to those of conventional die casting, although the ductility values are improved. Some of the recent results on tensile strength and elongation of thixomoulded AZ91D alloy are presented in Fig. 30.^{201–203} It is interesting to note that both the tensile strength and ductility of thixomoulded AZ91D alloys decrease



30 Literature values^{201–203} of a tensile strength and b elongation of thixomoulded AZ91D alloy plotted as function of volume fraction of primary solid phase

with increasing solid fraction, with ductility having a much stronger dependence on the solid fraction. The ASTM standards for tensile strength and ductility of AZ91D alloy are 230 MPa and 3%, respectively. Therefore, up to 0.2 solid fraction, the thixomoulded samples are above the corresponding limit. In addition, there has been a report²⁰⁴ that the average yield strength of thixocast AZ91D alloy is lower than that of the feedstock by 20% in the as cast state and by 10% in the heat treated state. The improved ductility of SSM processed samples over that of die cast samples was attributed to less entrapped air during mould filling and reduced shrinkage porosity due to lower casting temperature.^{203,204}

Technologies for SSM processing

Technologies for SSM processing can be generally divided into two basic routes: rheo-route and thixo-route. The rheo-route involves preparation of a SSM slurry from liquid alloys by shearing during solidification and transferring directly the prepared SSM slurry to a die or mould for component shaping. The thixo-route is basically a two step process, involving preparation of a feedstock material with thixotropic characteristics, then reheating the feedstock material to semisolid temperature to produce the SSM slurry, which is subsequently used for component shaping. In this review, the technologies available for SSM processing from both the routes are described.

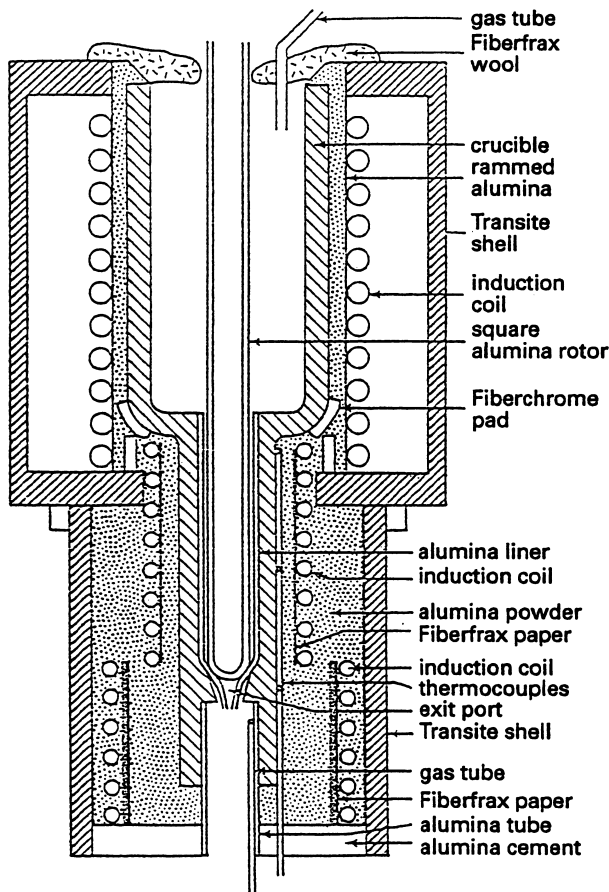
Technologies for production of non-dendritic feedstock

The objective of feedstock production is to provide a material with a characteristic thixotropic microstructure where a non-dendritic (or globular) primary phase with a fine grain size is uniformly distributed in a matrix of lower melting point. Although thixotropic feedstock materials in their semisolid state may be directly used for component shaping, they are often used as a raw material in the solid state for subsequent reheating into the semisolid state and component shaping through thixoforming. Thixotropic feedstock production can start either from a liquid alloy through controlled solidification under specific conditions, or from solid state through heavy plastic deformation and recrystallisation. Currently, there is little choice in commercially available feedstock materials, and alloys are usually limited to aluminium based materials, mostly A356 and A357 type cast alloys with 3–6 inch billet diameter, produced by MHD stirring.²⁰⁵ However, there are a number of other production techniques, which are at different stages of research and development. In this section, the basic features of those techniques available for feedstock production are summarised.

Mechanical stirring

The technologies originated at MIT were based on mechanical stirring.^{3,206} Melt agitation is commonly generated by means of augers, impellers, or multi-paddle agitators mounted on a central rotating shaft. Shear rate can be roughly estimated by the ratio of the velocity of the impeller extremity to the clearance between the impeller tip and the mould wall.²⁰⁶ The shear offered by the stirrer during solidification promotes the formation of non-dendritic structure. The mechanical stirring approach was developed from a batch process into a continuous process, as illustrated in Fig. 31. In the continuous process, superheated liquid in the holding vessel flows down into an annulus between the stirring rod and the outer cylinder where it is simultaneously stirred and cooled. Slurry flows from the bottom of the rheocaster either to be cast directly to shape (rheocasting), or to be solidified as feedstock material for subsequent reheating and thixoforming. The resulting solid particles are usually coarse rosettes.²⁰⁷ This early version of rheocasting has not reached a commercial stage. Historically, this was attributed to a number of technical difficulties at that time, such as contamination of the melt through oxidation and chemical reaction with the stirring system.

Recently, due to the technical and commercial concerns associated with other methods for feedstock production, there has been renewed interest in this technology. Modifications to the early version of the rheocaster were made to develop a process for feedstock production employing mechanical stirring.²⁰⁸ In the modified rheocasting process, shearing and solidification are caused to occur in separate volumes, and thus are effectively decoupled. The objective of the modification was to improve the microstructural uniformity in the cross-section of the continuous cast billet.



31 Schematic diagram of high temperature continuous rheocaster (after Ref. 206)

Magnetohydrodynamic (MHD) stirring

To overcome the problems associated with the original rheocasting process using direct mechanical stirring, a MHD stirring process was developed by ITT in the USA, and is described in a series of patents originally held by Alumax Inc.²⁰⁹ In this technique, local shear is generated by rotating electromagnetic fields within the continuous casting mould, and continuous billets of solidified non-dendritic alloy can be produced. The stirring is deep in the sump of the liquid, which has previously been filtered and degassed, so that contamination is virtually eliminated. Since the birth of this technology for thixotropic feedstock production, it has been subject to intensive research.^{209–218} At present, MHD stirring has established itself as the most widespread practice for feedstock production.²¹⁹

Electromagnetic stirring can be achieved through three different modes: vertical flow,^{146,220} horizontal flow,^{210,221} and helical flow¹⁶¹, with the helical mode being ultimately a combination of the vertical and horizontal modes. In the horizontal flow mode, the motion of the solid particles takes place in a quasi-isothermal plane so that mechanical shearing is probably the dominant mechanism for spheroidisation. In the vertical flow mode, the dendrites located near the solidification front are recirculated to the hotter zone of the stirring chamber and partially remelted, and therefore thermal processing is dominant over mechanical shearing.^{136,161}

The continuous casting is made through either a vertical or horizontal arrangement, depending on the casting direction in relation to the gravity direction. While vertical stirring has so far been employed in vertical continuous casting only, horizontal stirring has been used in both vertical and horizontal casting systems. According to Niedermaier *et al.*,²¹⁹ the major advantages of horizontal continuous casting include better economy, continuous production, and low investment costs, but the quality of the billet is influenced by the gravity. On the other hand, the vertical casting system benefits from symmetrical solidification and there is no limitation of the billet diameter. However, the vertical system suffers from drawbacks such as discontinuous production, high investment costs, and high production costs.

The major hurdles to the wide acceptance of this technology for thixotropic feedstock production include high production costs (accounting for up to 50% of the component cost),²²² microstructural non-uniformity in the cross-section of the cast billet, and non-spherical (although non-dendritic) particle morphology. Such a microstructural deficiency will cause prolonged reheating time and difficulties during subsequent thixoforming, consequently resulting in a further increase of the production costs.

Stress induced and melt activated (SIMA) process

An alternative to the liquid agitation route is the SIMA process. This process, originally developed by Young *et al.*,²²³ involves:

- cold deformation of a hot extruded and quenched billet to induce residual plastic strain
- reheating the cold worked billet to a semisolid temperature to produce the globular structure
- thixoforming the billet in its semisolid state.

This process is based on the scientific understanding that high angle grain boundaries induced by plastic deformation and recrystallisation will be wetted by liquid metal at the semisolid temperature, resulting in a fine and globular structure. A modification of the SIMA process was made by Kirkwood and co-workers^{224,225} by changing the cold working to warm working at a temperature below the recrystallisation temperature to ensure the maximum strain hardening. Further research work on the SIMA process for other alloys^{70,226–232} has allowed increased understanding of the effects of processing parameters (such as amount of plastic deformation, reheating temperature, and time duration) on the resulting microstructure in the semisolid state. With appropriate choice of processing conditions, the resulting solid phase particles are usually fine in size, globular in morphology, and uniform in distribution.

The SIMA process produces high quality feedstock for thixoforming and has the potential for wrought alloys and high melting temperature alloys such as steel and superalloys. However, the SIMA process requires plastic deformation and recrystallisation of conventionally cast dendritic materials by thermomechanical treatments that are energy and processing intensive making it cost approximately 3–5 times more than the MHD stirring process.²⁰⁸ The SIMA process is therefore only effective for small niche applications and for small diameter feedstock.

Spray casting

Spray casting (Osprey process)^{128,146,233} is another non-agitation process for feedstock production. In this process, molten metal is directed through a nozzle to meet the high pressure inert gas (nitrogen or argon). The liquid metal stream is atomised by the high pressure gas into micrometre sized droplets that experience high cooling rate during their flight, the cooling rate being in the order of 10^3 K s^{-1} . While the large droplets remain fully liquid and the small droplets solidify during atomisation, those of intermediate sizes become semisolid. The droplets are collected on a moving substrate and consolidated to form a coherent preform. A second stage of solidification takes place on the substrate at the beginning of the deposition, and subsequently on the upper surface of the preform. Liquid and semisolid droplets with high liquid fraction splat upon impact, while solid and semisolid droplets with high solid fraction fragment.²³³ A portion of the solid grains undergoes remelting and resolidifies slowly. Typical local solidification time on the preform surface is of the order of 100 s indicating that more than 90% of the solidification time of a spray cast preform occurs in the deposit at high solid fraction. The resulting microstructure comprises very fine equiaxed grains. The spray casting process has been investigated extensively over the past two decades and several models have been proposed to describe the process in detail (see Ref. 128).

Various alloys produced by spray casting have been evaluated experimentally as feedstock materials for semisolid processing, e.g. see Ref. 232. It is generally believed that spray cast materials are suitable as feedstock for thixoforming, especially for high temperature alloys, such as steels and superalloys.

Liquidus casting

Liquidus casting, also known as low superheat casting, has been developed recently as an alternative technique for production of thixotropic feedstock.^{185,234–236} In liquidus casting, melt with a uniform temperature just above its liquidus is poured into a mould for solidification. The resulting microstructures are usually fine and non-dendritic. Upon reheating, the liquidus cast microstructure spheroidises rapidly to produce microstructural features suitable for thixoforming operations. So far, this technique has been tested on both cast^{236–238} and wrought^{185,186,234,239,240} aluminium alloys.

The effect of melt superheating was recognised nearly 40 years ago by Chalmers and co-workers.^{241–243} They found that reducing the pouring temperature promotes the formation of an equiaxed zone and suppresses the formation of the columnar grain zone. In addition, lowering the pouring temperature also refines the equiaxed grains. Such experimental observations have been explained by investigators^{234,240} using the Mullins–Sekerka instability theory,¹³³ which suggests that an alloy with very small undercooling coupled with a very high saturation of nucleation sites would form an equiaxed structure. However, it seems much effort is still required to establish the exact mechanism for the formation of the fine and non-dendritic structure during liquidus casting.

Recently, Fan *et al.*²⁴⁴ developed a liquidus rheocasting process. In this process, overheated liquid metal is poured into a twin screw extruder where it is continuously sheared and cooled to a temperature around its liquidus before being transferred to a mould for shaping or to a DC (direct chill) caster for continuous casting of thixotropic feedstock billets. The microstructural features offered by the liquidus rheocasting process include fine grain size, spherical particle morphology and much improved chemical and microstructural uniformity.²⁴⁵

Liquidus casting, with liquidus rheocasting in particular, is gaining more attention as a simple and cost effective technique for feedstock production and seems to have a promising future. However, the major obstacles for industrial application may arise from difficulties related to accuracy and uniformity of temperature control, and consistency and uniformity of resulting microstructure in large scale production.

Ultrasonic treatment

Application of high power ultrasonic vibration (or ultrasonic treatment) to a solidifying melt for refinement of as cast structure can be traced back to the mid-1970s.²⁴⁶ In the past few years, there has been renewed interest in this technology as a means for feedstock production.^{247–252} Experimentally, it is well established that application of ultrasonic treatment to a cooling melt at a starting temperature just above its liquidus can produce effectively a fine and non-dendritic microstructure, which is suitable for subsequent reheating and thixoforming operations.

Regarding the mechanism for the formation of such fine and non-dendritic structure, it is now generally believed that introduction of high power ultrasonic vibration into a liquid alloy can lead to two basic physical phenomena:^{249,251,252} cavitation and acoustic streaming. Cavitation involves the formation, growth, pulsation, and collapsing of tiny bubbles in the melt. The compression rate of these unsteady bubbles can be so high that their collapsing generates hydraulic waves, thus producing artificial sources of nuclei. The propagation of a high intensity ultrasonic wave involves the initiation of steady state acoustic streaming in the melt. The overall effect of various types of stream is to vigorously mix and homogenise the melt. Therefore, hydraulic shock waves generated by the collapse of cavitation bubbles fragment dendritic arms, and acoustic streams will distribute the dendritic arm fragments homogeneously throughout the melt. When ultrasonic vibration is coupled to the solidifying metal, the structural changes include grain refinement, suppression of the columnar grain structure, increased homogeneity, and reduced segregation.

Chemical grain refining

Chemical grain refinement is nowadays a common practice in continuous casting of aluminium alloys.²⁵³ This technique has also been considered for feedstock production. In most cases, a prealloyed wire is proportioned into the hot metal flow into the launder where it releases heterogeneous nucleation agents, usually titanium and boron based. Owing to the enhanced heterogeneous nucleation rate and suppression of dendritic growth, a fine and equiaxed structure can be achieved. With an appropriate grain refining

procedure, such a structure can also be suitable for subsequent reheating and thixoforming. However, chemical grain refining is not used alone, but used in conjunction with other feedstock production methods, such as MHD stirring and liquidus casting.²³⁶ One disadvantage of the chemical grain refinement method is that nucleation agents are only effective to specific alloy systems, another is that in some cases these additives will remain present in the product as non-metallic inclusions, which may impair both the processability of the semifinished stock and the mechanical properties of the final product.²¹²

For more detailed information, readers are directed to the recent comprehensive review by Easton and St John.²⁵³

Other methods

A number of other techniques have also been proposed and investigated for the production of thixotropic feedstock. These include early techniques, such as static mixing techniques,^{254,255} the powder compaction method,^{256–258} and thermal transformation of an initially dendritic feedstock into a globular thixotropic structure.^{259–261} More recent techniques include the shear cooling roll process,^{262,263} MHD stirring in shot sleeve,²⁶⁴ the cooling slope process,^{265,266} and the single slug process.²⁶⁷

Technologies for component shaping

Rheocasting

The process of production of non-dendritic semisolid slurry by shearing during solidification has been identified as rheocasting. Direct transfer of the semisolid slurry into a die or mould to produce a finished product has also been identified as rheocasting or stir casting. Although rheocasting was identified as the production technology at the very beginning of semisolid processing research, it has not been commercialised to any great extent so far. This is possibly because of the quality of the semisolid slurry produced by such stirring processes. Mechanical stirring using either rod or impeller as stirrer results in the formation of very coarse rosettes with a diameter of a few hundred micrometres or approaching millimetre level. The slurries produced under such conditions do not have adequate thixotropic characteristics for successful direct shaping by either a casting or a forging route. In this regard, MHD stirred slurries are not better than mechanically stirred slurries. The MHD stirring process usually gives rise to degenerated equiaxed dendrites, which are inherently unsuitable for direct component shaping unless they are held at semisolid temperature for sufficiently long time. The other possible reason for the failure of commercialisation might be insufficient process control and low productivity associated with the original version of rheocasting. However, component shaping directly from SSM slurries is inherently attractive due to its characteristics, such as overall efficiency in production and energy management. The recent effort on the development of so called 'slurry-on-demand' processes is in this direction.

One of the slurry-on-demand processes is the recently developed new rheocasting (NRC) process, which was patented by UBE Industries Ltd²⁶⁸ and

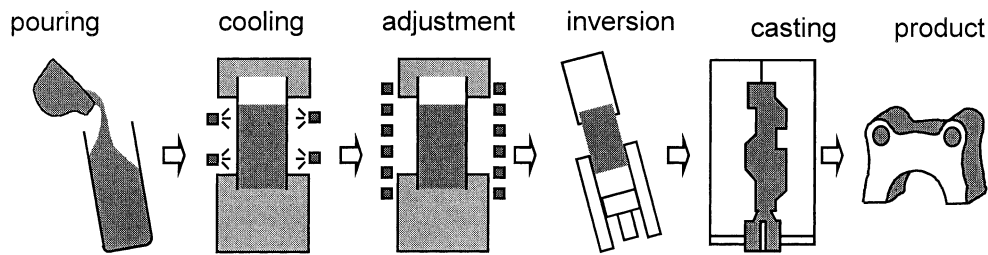
described first in Ref. 269. In the NRC process, as shown schematically in Fig. 32, a slightly overheated melt liquid metal is poured into specially designed steel crucibles, which are placed on a carousel next to a vertical SQC machine. In the crucible, semisolid slurry is formed by controlled cooling through a mechanism similar to the case of liquidus casting described in the previous section. By controlling the slurry temperature (therefore solid fraction), a stable skeleton of the solid phase is formed within a few minutes after pouring. The solid-like slug of cylindrical shape is then heated by induction heating to homogenise the slug temperature before being transferred into the sleeve of the vertical SQC machine, where it is cast into its final shape. So far, the NRC process has been evaluated by processing cast aluminium alloys,^{270–272} wrought aluminium alloys,¹⁸⁷ and magnesium alloys.²⁷³

Since conventional alloys can be used, NRC offers a significant cost advantage over thixoforming and SQC processes.²²² It also allows the use of a wider range of alloys; of particular interest are the magnesium alloys, where a thixotropic feedstock material is not readily available in the marketplace at present.

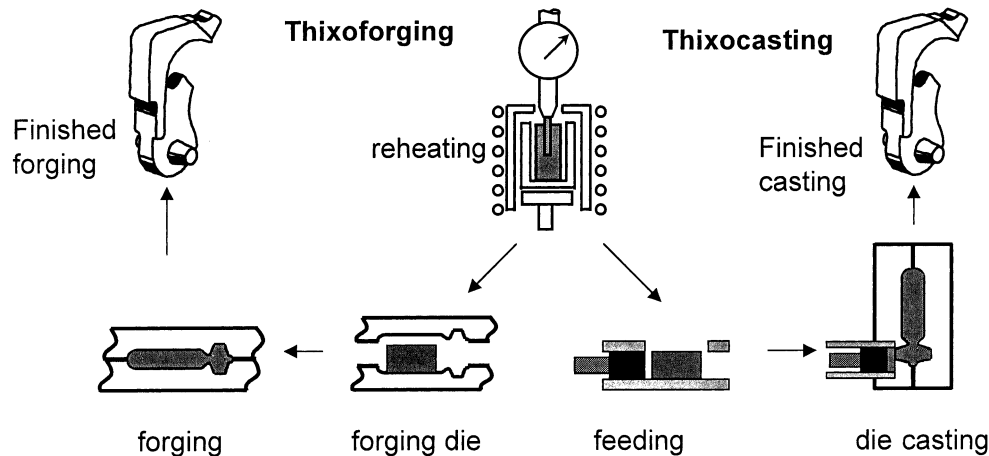
Thixoforming

Thixoforming is a general term coined to describe the near net shape forming processes from a partially melted non-dendritic alloy slug within a metal die. If the component shaping is performed in a closed die, it is referred to as thixocasting, while if the shaping is achieved in an open die, it is called thixoforging, as schematically illustrated in Fig. 33. There are two separate stages involved in the thixoforming process. The first stage is uniform heating and partial remelting of the alloy slug so that it is homogeneous throughout. In the second stage, the semisolid slug is transferred to a forging die or shot chamber by robot handling where it is injected in a controlled manner into a die cavity by a hydraulic ram. After solidification, the shaped component is removed from the mould for further processing, such as minor machining or grinding.

Reheating to the semisolid state is a particularly important phase in the thixoforming process.¹⁶¹ It aims to provide semisolid slug with an accurately controlled solid fraction of fine and spherical particles uniformly dispersed in a liquid matrix of low melting point. To achieve this semisolid microstructure, the important processing parameters during the reheating process include accuracy and uniformity of heating temperature and heating duration. It is the heating temperature that determines the solid fraction in the slug. Too high a heating temperature causes instability of the slug resulting in difficulties for slug handling, while too low a heating temperature leads to unmelted, coalesced, polyhedral silicon phase in the slug in the case of hypoeutectic cast aluminium alloys having a detrimental effect on the rheological properties during die filling and on the ductility of the finished parts. In addition, as discussed previously, the composition of the alloys currently used are not optimised for SSM processing, a small variation in temperature can cause a large difference in solid fraction. Therefore, temperature accuracy affects the



32 Schematic illustration of new rheocasting (NRC) process



33 Schematic illustration of thixoforming processes

stability of the forming process and the consistency of the product quality. Furthermore, a uniform temperature distribution throughout the slug is important, because a non-uniform distribution of temperature may lead to fluctuation in solid fraction and rheological characteristics, which in turn may cause solid/liquid separation during mould filling. Finally, the heating duration has to be optimised; too long a heating time will cause structural coarsening, while too short a heating time will lead to incomplete spheroidisation of the solid particles compromising the rheological properties and leading to difficulties during mould filling.

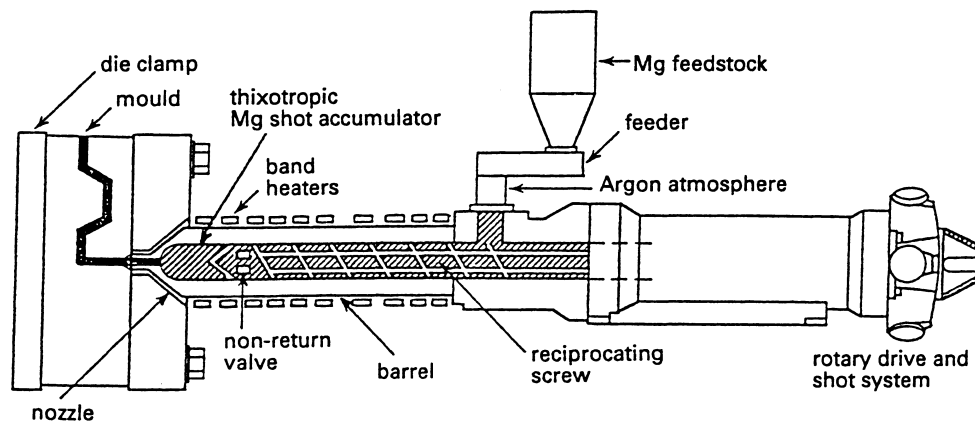
Currently, reheating is achieved mainly by induction heating, although a convection furnace is also used in some cases.²⁰⁵ Induction heating has the advantage of precise and fast heating, which is necessary for SSM processing. The relatively low energy efficiency of the induction heating station is a drawback. Possible improvement of energy efficiency can be achieved by preliminary heating to a critical temperature in a convection furnace followed by induction heating for temperature homogenisation. Induction heating is currently implemented in two different ways: vertical and horizontal heating.²⁰⁵ A vertical heating system has been conventionally used. It suffers from the slug instability problem when the height/diameter ratio is not correctly chosen. The horizontal heating system is a relatively new development, in which the slug lies in a tray and is heated to the optimal processing state monitored by an automatic control loop. Advantages of the horizontal heating system include reduction of the shape stability problem, possibly using higher liquid fractions and

alloys with a short freezing range. However, it has a higher system cost and higher space requirement.

It is clear from the above discussion that reheating is a complex process. Optimisation of the processing parameters is a critical step to ensure a high quality of formed parts. There have been substantial research efforts directed towards process optimisation^{157,274-277} and modelling of the heating process.²⁷⁸⁻²⁸³

The forming process takes place either with casting (thixocasting) or with forging (thixoforging). At present, thixocasting through horizontal cold chamber die casting is the dominant process. A robot arm transfers the semisolid slug into the shot chamber and the plunger injects the materials into the die cavity. All the thixocasting machines are real-time controlled and thus permit a reaction to possible fluctuation during the forming process. At this stage, smooth laminar mould filling is the crucial step for the forming process. This can be achieved by an optimised shot profile tailored for specific alloys and their physical conditions. Another important aspect during the forming process concerns the design of the gating system and die cavity and the correct choice of die temperature. Such a design process has to consider the flow characteristics of the semisolid metals. The forming process can be optimised through process simulations using various computer modelling techniques.

Flemings⁵ has recently summarised the major advantages and disadvantages of the thixoforming process. The main specific advantage of the thixoforming route is that the forming facility is free from handling liquid metal, and the process can be highly



34 Schematic diagram of Dow Thixomolder (after Ref. 285)

11

automated using approaches similar to those employed in forging and stamping. This basic concept of completely separating the two main parts of the process (forming of the desired structure and forming of the part) has been intuitively appealing and much work has been done in developing this process route industrially. As time progresses, the disadvantages of the thixocasting route are also becoming apparent. It has been difficult to obtain fully homogenised billets in MHD stirred continuous castings. Typical billets have some degree of inhomogeneity with respect to both structure and composition.²⁸⁴ There is metal loss during the reheating process, which may amount to as much as 10% of the total part weight.²²² Gates and risers cannot be recycled within the forming facilities, but must be sent back to the ingot producer. Thus, the metal former pays a premium to the continuous caster not only for the unique thixotropic structure in the metal, but also for the recycled materials. Currently, the cost for thixotropic feedstock could account for up to 50% of the total component cost.

Thixomoulding

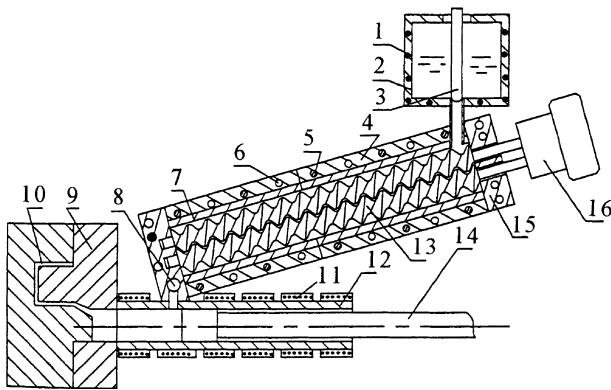
Thixomoulding is a relatively new process for production of near net shaped components from magnesium alloys in a single integrated machine,²⁸⁵ as shown schematically in Fig. 34. The raw material for thixomoulding is magnesium alloy chips of 2–5 mm in size obtained during metal working of conventional solid magnesium alloys. A volumetric metering device feeds the magnesium chips into an electrically heated plasticising and conveying unit where they are partially melted and transformed under continuous shear force into semisolid slurry. The core of this unit is the screw, which performs both a rotary and translational movement. Upon entering the unit at the feed throat, the chips are forced to pass from the heating zone to the front of the screw while the screw retracts. Once the plasticising volume corresponds to the weight of the part to be moulded, the screw advances at high speed and injects the material into a mould. A non-return valve keeps the material from flowing back from the front of the screw to the in-feed zone. To prevent the magnesium alloy from oxidising and igniting as it is heated, an argon atmosphere is usually maintained at the in-feed, displacing the air between the magnesium chips.

A major advantage of thixomoulding compared with other SSM processing technologies is that it combines effectively the slurry making and component forming operations into a one-step process leading to high efficiency of productivity and energy management. The other advantage of thixomoulding is the elimination of liquid metal handling operations, hence creating a cleaner and safer working environment, which is particularly advantageous for processing magnesium alloys. A number of thixomoulding machines are now in operation for production of magnesium castings, particularly electronic housing. At present, it appears that this process is limited to relatively low solid fraction and to magnesium alloys for thin wall components.

Rheomoulding

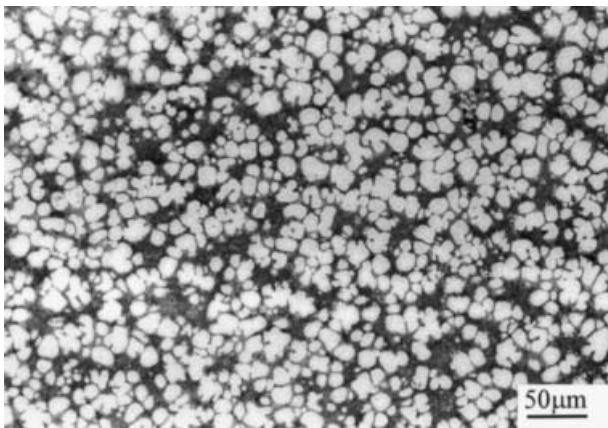
Similar to the thixomoulding process, rheomoulding is a technology adopted from the polymer processing field. However, instead of using solid alloy chips, as in the thixomoulding process, liquid metal is used as feeding material in the rheomoulding process. Currently, there are two different types of rheomoulding process: single screw and twin screw. The first rheomoulding prototype is a vertical injection and vertical clamping single screw machine patented by Cornell University.²⁸⁶ In this process, liquid metal is fed from an inert gas shielded hopper into a barrel where it is cooled while being mechanically stirred by a rotating screw converting the liquid metal into a semisolid slurry, which is then injected from a nozzle into a mould cavity for component shaping. This rheomoulding process has been applied to mould Sn–Pb and Zn–Al–Cu based alloys, and has been described in a number of publications.^{286,287} More recently, this single screw rheomoulding process has been extended to a horizontal injection and horizontal clamping single screw machine for moulding magnesium alloy parts.²⁸⁸

By realising the importance of turbulent flow on the microstructural evolution during the formation of semisolid slurry,^{115,116} Fan and co-workers^{118,137} have developed a twin screw rheomoulding (TSRM) process, which is schematically illustrated in Fig. 35. Fluid flow in the TSRM process is characterised by high shear rate, high intensity of turbulence, and cyclic variation of shear rate.¹¹⁸ As a consequence of



1 heating elements; 2 crucible; 3 stopping rod; 4 barrel; 5 heating elements; 6 cooling channels; 7 barrel liner; 8 transfer valve; 9 die; 10 mould cavity; 11 heating elements; 12 shot sleeve; 13 twin screw; 14 piston; 15 end cup; 16 driving system

35 Schematic diagram of twin screw rheomoulding process¹¹⁸



36 Microstructure of rheomoulded Mg-30Zn alloy with 0.5 solid fraction under shear rate of 2014 s^{-1} (Ref. 118)

such fluid flow characteristics and the accurate temperature control, the temperature and composition fields inside the barrel are extremely uniform. So far, this technology has been tested using Sn-Pb and magnesium based alloys.¹¹⁸ The SSM slurry produced by the TSRM process is characterised by fine and spherical particles of uniform size, as shown in Fig. 36 for a Mg-30Zn alloy. Such a slurry structure allows direct shaping operations, such as casting, extrusion, and forging.

Recently, the TSRM process has been extended to a rheomixing process for processing usually immiscible liquid alloys.^{289,290} In addition, the rheomoulding technology has also been extended to strip production by a twin roll rheocasting process²⁹¹ and to continuous cast billet production by a liquidus rheocasting process.²⁴⁴

Industrial applications

Every forming process has an appropriate niche where it can be deemed best suited and most cost effective. Semisolid metal processes need to be recognised for their enabling features, and must be judged among

processes that are similarly capable of producing high quality parts.¹⁷⁷ Before identifying the enabling features provided by SSM processes, it is necessary to analyse the competing processes in relation to SSM processing.

The conventional high pressure die casting (HPDC) process is unquestionably most widely selected for mass production of non-ferrous cast products. The process is relatively inexpensive and is suitable for various components differing in size and in complexity. The die casting process is, however, not capable of the same high product integrity and reliability achievable through SSM processing. Die castings always contain some level of porosity, which causes variability in properties and makes the components non-heat treatable.

Squeeze casting (SQC) is used for various high integrity parts, especially automobile chassis and suspension components with relatively thick sections. This process is equally capable of the high integrity, heat treatability, strength, and ductility achievable by SSM processing, but it is not suitable for production of the relatively thin sections possible with SSM.

Permanent mould casting (PMC), especially the low pressure version, is also capable of high integrity and is used to cast aluminium wheels and other structural components. The PMC process also accomplishes approximately the same soundness, heat treatability, strength, and ductility as SSM. In common with SQC, the PMC process is not suitable for casting thin sectioned components.

Forging generally provides the most desirable properties available in formed aluminium product and is therefore used for many aerospace and automobile structural components. However, forging does not provide the net shape, thin sections or tight dimensional control achievable with SSM.

Jorstad¹⁷⁷ compared the overall cost of component produced by SSM forming, conventional HPDC, SQC, and PMC, as listed in Table 3. This comparison clearly shows that SSM processing does not compete cost-wise with conventional HPDC, mainly because of the high cost of feedstock materials. However, SSM forming does compare favourably cost-wise with both SQC and PMC.

Flemings summarised the characteristics of SSM processing and potential benefits for further exploi-

Table 3 Comparison of cost elements and relative bottom-line component cost:¹⁷⁷ 1 represents lowest cost alternative; comparison values represent relative multiple of that

Cost	SSM forming	Die casting	Squeeze casting	Permanent mould casting
Material	2.5	1	1.25	1.25
Tooling	1	2	3	1.5
Capital	1.2	1	1.2	1
Labour	1.2	1.1	1.3	1
Heat treating	1	NA	3	3
Machining	1	1	1.2	2
Finishing	1	1.5	1	2
Bottom-line casting	2	1	2.2	3

tation at the first conference on SSM (see Table 4⁵). Many of the potential benefits listed have now been realised commercially at different levels. Based on this list, the enabling characteristics of SSM processing can be identified as the ability to:

- provide high integrity components, which are heat treatable
- provide improved mechanical properties of finished components
- produce components with complex shapes and tight dimensional control
- produce castings with thin walls
- cast materials not normally considered castable by conventional die casting, such as wrought alloys and alloys with high melting point
- provide high production rate.

With these enabling features in mind, there are several areas where SSM processing finds most of its applications:

- existing permanent mould parts where the near net shape capability of SSM can eliminate much of the machining and finishing
- parts that must be pressure tight and cannot be produced in conventional die casting, such as master brake cylinders, fuel rails, air conditioner compressor housing, and safety-critical parts
- high strength parts, such as engine mounts, steering knuckles, alloy wheels, tie rods, control arms, and seat belt retainer housings
- wear resistant parts that require hypereutectic alloys, such as unanodised mast cylinder, compressor piston, brake drums, and gearshift levers

Table 4 Characteristics of SSM processing for further exploitation⁵

Characteristics	Potential benefits and application
Lower heat content than liquid metal	Higher speed part forming Higher speed continuous casting Lower mould erosion Ferrous part forming Forming of high melting point materials Forming of reactive metals
Solid present at time of mould filling	Less shrinkage voids Less feeding required Less macrosegregation Fine grain structure
Viscosity higher than liquid metals, and controllable	Less entrapped mould gases Reduced oxides—improved mechinability Less mould attack Higher speed part forming Improved surface forming Automation New processes
Flow stress lower than for solid metals	Forming of intricate parts High speed part forming Lower cost part forming High speed forming of continuous shapes New processes
Ability to incorporate other materials	Composites
Ability to separate liquid and solid	Purification

● parts that are forged requiring excessive tooling. So far, there have been a number of successful applications of SSM processing technologies, as has been summarised in Refs. 163 and 292. In Europe, the three main current applications appear to be suspension parts, engine brackets, and fuel rails. Since 1998, Mercedes suspension arms and triangles have been in production at Alusuisse Singen. Stampal, while still producing the multilink parts of the Alfa Romeo Spider, is starting up an Alfa 156 front triangle. The Fiat Punto 8V and 16V engine brackets are produced by Stampal at a rate in excess of 2000 components per day. Florence Peillon is casting a component of Peugeot 206 bracket and other brackets are being developed. In Europe and in Brazil, Magneti Marelli produces a large number of fuel rails. Structural parts are a new sector for thixocasting. The three nodes for the new Renault (Matra) Avantime are examples of this type of part.¹⁷⁵ In the USA, the applications seem to be more diverse. In addition to fuel rails such as those produced by MKC, various mechanical parts are supplied, not only to the automobile industry, but also to the vast recreational market including snowmobiles and mountain bikes. In Asia, the applications of SSM processing appear to be focused mainly on electronic components using the thixomoulding process. These components include notebook computer cases, mobile phone cases, and other housing components.

In spite of the above mentioned industrial applications, the industrial acceptance of SSM processing as a production technology has to be said to be very slow after 30 years' research and development. It was argued by Eisen and Young²⁹³ that this rather slow market acceptance is due to two main barriers: the high materials price coupled with a limited number of suppliers and the inability for in-house material recycling. This argument is definitely valid, but may not fully explain the current situation. The research community is promoting SSM processing to industry, in particular the automobile industry, as a new full process technology. However, in this economically competitive world, a product is not judged only by its innovativeness, but also by its economics. Industry cannot be blamed for not accepting the technology on offer. Therefore, thinking should be concentrated on whether the technology in its current shape is good enough to be accepted industrially. Although the concept of SSM processing as a whole is undoubtedly innovative, thixocasting technology may not be robust enough as an industrial process. The recently revived rheocasting processes, such as NRC and TSRM, may speed up industrial acceptance, and promise a much brighter future for SSM processing.

Finally, in this section, the application of SSM processing technologies for the production of MMCs should be mentioned. As indicated in Flemings' summary (Table 4),⁵ the major advantage of SSM processing of MMCs is that the controllable viscosity of SSM slurries can be utilised to prevent macrosegregation of ceramic particles. Another advantage is the reduced interfacial reaction due to the reduced processing temperature. However, at microstructural level, SSM processing creates a less uniform distribution of ceramic particles compared to some of the

conventional MMC production routes. The resulting microstructure is effectively a hierarchical structure: the primary metallic phase of one or a few hundreds of micrometres in size is uniformly distributed in a MMC matrix with high volume fraction of ceramic particles of sizes ranging between a few and a few tens of micrometres.^{147,217} The amount of ceramic phase that can be successfully incorporated into the final MMC depends on the liquid fraction at SSM temperature.¹⁴⁷ If the liquid fraction is too high, the SSM processing advantage is lost, while too low a liquid fraction will only allow a limited amount of ceramic phase to be incorporated. Furthermore, the SSM processed MMC matrix is usually continuous and very brittle, and hence is responsible for the low strength and extremely low ductility observed for such MMCs (e.g. Ref. 294). Therefore, more effort is required to establish the overall benefit of SSM processing of MMCs. However, in other types of MMC, SSM processing might be useful. For example, thixoforming of spray formed, high silicon, aluminium alloys can increase the amount of silicon addition without the formation of a detrimental 3D silicon network and improve mechanical properties (e.g. Ref. 162); rheocasting of TiAl based intermetallic matrix composites has led to refined microstructure and improved mechanical properties (e.g. Ref. 295). Another potential application is to utilise fine ceramic particles for reducing the tendency for primary particle agglomeration during SSM processing. For this purpose, only a limited amount of ceramic particles is required.

Future development

In the previous sections, the progress made in various aspects of SSM processing has been reviewed. This would be useful for understanding the current status and the future prospects of SSM processing. In general, the progress made in the past 30 years on SSM processing, although a little slow, is very encouraging and has laid down a solid foundation for faster expansion both in scientific understanding and in technological development. There is no doubt that SSM processing will have a bright future and may give a facelift to the metallurgical processing industry. However, to achieve this goal, there is still a long way to go. Based on the current situation, it appears that future efforts should be directed to the following five areas: development of new processes, understanding the mechanisms for the formation of globular structure, development of new alloys for SSM processing, the rheological behaviour of SSM slurries, and microstructure–property relationships in SSM formed materials.

Process development

Currently, SSM processing is dominated by thixocasting using the feedstock produced by MHD continuous casting, which is a two-step process. One important fact responsible for the current situation is that the microstructure produced by MHD casting contains usually degenerated dendrites or rosettes, but not the spherical particles desirable for thixoforming. The MHD microstructure is therefore unsuitable for direct

forming, and reheating is required for morphological adjustment. However, in consideration of cost saving, energy efficiency, and process management, direct forming of slurries produced from the liquid alloy seems intuitively more attractive. This opinion was reflected strongly in the recent SSM conference held in Turin, Italy in September 2000.¹¹ A number of papers presented during the conference proposed that research effort should be directed towards the identification of new processing technologies, e.g. Refs. 11, 154, 155, 158–160.

It appears that an ideal process for SSM processing should contain the following characteristics:

- integration of slurry making and component shaping operation into one single process
- the slurry making operation should be efficient and capable of providing a microstructure comprising fine and spherical particles distributed uniformly in a liquid matrix
- efficient and accurate process control.

Mechanisms for formation of globular structure

Understanding of the mechanisms for the formation of globular structure is crucial to the successful development of SSM processing technologies. Although much progress has been made on this important aspect, there are still a number of fundamental questions deserving closer inspection. It appears that further research efforts should be directed to the following topics.

First, at present, the exact mechanism for the formation of globular structure during solidification under forced convection seems still unclear. More accurately controlled solidification experiments are required to establish the important factors influencing both nucleation and growth behaviour under forced convection. These factors may include: alloy composition, pouring temperature, the nature (laminar or turbulent) and intensity of melt flow, cooling rate, and the presence of grain refining agents. For this purpose, both analytical and numerical modelling may also prove to be very useful.

Second, it is important to understand the effects of the intensity and nature of the fluid flow (laminar or turbulent) on the nucleation and growth behaviour. So far, most of the investigations in this area have been focused primarily on laminar flows created by either mechanical or MHD stirring usually with relatively low intensity. The recent work^{115,116,119} using a TSRM machine capable of producing high shear rate and high intensity of turbulence has clearly identified the importance of turbulent flow with regard to the formation of fine and spherical solid particles. However, further work is required to quantify turbulent flow and to understand the physical interaction between turbulent flow and the solidification process.

Third, the solidification behaviour of the remaining liquid in the SSM slurry needs to be understood. If the formation of the solid particles in the SSM slurry is identified as primary solidification, the solidification of the remaining liquid in the SSM slurry can be called secondary solidification. The secondary solidi-

fication may have little significance to SSM processing itself, but it does have great implications regarding the mechanical properties of the final product. So far, there has been little attention paid to the secondary solidification.

Fourth, efforts are needed to understand solidification behaviour under various externally applied fields. This is not only scientifically important, but also has great implications with regard to the search for new processing technologies. Phenomenologically, it is well established that shear stress–strain field (mechanical stirring), magnetic field (MHD stirring), and ultrasonic field (ultrasonic vibration) have a strong influence on solidification behaviour. There have been reports in the literature that application of pulsed electrical field can also change significantly the solidification behaviour of alloys.^{296–299}

Finally, a better understanding of the physical nature of liquid metals and alloys may be very useful to both understanding the solidification process, nucleation in particular, and developing new solidification technologies. Historically, nearly all the research effort in solidification has been concentrated on the natural solidification process of alloys with a fixed composition at temperatures below their liquidus. So far, there have been few attempts to understand the physical nature of alloys above their liquidus.³⁰⁰ However, a significant difference between SSM processing and other solidification processes is the artificial interference with the solidification process of an external means. An insight into the physical nature of liquid metals may help to identify physical methods to interfere more effectively and positively with the nucleation process and eventually to develop more efficient solidification technologies.

Alloy development for SSM processing

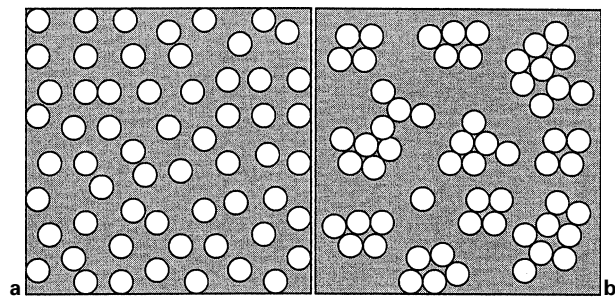
Currently, the alloys used for SSM processing are mainly cast alloys with a limited number of wrought alloys. However, wrought alloys have narrow processing windows for available SSM technologies, thus limiting further realisation of the full potential of SSM processing. Therefore, there has been a great demand for new alloys designed especially for SSM processing.

From this review, it appears that future work on alloy development for SSM processing should focus on the following areas:

- alloys designed for improved strength and ductility to match or exceed those of wrought alloys
- alloys designed to take specific advantages of SSM processing technologies such as heat treatability
- alloys designed to facilitate SSM processing, such as those with enlarged processing windows and lower tendency for particle agglomeration
- alloys designed for specific applications; this might be particularly necessary for automobile components.

Rheology of SSM slurries

Understanding the rheological behaviour has a direct influence on the successful development and effective control of SSM processes. Tremendous efforts have been made in the past decade initially on the rheology



a well dispersed; b heavily agglomerated

37 Schematic illustration of SSM processed microstructures with different distribution of primary phase

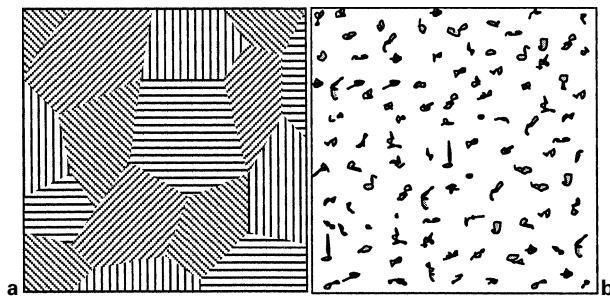
of SSM slurries of low solid fraction and more recently on those of high solid fraction. However, owing to the complexity of the rheology of SSM processing and the experimental difficulties associated with high temperature and high chemical reactivity, the rheology of SSM slurry is not well understood and accurate and well defined viscosity data are still scarce. It appears that future effort on this aspect should be directed to the following areas:

- development of more reliable techniques for rheological characterisation of SSM slurries
- understanding the effects of particle size and morphology on the rheological behaviour
- development of more realistic rheological models for SSM slurries, rigorous physical models for an improved scientific understanding, and phenomenological models for process simulation.

Microstructure–property relationships in SSM formed samples

The final microstructure of SSM formed parts can be generally described as a two phase microstructure in which a given volume fraction of the soft primary phase of globular morphology is distributed in a relatively hard matrix formed by solidification of the remaining liquid phase in the semisolid state. Basically, this is a composite structure, as illustrated schematically in Fig. 37 for solid fraction $f_s = 0.34$. However, different from the conventional composite structure, the variation of the primary volume fraction in SSM formed microstructure changes not only the mechanical properties of the primary phase, but also those of the matrix due to the change of chemical composition of both the primary phase and the matrix. Moreover, the matrix is not a homogeneous single phase, but a multiphase mixture, as shown in Fig. 38.

Such characteristics of SSM formed microstructure will result in a complex relationship between the microstructure and the mechanical properties. At a specified solid fraction, a homogeneous dispersion of the solid phase (Fig. 37a) results in a 0–3 structure, where the solid phase is 0D continuous and the matrix is 3D continuous. This resembles a metal toughened ceramic matrix composite. According to general composite theory, a less uniform distribution of the solid phase (e.g. Fig. 37b) might be more suitable for improving ductility than a homogeneous



a regular; b divorced

38 Schematic illustration of possible eutectic morphologies in SSM processed alloys

dispersion. In addition, the phase distribution in the matrix may play an important role in determining the mechanical properties of the final component, if not more important than the primary phase. The matrix usually contains a brittle phase, such as silicon and/or intermetallics. A coupled eutectic structure (Fig. 38a) results in higher strength but lower ductility, while a divorced eutectic structure (Fig. 38b) can offer a better combination of strength and ductility. Of course, the final properties of the SSM formed parts depend on the interplay between volume fraction, size, morphology, and distribution of all the relevant phases, which, in turn, are affected by processing conditions.

It is desirable to understand the effects on mechanical properties of microstructural parameters, such as volume fraction, size, morphology, and distribution of the primary phase, and of the phase arrangement in the matrix. So far, there has been very limited attention devoted to this aspect of SSM processing research. More investigations should be made both theoretically and experimentally to establish the relationships between SSM formed microstructure and the mechanical properties of the final part. This is a complex task, which may involve process development, alloy design, and schedules for heat treatment. For this purpose, the available knowledge of composite materials may provide useful guidance.

Acknowledgements

The author would like to thank Professor M. J. Bevis for his useful comments, and colleagues, Dr S. Ji, Dr A. Das, Dr Y. Q. Liu, and Dr X. Fang, for their valuable comments and help with the preparation of the manuscript.

References

1. D. B. SPENCER: PhD thesis, MIT, Cambridge, MA, 1971.
2. D. B. SPENCER, R. MEHRABIAN, and M. C. FLEMINGS: *Metall. Trans.*, 1972, **3**, 1925–1932.
3. R. MEHRABIAN and M. C. FLEMINGS: *Trans. AFS*, 1972, **80**, 173–182.
4. S. B. BROWN and M. C. FLEMINGS: *Adv. Mater. Process.*, 1993, **143**, 36–40.
5. M. C. FLEMINGS: Proc. 6th Int. Conf. on 'Semisolid processing of alloys and composites', (ed. G. L. Chiarmetta and M. Rosso), Turin, Italy, Sept. 2000, 11–14; 2000, Brescia, Edimet.
6. 1st Int. Conf. on 'Semisolid processing of alloys and composites', Ecole Nationale Supérieure des Mines de Paris, Société

Française de Metallurgie, Cemef, Sophia-Antipolis, France, 1990 (Abstracts).

7. S. B. BROWN and M. C. FLEMINGS (eds.): Proc. 2nd Int. Conf. on 'Semisolid processing of alloys and composites', Cambridge, MA, June 1992; 1992, Warrendale, PA, TMS.
8. M. KIUCHI (ed.): Proc. 3rd Int. Conf. on 'Semisolid processing of alloys and composites', University of Tokyo, Japan, 1994; 1994, Tokyo, Institute of Industrial Science.
9. D. H. KIRKWOOD and P. KAPRANOS (eds.): Proc. 4th Int. Conf. on 'Semisolid processing of alloys and composites', Sheffield, UK, June 1996; 1996, The University of Sheffield.
10. A. K. BHASIN, J. J. MOORE, K. P. YOUNG, and S. MIDSON (eds.): Proc. 5th Int. Conf. on 'Semisolid processing of alloys and composites', Golden, CO, June 1998; 1998, Golden, CO, Colorado School of Mines.
11. G. L. CHIARMETTA and M. ROSSO (eds.): Proc. 6th Int. Conf. on 'Semisolid processing of alloys and composites', Turin, Italy, Sept. 2000; 2000, Brescia, Edimet.
12. M. C. FLEMINGS: *Metall. Trans. A*, 1991, **22A**, 957–981.
13. D. H. KIRKWOOD: *Int. Mater. Rev.*, 1994, **39**, 173–189.
14. P. A. JOLY and R. MEHRABIAN: *J. Mater. Sci.*, 1976, **11**, 1393–1418.
15. M. SUERY, C. L. MARTIN, and L. SALVO: in Ref. 9, pp. 21–29.
16. H. K. MOON: 'Rheological behavior and microstructure of ceramic particulate/aluminum alloy composites', PhD thesis, MIT, Cambridge, MA, 1990.
17. L. S. TURNG and K. K. WANG: *J. Mater. Sci.*, 1991, **26**, 2173–2183.
18. P. KUMAR, C. L. MARTIN, and S. B. BROWN: *Metall. Trans. A*, 1993, **24A**, 1107–1116.
19. A. J. QUAAK and W. H. KOOL: *Mater. Sci. Eng.*, 1994, **A188**, 277–282.
20. M. MADA and F. AJERSCH: *Mater. Sci. Eng.*, 1996, **A212**, 171–177.
21. A. R. A. McLELLAND, N. G. HENDERSON, H. V. ATKINSON, and D. H. KIRKWOOD: *Mater. Sci. Eng.*, 1997, **A232**, 110–118.
22. F. C. YEE: PhD thesis, Nanyang University of Technology, Singapore, 1999.
23. M. MODIGELL and J. KOKE: *Mech. Time-Depend. Mater.*, 1999, **3**, 15–30.
24. M. MODIGELL, J. KOKE, R. KOPP, D. NEUDENBERGER, P. R. SAHM, and O. KLAASSEN: in Ref. 11, pp. 605–609.
25. V. LAXMANAN and M. C. FLEMINGS: *Metall. Trans. A*, 1980, **11A**, 1927–1937.
26. M. SUERY and M. C. FLEMINGS: *Metall. Trans. A*, 1982, **13A**, 1809–1819.
27. A. L. MARTIN, D. FAVIER, and Y. M. SUÉRY: *Int. J. Plast.*, 1997, **13**, 215–235, 237–259.
28. P. KAPRANOS, D. H. KIRKWOOD, and M. R. BARKHUDROV: in Ref. 10, pp. 11–19.
29. E. TZIMAS and A. ZAVALIANGOS: *Acta Mater.*, 1999, **47**, 517–528.
30. A. M. DE FIGUEREDO, A. KATO, and M. C. FLEMINGS: in Ref. 11, pp. 477–482.
31. W. R. LOUE, M. SUERY, and J. L. QUERBES: in Ref. 7, p. 266.
32. P. SECONDEL, E. VALETTE, and F. LEROY: in Ref. 7, p. 306.
33. P. SCHUMMER and R. H. WORTHOFF: *Chem. Eng. Sci.*, 1978, **33**, 759–763.
34. J. KOKE and M. MODIGELL: Proc. Int. Symp. on 'Advanced forming die manufacturing technology', Pusan, Korea, 1999, 101–106; *J. Mater. Process. Technol.*, 2001, **111**, (1–3), 53–58.
35. H. PENG and K. K. WANG: in Ref. 9, pp. 2–9.
36. J. KOKE, M. HUFSCHEIDT, M. MODIGELL, C. HEINE, S. HAN, S. STAPF, and J. PETERA: in Ref. 11, pp. 623–628.
37. H. LEHUY, J. MASOUNAVE, and J. BLAIN: *J. Mater. Sci.*, 1985, **20**, 105–113.
38. W. S. NAN, S. GUANGJI, and Y. HANGUO: *Mater. Trans., JIM*, 1990, **31**, 715–722.
39. T. Z. KATTAMIS and T. J. PICCONE: *Mater. Sci. Eng.*, 1991, **A131**, 265–272.
40. Y. ITO, M. C. FLEMINGS, and J. A. CORNEI: in 'Nature and properties of semi-solid materials', (ed. J. A. Sekhar and J. A. Dantzig), 3–17, 1992, Warrendale, PA, TMS.
41. W. R. LOUE: PhD thesis, INPG, Grenoble, 1992.
42. M. A. TAHA, N. A. ELMAHALLAWY, and A. M. ASSAR: *J. Mater. Sci.*, 1988, **23**, 1379–1390.
43. M. C. FLEMINGS, S. F. CHEN, I. DIENWANIT, and J. A. CORNEI: in Ref. 7, pp. 202–210.
44. C. J. QUAAK, L. KATGERMAN, and W. H. KOOL: in Ref. 9, pp. 35–39.
45. H. A. BARNES and K. WALTERS: *Rheol. Acta*, 1985, **24**, 323–326.

46. J. P. HARTNETT and R. Y. Z. HU: *J. Rheol.*, 1989, **33**, 671–679.
47. G. K. SIGWORTH: *Can. Metall. Q.*, 1996, **35**, 101–122.
48. S. SANNES, H. GJESTLAND, L. ARNBERG, and J. K. SOLBERG: in Ref. 8, pp. 271–280.
49. C. L. MARTIN, P. KUMAR, and S. B. BROWN: *Acta Metall. Mater.*, 1994, **42**, 3603–3614.
50. M. MODIGELL, J. KOKE, and J. PETERA: in Ref. 10, pp. 317–326.
51. M. MADA and F. AJERSCH: *Mater. Sci. Eng.*, 1996, **A212**, 157–170.
52. M. SUERY and A. ZAVALIANGOS: in Ref. 11, pp. 129–135.
53. A. N. ALEXANDROU, G. R. BURGOS, and V. M. ENTOV: in Ref. 11, pp. 161–167.
54. P. KUMAR, C. L. MARTIN, and S. B. BROWN: *Acta Metall. Mater.*, 1994, **42**, 3595–3602.
55. M. PEREZ, J. C. BARBE, Z. NEDA, Y. BRECHET, and L. SALVO: *Acta Mater.*, 2000, **48**, 3773–3782.
56. J. Y. CHEN and Z. FAN: *Mater. Sci. Technol.*, 2002, **18**, (3), 237–242.
57. Z. FAN and J. Y. CHEN: *Mater. Sci. Technol.*, 2002, **18**, (3), 243–249.
58. W. H. HERSCHEL and R. BUCKLEY: *Proc. ASTM*, 1962, Vol. 26, pp. 621–633.
59. H. A. BARNES: *J. Non-Newton. Fluid Mech.*, 1999, **18**, 133–178.
60. M. M. CROSS: *J. Colloid. Sci.*, 1965, **20**, 417–437.
61. D. C.-H. CHENG: *Int. J. Cosmetic Sci.*, 1987, **9**, 151–191.
62. D. H. KIRKWOOD, P. J. WARD, M. BARKHUDAROV, S. B. CHIN, H. V. ATKINSON, and T. Y. LIU: in Ref. 11, pp. 545–551.
63. A. ZAVALIANGOS and A. LAWLEY: *J. Mater. Eng. Perform.*, 1995, **4**, 40–47.
64. A. L. MARTIN, S. B. BROWN, D. FAVIER, and M. SUERY: *Mater. Sci. Eng.*, 1995, **A202**, 112–122.
65. J. KOKE, M. MODIGELL, and J. PETERA: *Appl. Mech. Eng.*, 1999, **4**, 345–350.
66. G. R. BURGOS and A. N. ALEXANDROU: *J. Rheol.*, 1999, **43**, 485–498.
67. J. Y. CHEN and Z. FAN: *Mater. Sci. Technol.*, 2002, **18**, (3), 250–257.
68. M. HIRAI, K. TAKEBAYASHI, Y. YOSHIKAWA, and R. YAMAGUCHI: *ISIJ Int.*, 1993, **33**, 405–412.
69. W. R. LOUE, J. L. QUERBES, and M. SUERY: in Ref. 7, p. 266.
70. W. R. LOUE and M. SUERY: *Mater. Sci. Eng.*, 1995, **A203**, 1–13.
71. R. S. QIN and Z. FAN: *Mater. Sci. Technol.*, 2001, **17**, 1149–1152.
72. Z. FAN and J. Y. CHEN: *Mater. Sci. Technol.*, 2002, **18**, (3), 258–267.
73. J. A. YURKO, A. M. DE FIGUEREDO, and M. C. FLEMINGS: in Ref. 11, pp. 681–686.
74. T. BASNER, R. PEHLKE, and A. SACHDEV: *Metall. Trans. A*, 2000, **31A**, 57–62.
75. L. SALVO, M. SUERY, Y. DE CHARENTENAY, and W. LOUE: in Ref. 9, pp. 10–15.
76. A. ZAVALIANGOS, E. TZIMAS, A. LAWLEY, and C. PUMBURGER: in Ref. 9, pp. 40–46.
77. T. G. N'GUYEN, D. FAVIER, and M. SUERY: *Int. J. Plast.*, 1994, **10**, 663–693.
78. J. C. GEBELIN, D. FAVIER, and M. SUERY: in Ref. 10, pp. 309–316.
79. G. R. BURGOS, A. N. ALEXANDROU, and V. ENTOV: in Ref. 10, pp. 217–224.
80. C. C. MEI and J.-L. AURIAULT: *J. Fluids Mech.*, 1991, **222**, 647–663.
81. J.-C. GEBELIN, C. GEINDREAU, L. ORGEAS, P. POYER, D. FAVIER, and J.-L. AURIAULT: in Ref. 11, pp. 155–160.
82. J.-C. GEBELIN: PhD thesis, INPG, Grenoble, France, 2000.
83. E. SKEJETNE and J.-L. AURIAULT: *Trans. Porous Media*, 1999, **36**, 131–47.
84. L. A. LALLI: *Metall. Trans. A*, 1985, **16A**, 1393–1403.
85. M. ABOUAF and J. L. CHENOT: *J. Theor. Appl. Mech.*, 1986, **5**, 121–140.
86. A. ZAVALIANGOS and L. ANAND: *J. Mech. Solids*, 1993, **41**, 1087–1118.
87. A. ZAVALIANGOS: *Int. J. Mech. Sci.*, 1999, **40**, 1029–1041.
88. E. E. UNDERWOOD: 'Quantitative stereology'; 1972, Reading, MA, Addison-Wesley.
89. E. TZIMAS and A. ZAVALIANGOS: *J. Mater. Sci.*, 2000, **35**, 5319–5329.
90. J. S. LANGER: *Rev. Mod. Phys.*, 1980, **52**, 1–58.
91. B. B. MANDELROT, D. E. PASSOJA, and A. J. PAULLAY: *Nature*, 1984, **308**, 721.
92. K. J. MALOY, A. HANSEN, E. L. HINRICHSON, and S. ROUX: *Phys. Rev. Lett.*, 1992, **68**, 213–216.
93. J. J. FRIEL and C. S. PANDE: *J. Mater. Res.*, 1993, **8**, 100.
94. J. M. LI, L. LU, Y. SU, and M. O. LAI: *J. Appl. Phys.*, 1999, **86**, 2526–2532.
95. P. MEAKIN: *Phys. Rev.*, 1983, **27A**, 1495–1507.
96. S. VERRIER, C. JOSSEYOND, L. SALVO, M. SUERY, P. CLOETENS, and W. LUDWIG: in Ref. 11, pp. 423–428.
97. J. GURLAND: *Trans. AIME*, 1958, **212**, 452.
98. H. C. LEE and J. GURLAND: *Mater. Sci. Eng.*, 1978, **33A**, 125.
99. G. C. GULLO, K. STEINHOFF, and P. J. UGGOWITZER: in Ref. 11, pp. 367–372.
100. K. STEINHOFF, G. C. GULLO, R. KOPP, and P. J. UGGOWITZER: in Ref. 11, pp. 121–127.
101. S. SANNES, H. GJESTLAND, L. AMBERG, and J. K. SOLBERG: in Ref. 8, pp. 75–84.
102. T. L. WOLFSBORF, W. H. BENDER, and P. W. VOORHEES: *Acta Mater.*, 1997, **45**, 2279–2295.
103. B. NIROUMAND and K. XIA: in Ref. 10, pp. 637–644.
104. B. NIROUMAND and K. XIA: *Mater. Sci. Eng.*, 1999, **A283**, 70–75.
105. L. ARNBERG, A. BARDAL, and H. SAUD: *Mater. Sci. Eng.*, 1999, **A262**, 300–303.
106. M. C. FLEMINGS: 'Solidification processing'; 1974, New York, McGraw-Hill.
107. W. J. BOETTINGER, S. R. CORIELL, A. L. GREER, A. KARMA, W. KURZ, M. RAPPAZ, and R. TRIVEDI: *Acta Mater.*, 2000, **48**, 43–70.
108. A. M. MULLIS, S. E. BATTERSBY, and H. L. FLETCHER: in Ref. 10, pp. 233–240.
109. A. VOGEL, R. D. DOHERTY, and B. CANTOR: in 'Solidification and casting of metals', 518–525; 1979, London, The Metals Society.
110. M. A. TAHA and N. A. EL-MAHALLAWY: Proc. 46th Int. foundry Congress, Madrid, Spain, 1979, paper 15.
111. N. APAYDIN, K. V. PRABHAKAR, and R. D. DOHERTY: *Mater. Sci. Eng.*, 1980, **46**, 145–150.
112. J. C. van DAM and F. H. MISCHGOSFSKY: *J. Mater. Sci.*, 1982, **17**, 989–993.
113. J. M. M. MOLENAAR, F. W. H. C. SALEMANS, and L. KATGERMAN: *J. Mater. Sci.*, 1985, **20**, 4335–4344.
114. D. M. SMITH, J. A. EADYL, M. HOGAN, and D. W. IRWIN: *Metall. Trans. A*, 1991, **22A**, 575–584.
115. S. JI and Z. FAN: in Ref. 11, pp. 723–728.
116. S. JI and Z. FAN: *Metall. Mater. Trans.*, submitted 2001.
117. Y. H. RYOO and D. H. KIM: in Ref. 8, pp. 95–104.
118. S. JI, Z. FAN, and M. J. BEVIS: *Mater. Sci. Eng.*, 2001, **A299**, 210–217.
119. A. DAS, S. JI, and Z. FAN: *Mater. Sci. Eng. A*, submitted 2001.
120. J. F. SECONDE and M. SUERY: *J. Mater. Sci.*, 1984, **19**, 3995–4006.
121. Y. S. YANG and C. Y. A. TSAO: *Scr. Metall. Mater.*, 1994, **30**, 1541–1546.
122. C. P. CHEN and C. Y. A. TSAO: *J. Mater. Sci.*, 1995, **30**, 4019–4026.
123. J. L. WANG, Y. H. SU, and C. Y. A. TSAO: *Scr. Mater.*, 1997, **37**, 2003–2007.
124. S. JI and Z. FAN: *J. Mater. Sci.*, submitted 2001.
125. A. MORTENSEN: *Metall. Trans. A*, 1989, **20A**, 247.
126. K. P. YOUNG and D. H. KIRKWOOD: *Metall. Trans. A*, 1975, **6A**, 197.
127. T. Z. KATTAMIS, J. C. COUGHLIN, and M. C. FLEMINGS: *Trans. AIME*, 1967, **239**, 1504.
128. S. ANNAVAPU and R. D. DOHERTY: *Acta Metall. Mater.*, 1995, **43**, 3207–3230.
129. S. JI and Z. FAN: 'Metastable effects obtained by solidification of eutectic Sn–Pb alloy under intensive forced convection', Internal Report, Brunel University, Uxbridge, UK, 2002.
130. A. VOGEL and B. CANTOR: *J. Cryst. Growth*, 1977, **37**, 309–316.
131. B. CANTOR and A. VOGEL: *J. Cryst. Growth*, 1977, **41**, 109–123.
132. A. VOGEL: PhD thesis, University of Sussex, UK, 1977.
133. W. M. MULLINS and R. F. SEKERKA: *J. Appl. Phys.*, 1963, **34**, 323.
134. R. D. DOHERTY, H. I. LEE, and E. A. FEEST: *Mater. Sci. Eng.*, 1984, **A65**, 181–189.
135. H. I. LEE, R. D. DOHERTY, E. A. FEEST, and J. M. TITCHMARSH: in 'Solidification technology in the foundry and casthouse', 119; 1983, London, The Metals Society.
136. A. HELLAWELL: in Ref. 9, pp. 60–65.
137. Z. FAN, M. J. BEVIS, and S. JI: 'Method and apparatus for producing semisolid metal slurries and shaped components', PCT/WO/01/21343 A1, 1999.
138. A. M. MULLIS: *Acta Mater.*, 1999, **47**, 1783–1789.
139. R. S. QIN and Z. FAN: in Ref. 11, pp. 819–824.
140. A. DAS, S. JI, and Z. FAN: *Acta Mater.*, submitted 2001.
141. I. SEYHAN, L. RATKE, W. BENDER and P. W. VOORHEES: *Metall. Mater. Trans.*, 1996, **17A**, 2470–2478.

142. M. BRACCINI, L. SALVO, and M. SUERY: in Ref. 10, pp. 371–378.
143. E. J. ZOQUI and M. H. ROBERT: *J. Mater. Process. Technol.*, 2001, **109**, 215–219.
144. I. M. LIFSHITZ and V. V. SLYOZOV: *J. Phys. Chem. Solids*, 1961, **19**, 35–50.
145. C. WAGNER: *Z. Elektrochem.*, 1961, **65**, 581–591.
146. S. BLAIS, W. LOUE, and C. PLUCHON: in Ref. 9, pp. 187–192.
147. T. W. HONG, S. K. KIM, H. S. HA, M. G. KIM, D. B. LEE, and Y. J. KIM: *Mater. Sci. Technol.*, 2000, **16**, 887–892.
148. W. YUNHUA, Z. MINGFANG, G. ZHIQIANG, and S. HUAQIN: in Ref. 10, pp. 693–698.
149. E. TZIMAS and A. ZAVALIANGOS: *Mater. Sci. Eng.*, 2000, **A289**, 217–227.
150. S. TAKAJO, W. A. KAYSSER, and G. PETZOW: *Acta Metall.*, 1984, **32**, 107–113.
151. G. WAN and P. R. SAHM: in Ref. 7, pp. 328–335.
152. S. P. MARSH, M. E. GLICKSMAN, L. MELERO, and K. TSUTSUMI: in 'Modelling of casting and welding processes IV'; 1988, Warrendale, PA, TMS.
153. T. WITULSKI, U. MORJAN, I. NIEDICK, and G. HIRT: in Ref. 10, pp. 353–360.
154. S. EAGLER, D. HARTMAN, and I. NIEDICK: in Ref. 11, pp. 483–488.
155. H. V. ATKINSON, P. KAPRANOS, and D. H. KIRKWOOD: in Ref. 11, pp. 443–450.
156. Y. Q. LIU and Z. FAN: 'Critical assessment of thermal properties of Al-alloys', Internal Report, Brunel University, Uxbridge, UK, 2001.
157. R. CREMER, A. WINKELMANN, and G. HIRT: in Ref. 9, pp. 159–164.
158. D. APELIAN: in Ref. 11, pp. 47–54.
159. G. HIRT: in Ref. 11, pp. 55–60.
160. W. L. WINTERBOTTOM: in Ref. 11, pp. 73–78.
161. M. GARAT, S. BLAIS, C. PLUCHON, and W. R. LOUE: in Ref. 10, pp. 199–213.
162. P. J. WARD, H. V. ATKINSON, P. R. G. ANDERSON, L. G. ELIAS, B. GARCIA, L. KAHLEN, and J. M. RODRIGUEZ-IBABE: *Acta Mater.*, 1996, **44**, 1717–1727.
163. M. GARAT, L. MAENNER, and Ch. SZTUR: in Ref. 11, pp. 187–194.
164. W. WAGENER and D. HARTMANN: in Ref. 11, pp. 301–306.
165. G. COLE: in Proc. International Magnesium Association Conf.: IMA52, San Francisco, CA, May 1995, 1; 1995, McLean, VA, IMA.
166. Y. Q. LIU and Z. FAN: *Mater. Sci. Eng. A*, submitted 2001.
167. S. H. JUANG, S.-M. WU, C.-Y. MA, and H. PENG: in Ref. 11, pp. 705–710.
168. X. P. NIU, B. H. HU, S. W. HAO, F. C. YEE, and I. PINWILL: in Ref. 10, pp. 141–148.
169. R. SHIBATA, T. KANEUCHI, T. SOUDA, H. YAMANE, and T. UMEDA: in Ref. 10, pp. 465–470.
170. K. SUKUMARAN, S. G. K. PILLAI, K. K. RAVIKUMAR, K. S. PRAVEEN, V. S. KELUKUTTY, and T. SOMAN: in Ref. 10, pp. 379–385.
171. G. L. CHIARMETTA: in Ref. 9, pp. 204–207.
172. S. C. BERGSMA, X. LI, and M. E. KASSNER: *Mater. Sci. Eng.*, 2001, **A297**, 69–77.
173. B. WINDINGER: in Ref. 9, pp. 239–241.
174. R. FINK and T. WITULSKI: in Ref. 10, pp. 557–564.
175. P. GIORDANO, F. BOERO, and G. L. CHIARMETTA: in Ref. 11, pp. 29–34.
176. K. P. YOUNG and P. EISEN: in Ref. 11, pp. 97–102.
177. J. L. JORSTAD: in Ref. 11, pp. 227–233.
178. S. C. BERGSMA, M. E. KASSNER, E. EVANGELISTA, and E. CERRI: in Ref. 11, pp. 319–324.
179. S. C. BERGSMA, M. C. TOLLE, M. E. KASSNER, X. LI, and E. EVANGELISTA: *Mater. Sci. Eng.*, 1997, **A237**, 24–34.
180. J. R. DAVIS: 'Aluminium and aluminium alloys', 102–114, 533, 722–725; 1993, Materials Park, OH, ASM International.
181. F. BOERO, G. L. CHIARMETTA, and P. GIORDANO: in Ref. 11, pp. 581–586.
182. M. ROSSO, C. MUS, and G. L. CHIARMETTA: in Ref. 11, pp. 209–214.
183. P. KAPRANOS, D. H. KIRKWOOD, H. V. ATKINSON, J. T. RHEINLANDER, J. J. BENTZEN, P. T. TOFT, C. P. DEBEL, G. LESLAZ, L. MAENNER, S. BLAIS, J. M. RODRIGUEZ-IBABE, L. LASA, P. GIORDANO, and G. L. CHIARMETTA: in Ref. 11, pp. 741–745.
184. J. R. DAVIS: 'Aluminium and aluminium alloys', 653–698; 1993, Materials Park, OH, ASM International.
185. G. TAUSIG and K. XIA: in Ref. 10, pp. 473–480.
186. G. TAUSIG: in Ref. 11, pp. 489–494.
187. H. KAUFMANN, H. WABUSSEG, and P. J. UGGOWITZER: in Ref. 11, pp. 457–462.
188. E. O. HALL: *Proc. Phys. Soc. London*, 1951, **864B**, 747.
189. N. J. PETCH: *J. Iron Steel Inst.*, 1953, **174**, 25.
190. Z. FAN: *Mater. Sci. Eng.*, 1995, **A191**, 73–83.
191. M. BADIALI, C. J. DAVIDSON, J. R. GRIFFITHS, and A. ZANADA: in Ref. 11, pp. 349–354.
192. J.-P. GABATHULER, H. J. HUBBR, and J. ERLING: Proc. Int. Conf. on 'Aluminium alloys: new processing technologies', Ravenna, Italy, June 1993, 169–180; 1993, Milan, Associazione Italiana di Metallurgia.
193. J. VALER GONI, J. M. RODRIGUEZ-IBABE, and J. J. URCOLA: *Scr. Mater.*, 1995, **34**, 483–489.
194. J. VALER, J. M. RODRIGUEZ-IBABE, and J. J. URCOLA: in Ref. 9, pp. 326–330.
195. C. C. FERREIRA and J. P. TEIXEIRA: in Ref. 11, pp. 337–342.
196. K. P. YOUNG: in Ref. 9, pp. 229–233.
197. S. LEBEAU and R. DECKER: in Ref. 10, pp. 387–395.
198. S. SUK, B. LISIECKI, and J. COLLOT: in Ref. 11, pp. 729–734.
199. M. M. AVEDESIAN and H. BAKER: 'Magnesium and magnesium alloys', 92; 1999, Materials Park, OH, ASM International.
200. R. D. CARNAHAN: in Ref. 8, pp. 65–74.
201. R. D. CARNAHAN, R. HATHAWAY, R. KILBERT, L. PASTERNAK, and P. ROHATGI: Proc. Int. Symp. on 'Light metals processing and applications', Quebec City, PQ, Aug./Sept. 1993, 325; 1993, Montreal, PQ, CIM.
202. D. GHOSH, K. KANG, C. BACH, J. G. ROEMER, and C. van SCHILT: Proc. 34th Ann. Conf. of Metallurgists 'Recent metallurgical advances in light metals industries', Vancouver, BC, Aug. 1995, 481; 1995, Montreal, PQ, CIM.
203. F. CZERWINSKI, A. ZIELINSKA, P. J. PINET, and J. OVERBEEKE: *Acta Mater.*, 2001, **49**, 1225–1235.
204. T. LIECHTI, Z. W. CHEN, C. J. DAVIDSON, and A. K. DAHLE: in Ref. 10, pp. 505–512.
205. P. R. SAHM: in Ref. 10, pp. XL1–L.
206. M. C. FLEMINGS, R. G. RIEK, and K. P. YOUNG: *Mater. Sci. Eng.*, 1976, **25**, 103–117.
207. Y. SUMARTHA, A. M. DE FIGUEREDO, and M. C. FLEMINGS: in Ref. 10, pp. 57–67.
208. E. L. BROWN and K. P. YOUNG: *Die Cast. Eng.*, Nov./Dec. 1999, 70–78.
209. M. P. KENNEY, J. A. COURTOIS, R. D. EVANS, G. M. FARRIOR, C. P. KYONKA, A. A. KOCH, and K. P. YOUNG: in 'Metals handbook', 9th edn, Vol. 15, 327–338; 1988, Metals Park, OH, ASM International.
210. J. P. GABATHULER, D. BARRAS, Y. KRÄHENBÜHL, and J. C. WEBER: in Ref. 7, pp. 33–46.
211. W. R. LOUE, M. BRIMONT, and M. GARAT: Proc. Conf. on 'Die casting technology', Indianapolis, IN, 1995, 389; 1995, Rosemont, IL, North American Die Casting Association.
212. M. ZILLGEN and G. HIRT: in Ref. 9, pp. 180–186.
213. W. KAHRMANN, R. SCHRAGNER, and K. P. YOUNG: in Ref. 9, pp. 154–158.
214. O. J. ILEGBUSI and J. SZEKELY: *Trans. Iron Steel Inst. Jpn*, 1988, **28**, 97–103.
215. K. E. BLAZEK, J. E. KELLY, and N. S. POTTORRE: *ISIJ Int.*, 1995, **35**, 813–818.
216. C. VIVES: *Metall. Trans. B*, 1992, **23B**, 189–206.
217. C. VIVES, J. BAS, G. BELTRAN, and G. FONTAINE: *Mater. Sci. Eng.*, 1993, **A173**, 239–242.
218. S. FINKE, M. SUERY, C. L. MARTIN, and W. WEI: in Ref. 11, pp. 169–174.
219. F. NIEDERMAIER, J. LANGGARTNER, G. HIRT, and I. NIEDICK: in Ref. 10, pp. 407–414.
220. C. PLUCHON, W. R. LOUE, P. Y. MENET, and M. GARAT: in 'Light metals 1995', (ed. J. W. Evans), 1233–1242; 1995, Warrendale, PA, TMS.
221. European Patent Specification: EP 0 071 822 B2, Alumax Inc., 1982.
222. K. HALL, H. KAUFMANN, and A. MUNDL: in Ref. 11, pp. 23–28.
223. K. P. YOUNG, C. P. KYONKA, and J. A. COURTOIS: 'Fine grained metal composition', US Patent 4,415,374, 1983.
224. L. ELIAS BOYED, D. H. KIRKWOOD, and C. M. SELLARS: Proc. 2nd World Basque Cong. on 'New structural materials', Spain, 1988, Servicio Central de Publicaciones del Gobierno Vasco, 285–295.
225. D. H. KIRKWOOD and P. KAPRANOS: *Met. Mater.*, 1989, **5**, (1), 16–19.
226. A. TURKELI and N. AKBAS: in Ref. 9, pp. 71–74.
227. J. C. CHOI, H. Y. CHO, G. S. MIN, H. J. PARK, and J. U. CHOI: *J. Korean Soc. Precis. Eng.*, 1996, **13**, 29–35.

228. J. C. CHOI and H. J. PARK: in Ref. 10, pp. 457–464.
229. J. VALER J. P. MENESES, F. SAINT-ANTONIN, and M. SUERY: *Mater. Sci. Eng.*, 1999, **A272**, 342–350.
230. J. VALER, F. SAINT-ANTONIN, P. MENESES, and M. SUERY: in Ref. 10, pp. 3–10.
231. J. C. CHOI and H. J. PARK: *J. Mater. Process. Technol.*, 1998, **82**, 107–116.
232. E. TZIMAS and A. ZAVALIANGOS: *Mater. Sci. Eng.*, 2000, **A289**, 228–240.
233. P. R. UNDERHILL, P. S. GRANT, D. J. BRYANT, and B. CANTOR: *J. Mater. Synth. Proc.*, 1995, **3**, 171.
234. K. XIA and G. TAUSIG: *Mater. Sci. Eng.*, 1998, **A246**, 1–10.
235. R. SHIBATA: in Ref. 10, pp. LI–LVI.
236. H. WANG, C. J. DAVIDSON, and D. H. St JOHN: in Ref. 11, pp. 149–154.
237. H. WANG, D. H. St JOHN, C. J. DAVIDSON, and M. J. COUPER: *Aluminium Trans.*, 2000, **2**, 57–66.
238. H. WANG, D. H. St JOHN, C. J. DAVIDSON, and M. J. COUPER: *Mater. Sci. Forum*, 2000, **329–330**, 449–454.
239. J. CUI, G. LU, J. DONG, and K. XIA: in Ref. 11, pp. 701–704.
240. J. A. YURKO, X. P. NIU, and I. PINWILL: *J. Mater. Sci. Lett.*, 1999, **18**, 1869–1870.
241. B. CHALMERS: *J. Australian Inst. Met.*, 1963, **8**, 255.
242. H. BILONI and B. CHALMERS: *J. Mater. Sci.*, 1968, **3**, 139.
243. D. R. UHLMANN, T. P. SEWARD III, and B. CHALMERS: *Trans. AIME*, 1966, **236**, 527.
244. Z. FAN, S. JI, and M. J. BEVIS: PCT/GB01/03596, 2000.
245. S. JI, A. DAS, and Z. FAN: 'Solidification structure of liquidus rheocast Sn–Pb alloys', Internal Report, Brunel University, Uxbridge, UK, 2001.
246. V. I. DOBATKIN, A. F. BELOV, and G. I. ESKIN: *Vestnik Akad. Nauk SSSR*, 1984, **1**, 139.
247. V. I. DOBATKIN and G. I. ESKIN: in Ref. 9, pp. 193–196.
248. C. LIU, Y. PAN, and S. AOYAMA: in Ref. 10, pp. 439–447.
249. G. I. ESKIN and V. N. SEREBRYANY: in Ref. 11, pp. 361–366.
250. V. O. ABRAMOV, O. V. ABRAMOV, B. B. STRAUMAL, and W. GUST: *Mater. Des.*, 1997, **18**, 323–326.
251. V. ABRAMOV, O. ABRAMOV, V. BULGAKOV, and F. SOMMER: *Mater. Lett.*, 1998, **37**, 27–34.
252. V. ABRAMOV: 'Ultrasound in liquid and solid metals'; 1994, Boca Raton, FL, CRC Press.
253. M. EASTON and D. St JOHN: *Metall. Mater. Trans. A*, 1999, **30A**, 1613–1623, 1625–1633.
254. P. L. ANTONA and R. MOSCHINI: *Mater. Sci. Technol.*, 1986, **4**, (2), 49–59.
255. P. L. ANTONA and R. MOSCHINI: *Foundry Trade J. Int.*, Dec. 1987, 173–178.
256. J. V. WOOD and B. TOLOUT: in 'Biomedical materials', MRS Symp. Proc. 55; 1986, Warrendale, PA, Materials Research Society.
257. R. M. K. YOUNG and T. W. CLYNE: *Powder Metall.*, 1986, **29**, 195–199.
258. M. TSUJIKAWA, K. TANAKA, C. USHIGOME, S. NISHIKAWA, and M. KAWAMOTO: in Ref. 9, pp. 165–168.
259. French Patent Specification 7 506 954, Aluminium Pechiney, 27 February 1975.
260. 'Process for manufacturing spheroidal hypoeutectic aluminum alloy', US Patent Specification 5,009,844, General Motors Corp., 23 April 1991.
261. Patent Specification WO 96/32519, North West Aluminium, 17 October 1996.
262. M. KIUCHI and S. SUGIYAMA: in Ref. 7, pp. 47–56.
263. M. KIUCHI and S. SUGIYAMA: *ISIJ Int.*, 1995, **35**, 790–797.
264. R. SHIBATA, K. KANEUCHI, T. SODA, and Y. IZUKA: in Ref. 9, pp. 296–300.
265. T. MOTEKI, N. OGAWA, K. KONDO, C. LIU, and S. AOYAMA: Proc. 6th Int. Conf. on 'Aluminium alloys' (ICAA-6), 297–326; 1998, Japan Institute of Light Metals.
266. T. HAGA and S. SUZUKI: in Ref. 11, pp. 735–740.
267. H. MULLER-SPATH, M. ACHTEN, and P. R. SAHM: in Ref. 9, pp. 174–179.
268. European Patent Specification, EP 0 745 694 A1, UBE Industries Ltd.
269. M. ADACHI: Proc. Japanese Die Casting Association, JD98–19, Tokyo, 1998, 123–128.
270. H. KAUFMANN, H. WABUSSEG, and P. J. UGGOWITZER: *Aluminium*, 2000, **76**, 70–75.
271. H. WABUSSEG, H. KAUFMANN, and P. J. UGGOWITZER: *Giesserei*, 2000, **87**, 39–43.
272. H. WABUSSEG, H. KAUFMANN, and P. J. UGGOWITZER: in Ref. 11, pp. 777–782.
273. R. POTZINGER, H. KAUFMANN, and P. J. UGGOWITZER: in Ref. 11, pp. 85–90.
274. R. SEBUS and G. HENNEBERGER: in Ref. 10, pp. 481–487.
275. F. MATSUURA and S. KITAMURA: in Ref. 10, pp. 489–496.
276. S. MIDSON, V. RUDNEV, and R. GALLIK: in Ref. 10, pp. 497–504.
277. H. K. JUNG and C. G. KANG: *Metall. Mater. Trans. A*, 1999, **30A**, 2967–2977.
278. G. HIRT, R. CREMER, A. WINKELMANN, T. WITULSKI, and M. ZILLGEN: in Ref. 8, pp. 107–116.
279. J. A. DANTZIG and S. P. MIDSON: in Ref. 7, pp. 105–118.
280. R. C. GIBSON: in Ref. 9, pp. 137–141.
281. P. KAPRANOS, R. C. GIBSON, D. H. KIRKWOOD, P. J. HAYES, and C. M. SELLARS: *Mater. Sci. Technol.*, 1996, **12**, 274–278.
282. P. KAPRANOS, R. C. GIBSON, D. H. KIRKWOOD, and C. M. SELLARS: in Ref. 9, pp. 148–152.
283. J. C. CHOI, H. J. PARK, and B. M. KIM: *J. Mater. Process. Technol.*, 1999, **87**, 46–52.
284. E. TZIMAS, A. ZAVALIANGOS, and A. LAWLEY: in Ref. 10, pp. 345–352.
285. L. PASTERNAK, R. CARNAHAN, R. DECKER, and R. KILBERT: in Ref. 7, pp. 159–169.
286. H. PENG, S. P. WANG, N. WANG, and K. K. WANG: in Ref. 8, pp. 191–200.
287. N. WANG, H. PENG, and K. K. WANG: in Ref. 9, pp. 342–346.
288. H. PENG and W.-M. HSU: in Ref. 11, pp. 313–317.
289. Z. FAN, M. J. BEVIS, and S. JI: 'Process and apparatus for manufacturing castings from immiscible metallic liquids', PCT/WO 01/23124 A1, 1999.
290. Z. FAN, S. JI, and J. ZHANG: *Mater. Sci. Technol.*, 2001, **17**, 837–842.
291. Z. FAN, S. JI, and M. J. BEVIS: UK Patent Application 0 019 855.6, 2000.
292. D. WALUKAS, S. LEBEAU, N. PREWITT, and R. DECKER: in Ref. 11, pp. 109–114.
293. P. EISEN and K. P. YOUNG: in Ref. 11, pp. 41–46.
294. M. GUPTA, S. C. LIM, and W. B. NG: *Mater. Sci. Technol.*, 1997, **13**, 584–589.
295. K. ICHIKAWA and Y. KINOSHITA: *Mater. Sci. Eng.*, 1997, **A240**, 493–502.
296. A. K. MUSRA: *Metall. Trans. A*, 1985, **16A**, 1254.
297. A. K. MUSRA: *Metall. Trans. A*, 1986, **17A**, 358.
298. J. P. BARNAK, A. F. SPRECHER, and H. CONRAD: *Scr. Metall. Mater.*, 1995, **32**, 879–884.
299. R. S. QIN and B. L. ZHOU: *Int. J. Non-Equilib. Process.*, 1998, **11**, 77–86.
300. T. IIDA and R. I. L. GUTHRIE: 'The physics of liquid metals'; 1988, Oxford, Clarendon Press.

Authors Queries

Journal: **International Materials Reviews**

Paper: **335**

Dear Author

During the preparation of your manuscript, the queries listed below have arisen. The text to which the queries pertain is indicated on the proof by a numbered box in the margin. Please answer the queries and return this form with your corrected proof. Many thanks for your co-operation.

<i>Query Refs</i>	<i>Query</i>	<i>Remarks</i>
1	Author: Please check all equations throughout.	
2	Author: OK, here, eta subscript 0 is the viscosity of the liquid matrix?	
3	Author: OK s^{-1} for unit of shear rate – as elsewhere?	
4	Author: OK the F_g in Fig. 11 is from equation 20? However, now that refs. 69 and 70 have been renumbered, this use of F_g (ref 69 is 1992) appears to predate the statement ‘Loue and Suery ⁷⁰ introduced ...’ that appears above equation 20 in the text (ref. 70 is 1995).	
5	Author: OK (equation (18)) added to Fig. 17 caption with regard to F_1 ?	
6	Author: OK ‘In this paper’ or ‘In this section’?	
7	Author: Does ‘both fragmentation and remelting mechanisms’ here mean ‘neither the fragmentation nor the remelting mechanism offers an explanation (i.e. the mechanisms considered separately), or ‘the fragmentation and remelting mechanisms combined do not offer’ (i.e. the mechanisms acting in combination)?	
8	Author: OK (equation (25)) added to Fig. 25 caption with regard to this F_g ?	
9	Author: OK rewording of sentence ‘The advantage of such alloys fl 4Vx ...’?	
10	Author: OK rewording ‘... making it cost approximately 3–5 times more than the MHD stirring process.’	
11	Author: OK ‘desired’?	
12	Author: Ref. 6, 8, 211 month held (if possible)?	

<i>Query Refs</i>	<i>Query</i>	<i>Remarks</i>
13	Author: Ref. 110 and 224: please do you have any further details for these conferences, e.g. month held, organiser, and (if published) the year of publication and name and location of Publisher?	
14	Author: Refs. 116, 119, 124,140, 166: just in case (since your e-mail) do you have any updates on the 'Submitted' refs yet please?	
15	Author: Ref. 244, can you give the title for this PCT ref?	